

**Mechanism and Function  
of *RAD6*-Mediated  
DNA Damage Tolerance**

Dissertation  
zur Erlangung des Doktorgrades  
der Fakultät für Biologie der  
Ludwig-Maximilians-Universität  
München

vorgelegt von  
Diplom Molekular Biologe- Genetiker  
Georgios Ioannis Karras

April 2010

## **Ehrenwörtliche Erklärung**

Hiermit erkläre ich, dass ich die vorliegende Dissertation selbständig und ohne unerlaubte Hilfe angefertigt habe. Ich habe weder anderweitig versucht, eine Dissertation einzureichen oder eine Doktorprüfung durchzuführen, noch habe ich diese Dissertation oder Teile derselben einer anderen Prüfungskommission vorgelegt.

Georgios I Karras

München, den 28. 04. 2010

Promotionsgesucht eingereicht:

03. 05. 2010

Tag der mündlichen Prüfung:

18. 06. 2010

Erster Gutachter:

Prof. Dr. Stefan Jentsch

Zweiter Gutachter:

Prof. Dr. Peter B. Becker

Die vorliegende Arbeit wurde zwischen November 2004 und Dezember 2009 unter Anleitung von Prof. Dr. Stefan Jentsch am Max-Planck-Institut für Biochemie in Martinsried durchgeführt.

Wesentliche Teile dieser Arbeit sind in folgenden Publikationen veröffentlicht:

Moertl S., **Karras G.I.**, Wismüller T., Ahne F., Eckardt-Schupp F. Regulation of double-stranded DNA gap repair by the *RAD6* pathway. *DNA Repair (Amst)*; 2008 (7, 11, 1893-1906)

**Karras G.I.** and Jentsch S. The *RAD6* DNA Damage Tolerance Pathway Operates Uncoupled From the Replication Fork and Is Functional Beyond S-phase. *Cell*; 2010 (141, 2, 255-267)

# TABLE OF CONTENTS

<b>I SUMMARY</b>	<b>1</b>
<b>II INTRODUCTION</b>	<b>2</b>
<b>II.1 Ubiquitin and Ubiquitin-Like Protein Modifiers</b>	<b>2</b>
II.1.1 Enzymology of Ubiquitin and SUMO Conjugation	2
II.1.2 Functions of Ubiquitin and SUMO	5
<b>II.2 DNA Repair</b>	<b>7</b>
II.2.1 Sensing DNA Replication Stress	9
II.2.2 DNA Damage Tolerance	11
<b>II.3 Aim of this work</b>	<b>15</b>
<b>III RESULTS</b>	<b>17</b>
<b>III.1 PCNA Ubiquitylation and DNA Replication</b>	<b>17</b>
III.1.1 Roles of Replication Forks in PCNA Ubiquitylation by the <i>RAD6</i> Pathway	
III.1.2 Loss of The Replication Fork Protein Pol32 Results in Spontaneous PCNA Ubiquitylation	19
III.1.3 Pol32 Does Not Function as an Enzymatic Inhibitor of PCNA Ubiquitylation	20
III.1.4 Defects in DNA Replication Triggers PCNA Ubiquitylation in <i>pol32Δ</i> Cells	22
<b>III. 2 PCNA Ubiquitylation And The Cell Cycle</b>	<b>25</b>
III.2.1 Role of Pol32 in Error-Free DDT Becomes Prominent at Low Temperatures	25



III.2.2 Ubiquitylated PCNA Persists Beyond S-Phase	27
III.2.3 Ubiquitylated PCNA Is Not Required for S-Phase Progression in The Presence of DNA Damage	31
<b>III. 3 Error-Prone DDT Proceeds Uncoupled From The Replication Fork</b>	<b>34</b>
III.3.1 The G2-Tag	34
III.3.2 Efficient and Specific Tolerance to DNA Damage by TLS Polymerases in G2/M	38
<b>III. 4 Error-Free DDT Involves Sgs1 Functions Behind The Replication Fork</b>	<b>42</b>
III.4.1 A Genetic Screen For Components of Error-Free DDT	42
III.4.2 Sgs1 Helicase Operates Downstream of Polyubiquitylated PCNA	43
III.4.3 Restriction of Sgs1 to G2/M Supports DDT, But Not its Functions at The Fork	47
<b>III. 5 <i>RAD6</i>-Dependent Error-Free DDT Proceeds Uncoupled From The Replication Fork</b>	<b>49</b>
III.5.1 Restriction of the <i>RAD6</i> Pathway to G2/M Has No Impact on DDT	49
III.5.2 Restricting Rad5 to G2/M Postpones DDT, Without Affecting S-Phase Progression	51
III.5.3 The <i>RAD6</i> Pathway Supports DDT in G2/M Specifically	54
<b>IV DISCUSSION</b>	<b>57</b>
<b>IV.1 The G2 tag</b>	<b>58</b>
IV.1.1 Evidence for the Validity and Efficiency of the G2 tag Strategy	58
IV.1.2 Advantages of the G2 tag	60
<b>IV.2 The DNA Substrate of <i>RAD6</i>-Mediated DDT</b>	<b>61</b>
IV.2.1 The <i>RAD6</i> Pathway Proceeds Uncoupled From The Replication Fork	61
IV.2.2 The DNA substrate(s) of the <i>RAD6</i> Pathway	62

<b>IV.3 Timing of DDT</b>	<b>65</b>
<b>IV.4 The Biological Role of Fork-Uncoupled DDT</b>	<b>66</b>
 <b>V MATERIALS AND METHODS</b>	 <b>69</b>
<b>V.1 Computational analyses</b>	<b>69</b>
<b>V.2 Microbiological and genetic techniques</b>	<b>69</b>
V.2.1 <i>E. coli</i> techniques	69
V.2.2 <i>S. cerevisiae</i> techniques	72
 <b>V.3 Molecular biology methods</b>	 <b>79</b>
V.3.1 Isolation of DNA	79
V.3.2 Molecular cloning methods	81
V.3.3 Polymerase chain reaction (PCR)	82
V.3.4 Site-directed mutagenesis	83
 <b>V.4. Protein biochemistry methods</b>	 <b>84</b>
V.4.1 Gel electrophoresis and immunoblot techniques	84
V.4.2 Preparation of cell extracts	85
 <b>VI LITERATURE</b>	 <b>86</b>
 <b>Abbreviations</b>	 <b>101</b>
<b>Acknowledgements</b>	<b>104</b>
<b>Lebenslauf</b>	<b>105</b>

## I SUMMARY

Life depends on the integrity of the genomic information that encodes it, which has to be maintained inside the hostile environment where organisms live. The carrier of genetic information, DNA, is particularly vulnerable to DNA damage during the process of DNA replication; replication forks can collapse and give rise to chromosomal aberrations, the hallmark of cancer.

To ensure DNA replication completion and protect genome stability, organisms have evolved DNA damage tolerance mechanisms. These mechanisms promote survival even when DNA damage cannot be removed from the genome. Although the molecular events are only partially understood, DNA damage tolerance in eukaryotes requires the *RAD6* pathway, which consists of two main branches, an error-free involving sister-chromatid recombination and an error-prone involving specialized translesion synthesis (TLS) polymerases. This pathway controls the modification of an essential replication fork component, PCNA by ubiquitin upon impact of the replication machinery with the DNA damage. Therefore, the *RAD6* pathway is believed to initiate and proceed in a manner coupled to the DNA replication fork in S-phase in order to ensure replication completion.

To address the validity of this model we needed to construct mutant versions of *RAD6* pathway members that are specifically excluded from replication forks, but retain accessibility to lesions left behind the forks. Because the specific mode of recruitment of these factors to the stalled fork remains elusive, we designed *RAD6* member mutants that are excluded from S-phase, instead. Surprisingly, we found that limiting TLS to the G2/M phase of the cell cycle does not influence lesion tolerance. Likewise, also the ubiquitin ligase Rad5 and Werner/Bloom (WRN/BLM)-related helicase Sgs1, which we found to be elementary for the error-free branch, efficiently and specifically uphold this pathway when restricted to G2/M.

In conclusion, our findings indicate that both branches of *RAD6*-mediated DNA damage tolerance unexpectedly operate effectively after chromosomal replication, outside S-phase. We therefore propose that the *RAD6* pathway acts on single-stranded gaps left behind newly restarted replication forks. This uncoupling may allow rapid replication completion and protect genomic integrity, while in parallel by facilitating decision-making may be important for evolution and pathogenesis.

## II INTRODUCTION

### II.1 Ubiquitin and Ubiquitin-Like Protein Modifiers

Protein modification offers a rapid and reversible way to regulate function. Among a large number of protein modifiers, ubiquitin excels in versatility. By utilizing diverse functional surfaces, the highly-conserved globular protein of 76 amino acids conducts a multitude of cellular activities in the eukaryotic cell (Jentsch, 1992). Yet, ubiquitin is not exceptional in this respect; Smt3/SUMO, Rub1/NEDD8, Atg12, Atg8, FAT10, ISG15, FUB1/MNSF, Urm1, and Ufm1 all possess a ubiquitin-like (Ubl) fold and function similar to ubiquitin as “modifiers” (Hochstrasser, 2006; Jentsch and Pyrowolakis, 2000). Protein modification by ubiquitin and Ubls has emerged as a versatile eukaryotic strategy for the regulation of cellular activities (Pickart, 2004).

#### II.1.1 Enzymology of Ubiquitin and SUMO Conjugation

Among the members of the ubiquitin fold family, ubiquitin and SUMO are the most thoroughly investigated. Covalent conjugation of Ub/Ubls onto protein targets employs an enzymatic cascade that attaches the modifier to the  $\epsilon$ -amino group of a target lysine. This cascade (ubiquitylation and SUMOylation for ubiquitin and SUMO, respectively) couples ATP hydrolysis to a handful of kinetically discrete steps that involve a large list of specialized catalysts (Hershko and Ciechanover, 1998; Pickart, 2001).

Ub/Ubl-conjugation starts with the hydrolysis of a molecule of ATP for the adenylation of the modifier by a dimeric Ub/Ubl-activating enzyme, E1, and its subsequent attachment to a cystein residue on the E1 enzyme via a high energy thioester bond. This reaction involves large conformational changes on the E1 protein (Olsen et al., 2010; Wang et al., 2009) that place the activated Ub/Ubl in a favorable position for its transfer to a cystein residue on a Ub/Ubl-conjugating

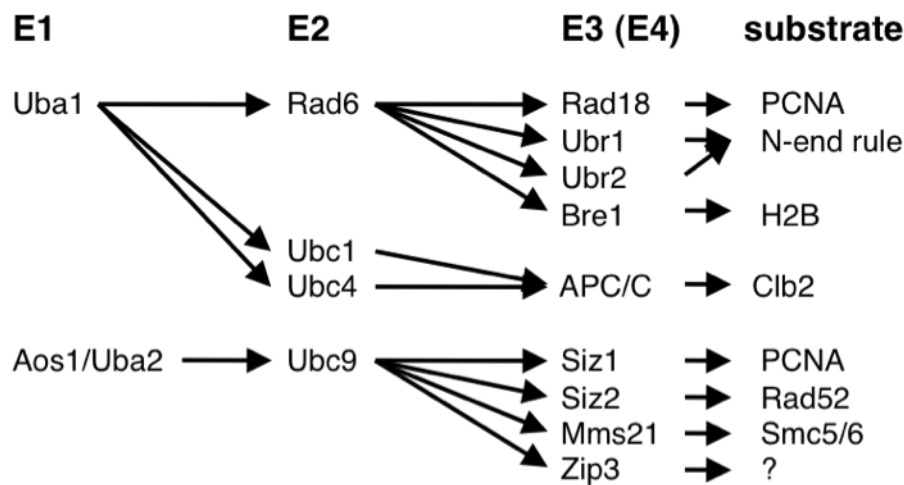


**Fig. 1: Ubiquitin and SUMO Conjugation Systems**

Examples of ubiquitin and SUMO conjugation cascades from *S.cerevisiae* involving specialized E1s, E2s, and E3s (occasionally also an E4 examples of which are not indicated) for the modification of specific protein substrates. The homodimeric E1 enzyme Uba1 is required for activation of ubiquitin and the heterodimeric Aos1/Uba2 for SUMO. For most of the above mentioned E3s more than a single substrate has been identified, but only one example is shown here. Note that the complexity usually increases with every step in the reaction.

enzyme, E2. In *S. cerevisiae* there is a single E1 dimer for each Ub/Ubl, although the number of E2s varies dramatically; while a single E2 enzyme (Ubc9) catalyzes SUMO conjugation in yeast, 11 E2s (Ubc1, Ubc2/Rad6, Ubc3/Cdc34, Ubc4, Ubc5, Ubc6, Ubc7, Ubc8, UbcX, Ubc11, and Ubc13) work with ubiquitin. E2s are often capable of direct substrate recognition (eg. Ubc9 recognizes sequence consensus  $\Psi KxE/D$ , where  $\Psi$  is any aliphatic amino acid), yet for most proteins, and in particular for ubiquitin targets, the reaction requires a Ub/Ubl ligase, E3 (**Fig. 1**). The participation of an E3 in the conjugation reaction does not always entail the formation of an E3~Ub/Ubl high energy intermediate – like for the case of the HECT (Homologous to E6-AP C-terminus) family of ubiquitin-ligases (Rotin and Kumar, 2009) – but may as well be restricted to substrate recruitment. In fact, most E3s play non-enzymatic roles in the reaction by bringing the Ub/Ubl-loaded E2s in close proximity to their substrates and/or enhancing conjugation activity of the E2 (Das et al., 2009; Pichler et al., 2004;

Reverter and Lima, 2005). Most of those E3s mediate E2-binding via a zinc-coordinating domain termed the RING finger. Importantly, there are about 40 RING finger proteins in budding yeast, four out of which (Siz1, Siz2, Mms21, and Zip3/CST9) are E3 ligases for SUMO, and over 350 in humans, in accordance with the fact that most E2s work in complex with several E3s (**Fig. 1**).

The exponential increase in complexity gained with each step during Ub/Ubl conjugation offers tremendous versatility to its function. On the one hand, it allows the regulation of discrete protein pools by tethering the ubiquitin ligase to specific cellular compartments or even to certain substrates via direct interaction. Examples of this mechanism are the membrane-bound Doa10 and Hrd1/Der3 ligases that promote endoplasmic reticulum-associated degradation (ERAD) (Kostova et al., 2007), the specific interaction and modification of lysine 164 (K164) of the replication polymerase processivity factor, PCNA, involving a specialized and conserved “PINIT” sequence motif on Siz1 ligase (Duval et al., 2003; Hoege et al., 2002; Reindle et al., 2006; Yunus and Lima, 2009), and the modular D (destruction)-box and “KEN” motifs respectively found in all substrates (Pds1 contains D-box, while Clb2 contains both motifs) of the APC/C<sup>Cdc20</sup> and APC/C<sup>Cdh1</sup> E3 complexes (Pfleger and Kirschner, 2000; Visintin et al., 1997; Wasch and Cross, 2002). In addition to substrate selection, the Ub/Ubl systems employ the modification of the modifier itself to boost versatility. In fact, the N-terminal NH<sub>2</sub> of ubiquitin or any of its seven lysines can be utilized for the formation of so-called “polyubiquitin” chains *in vitro* and *in vivo*. Residue selectivity for ubiquitin chain formation often depends on sterical restrictions enforced by the E2 enzyme. For instance, the E2 Ubc3/Cdc34 bears an acidic loop inside the core Ubc domain that restricts its activity to K48-linked ubiquitin chain assembly on target proteins (Petroski and Deshaies, 2005), although this reaction occurs with very slow kinetics (David et al., 2010). This reaction can be accelerated by the use of specialized E2s. Therefore, the multi-subunit ubiquitin ligase APC/Cyclosome first employs the E2 Ubc4 to form monoubiquitylated protein conjugates that will be subsequently extended by recruiting the E2 Ubc1

that bears a ubiquitin-binding module (ubiquitin-association (UBA) domain) into K48-linked chains (Rodrigo-Brenni and Morgan, 2007). Similarly, E4 factors may be utilized for ubiquitin chain elongation (Koegl et al., 1999). At least one E2 variant, Mms2, although deprived of enzymatic activity, serves towards chain selectivity by working in complex with the E2 Ubc13 (VanDemark et al., 2001). The heterodimer Mms2/Ubc13 forces the orientation of acceptor ubiquitin K63 towards the active site of Ubc13 (Eddins et al., 2006), thus favoring catalysis of K63-linked ubiquitin chains. Such intermediate steps distinguish Ub/Ubl conjugation from most other ligation reactions and increase the versatility of the system.

## II.1.2 Functions of Ubiquitin and SUMO

The eukaryotic cell exploits the versatility of these protein modification systems. Evidently, polymeric conjugates exhibit discrete functions from the monomeric; polySUMOylated proteins have roles during mitosis and meiosis that cannot be supported by the monoSUMOylated counterparts (Vertegaal, 2010) and protein polyubiquitylation is specifically employed in a multitude of pathways varying from protein activation to protein degradation.

The importance of ubiquitin for protein degradation has been known for decades (Ciechanover et al., 1984; Finley et al., 1984; Hershko and Ciechanover, 1998; Hochstrasser, 1996; Varshavsky, 1996). Cyclins, the master regulators of CDK activity and thus the cell cycle, have to be degraded to facilitate cell cycle progression (Glutzer et al., 1991; Wasch and Cross, 2002) and unfolded proteins that form after stress in the cytoplasm and membrane compartments must be recognized and disposed to avoid pathological condition (Ardley and Robinson, 2004), and ubiquitin is required for both. However, it has only been recently understood how quality control is achieved by this mechanism. It was found that ubiquitin chains of discrete shapes (K48- and K29-linked, and likely other types as well) and sizes (oligo- versus poly-) are

recognized by specialized receptors or escort-factors (Richly et al., 2005) that collaborate with ubiquitin ligases (E3s) and the chain elongation enzyme Ufd2 (E4s) and de-ubiquitylating enzymes (DUBs) to control the transfer of ubiquitylated cargo to a multi-subunit cytoplasmic protease complex, the 26S proteasome (26S Ps) (Jentsch and Rumpf, 2007; Koegl et al., 1999; Romisch, 2005). Both N-terminal and internal amino acids can strongly accelerate these events. Among the most widely studied, the presence of a D-box motif consisting of 9 amino acids (RxxLxxxxN consensus sequence, where x can be any amino acid) can bypass the need for escort by triggering the processive and robust polyubiquitylation of targets by the APC/C ubiquitin ligase complex (Cao et al., 2003; Rape et al., 2006) and their direct recognition by the 26S Ps (Fu et al.; Thrower et al., 2000). It has become apparent that polySUMO chains may also influence the degradation rate of certain protein targets (Perry et al., 2008).

However, a multitude of ubiquitin and SUMO functions is uncoupled to proteasomal degradation. Attachment of K63-linked ubiquitin chains on protein targets is employed for the NF- $\kappa$ B-dependent inflammatory response (Deng et al., 2000; Sun and Chen, 2004; Wu et al., 2006), DNA repair (Garcia-Higuera et al., 2001; Hoege et al., 2002; Hofmann and Pickart, 1999), and vesicular transport (Dupre et al., 2004; Haglund et al., 2003; Hicke and Dunn, 2003; Katzmann et al., 2001). K6-linked chains catalyzed by the BRCA1-BARD1 ubiquitin ligase play important roles in the response to DNA damage (Sobhian et al., 2007). Ubiquitin chains have also been implicated in transcriptional silencing, with histone 2B (H2B) ubiquitylation directly triggering Dot1-mediated histone 3 (H3) K79 methylation (Briggs et al., 2002; Jeltsch and Rathert, 2008; Osley, 2004; Sun and Allis, 2002). Monomeric ubiquitin and SUMO attachment to protein substrates among other functions also facilitates transcriptional silencing (Girdwood et al., 2003; Khan et al., 2001), induces conformational activation of DNA repair enzyme thymidine-DNA glycosylase (TDG) (Baba et al., 2005; Hardeland et al., 2002) promotes DNA damage induced mutagenesis (Hoege et al., 2002; Stelter and Ulrich, 2003), and mediates the recruitment of the



antirecombinogenic helicase Srs2 at replication forks (Papouli et al., 2005; Pfander et al., 2005).

Specialized recognition domains that bind with high-affinity ubiquitin or SUMO conjugates ensure the functional specificity of this diverse list of conjugates (Grabbe and Dikic, 2009; Liu and Walters, 2010). Structural studies have established that there are several ways to recognize ubiquitin (Matta-Camacho et al., 2009) and SUMO (Hannich et al., 2005; Minty et al., 2000; Song et al., 2004) even at the level of the monomer (Bomar et al., 2010; Sekiyama et al., 2010). This points to the conclusion that each modification type may involve one or more specific recognition domains. Moreover, mixed ubiquitin-SUMO chains of various linkages (including linear configuration) and sizes may “encode” specialized biological roles (Ikeda and Dikic, 2008). In essence, the existence of regulatory steps during Ub/Ubl conjugation and recognition provides the system with a seemingly unlimited versatility and specificity.

## **II.2 DNA Repair**

The robustness of all biological mechanisms depends on the integrity of the genomic information that encodes them. Therefore, protecting the genome from DNA damage is of critical importance. The response to DNA damage involves the concerted action of a horde of specialized factors that operate at the site of the DNA lesion to promote DNA repair and signal checkpoint responses that will delay cell cycle progression until the damage has been repaired (Zhou and Elledge, 2000).

DNA damage can arise by the reaction of common in nature chemical entities with DNA. Reactive-oxygen species (ROS), alkylating agents, and UV-light, or even spontaneous errors during the duplication of genomic DNA can result in genome instability, in various genetic disorders, premature aging, and carcinogenesis (Jackson and Bartek, 2009). To avoid these conditions, organisms

directly recognize and repair most of these lesions by mechanisms employing excision of the DNA damage (reversal) or the damaged nucleotide stretches (base-excision repair; BER, and global genomic nucleotide excision repair; GG-NER), or correction of mismatched Non-Watson-Crick base pairs (mismatch repair; MMR) created during erroneous DNA replication (Hoeijmakers, 2001). To ensure the integrity of the encoded information in addition to GG-NER cells utilize transcription-coupled NER (TC-NER), which allows them to enhance the efficiency of NER specifically at actively transcribed DNA strands that have been damaged. This mechanism operates upon arrest of an actively transcribing RNA polymerase II on the encountered DNA lesion (Tornaletti and Hanawalt, 1999). It is therefore appreciable that mutation of the genes regulating such mechanisms in mammals often results in cancer syndromes, associated with increased sensitivity to DNA damaging agents. Characteristic examples are Xeroderma pigmentosum and Cockayne syndromes.

Persistence of DNA damage can result in the accumulation of double-stranded breaks (DSBs). Because DSBs are highly recombinogenic and can engage into error-prone (non-homologous end-joining; NHEJ, versus homologous recombination; HR) repair reactions, these intermediates are often deleterious. Yet, homologous recombination (HR) promotes error-free repair of DSBs. In fact, this pathway is critical for meiosis of sexually reproducing eukaryotes (Keeney et al., 1997) and mating type switching in budding yeast (Schiestl and Wintersberger, 1992). It is notable that the HR mechanisms operating in the bacterium *Deinococcus radiodurans* support error-free repair of DNA damage doses sufficient to shatter its genome into hundreds of pieces (Blasius et al., 2008). However, DSBs only rarely occur *in vivo* even during the replication of difficult to replicate (eg. repetitive) sequences (Mizuno et al., 2009; Paek et al., 2009), likely to limit the possibility of gross-chromosomal rearrangement (GCR) formation that is a hallmark of cancer. An important contribution towards the protection from GCRs is the utilization of sensitive and robust checkpoint responses (Myung and Smith, 2008).

### II.2.1 Sensing DNA Replication Stress

DNA replication takes place during the S-phase of the cell cycle in a processive (**Fig. 2A**) and highly programmed manner (Alvino et al., 2007; Raghuraman et al., 2001). DNA replication bubbles and forks (**Fig. 2A and 2B**) are established at specific chromosomal locations containing autonomously-replicating sequences (ARSs) in yeast initiated by the concerted action of ORC, MCM and GINS and cell cycle kinases CDK and DDK (Bell and Dutta, 2002). S-phase is a very sensitive period of the cell cycle suggesting the recruitment of hundreds of protein factors to the replication fork (**Fig. 2B**) may ensure timely completion of DNA replication. One such component is the essential proliferating-cell nuclear

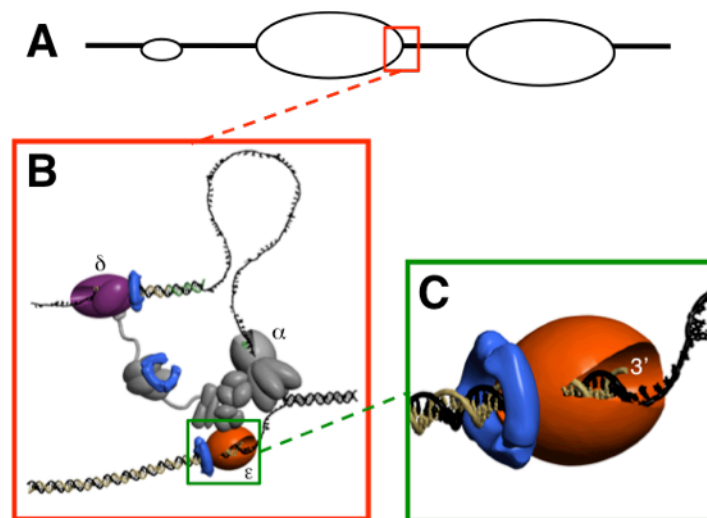


**Fig. 2: The Bulk of DNA Replication Involves PCNA**

(A) The synthetic (S) phase of the eukaryotic cell cycle hosts the duplication (replication) of genomic nuclear DNA. DNA replication initiates at specific genomic loci (termed origins in *S.cerevisiae*) with the establishment of two replication forks (red box) at each replication bubble (empty circles) that move in opposite directions expanding the bubble until it fuses with an adjacent one. (B) The chemistry of DNA synthesis directs synthesis of one of the two nascent strands of the replication fork to be discontinuous (lagging-strand). Three polymerases catalyze bulk DNA replication; Pol α and Pol δ synthesize the lagging-strand, while Pol ε (green box) the leading, as indicated. (C) PCNA (blue ring) is an integral component of the replication fork and is involved in tethering the replicative polymerases δ and ε to the 3' end of primed ssDNA templates on chromatin, thus significantly increasing their processivity. Template DNA strands are depicted in black, while nascent strands in gold.

antigen, PCNA, a homotrimeric, ring-shaped, DNA-encircling protein, which functions as a DNA polymerase processivity factor and as a platform for replication-linked activities (**Fig. 2C**) (Moldovan et al., 2007; Tsurimoto, 1999; Warbrick, 2000).

DNA lesions that remain unrepaired before entering S-phase pose a serious problem. The active sites of the replicative polymerases are only wide enough to incorporate a perfect Watson-Crick base pair and cannot accommodate even the smallest of modifications. In this way, bulky DNA lesions encountered during replication result in the accumulation of single-stranded (ss) DNA at stalled replication forks via uncoupling the MCM helicase activity from DNA synthesis (Baynton and Fuchs, 2000; Branzei and Foiani, 2010; Byun et al., 2005; Tourriere and Pasero, 2007). Beside the discontinuity of chromosomal replication they cause, stalled replication forks are particularly dangerous as they can collapse, resulting in chromosome breaks and subsequently genomic instability (Cox et al., 2000; Osborn et al., 2002; Smirnova and Klein, 2003). This is avoided by the action of the cellular checkpoints (Myung and Smith, 2008).

There are two major checkpoint responses to replication stress: the S-phase and the G2/M (or DNA damage) checkpoints. Both responses sense the accumulation of ssDNA via a mechanism that involves the ssDNA-binding protein RPA, the checkpoint sensor Ddc2/ATRIP and the Mec1/ATR checkpoint kinase. The S-phase checkpoint senses stalled and damaged forks and delays G2 onset (Bartek et al., 2004; Sancar et al., 2004). For this purpose Mec1 directly phosphorylates the fork component, Mrc1, to slow down fork movement (Alcasabas et al., 2001; Katou et al., 2003; Lou et al., 2008; Osborn and Elledge, 2003). An important branch of the S-phase checkpoint (termed intra-S) requires the helicase Sgs1 in the stabilization of DNA polymerases at the stalled fork (Cobb et al., 2003; Frei and Gasser, 2000), and thus the S-phase responses all operate at the fork. On the other hand, the G2/M checkpoint involves oligomers of the mediator protein Rad9/BRCA1 (Huen et al., 2010; Paulovich et al., 1998; Usui et al., 2009), which plays a minor role in replication progression (Paulovich

and Hartwell, 1995; Paulovich et al., 1997). However, both mediators activate the checkpoint kinase Rad53/CHK2 facilitating its phosphorylation by Mec1/ATR (Lee et al., 2004; Vialard et al., 1998). Both checkpoint responses are to some extent strengthened by chromatin loading of the PCNA-like checkpoint clamp, 9-1-1 (Parrilla-Castellar et al., 2004). Rad53 catalyzes phosphorylation of many substrates (Chen et al., 2010), mediating subsequent events in cell cycle control (inhibitory phosphorylation of polo-like kinase (Plk) that prevents its from inactivating Cdh1 and the APC/C and hence anaphase progression (Zhang et al., 2009)) and repair (like RPA, H2A, Rad55 phosphorylation)

### II.2.2 DNA Damage Tolerance

The S and G2/M phase checkpoints provide repair mechanisms with sufficient time to cope with DNA damage. Apparently all organisms achieve this via so-called DNA damage tolerance (DDT) pathways, which ensure cell survival in the presence of DNA polymerase-blocking damage (Andersen et al., 2008; Budzowska and Kanaar, 2009; Friedberg et al., 2002; Waters et al., 2009). Notably different from conventional DNA repair pathways, DDT does not result in repair of the primary DNA lesion (Ganesan, 1974), but rather cures their symptoms that manifest during replication (Bridges et al., 1968; Broomfield et al., 2001). Similarly to the activation of the cellular checkpoints at the fork DDT usually becomes activated as a result of a replication block-induced temporal uncoupling of DNA unwinding and synthesis (Chang and Cimprich, 2009; Janion, 2008). This leads to the formation of ssDNA, a key trigger of DDT (**Fig. 3A**) (Broomfield et al., 2001; Higgins et al., 1976; Little and Mount, 1982). However, repair of a class of bulky DNA lesions causing inter-strand DNA crosslinks activate DDT and checkpoint responses during fork collapse (Knipscheer et al., 2009).

Early studies in *E. coli* have indicated that bacterial DDT promotes restart of stalled replication forks, which frequently involves re-priming at the damaged

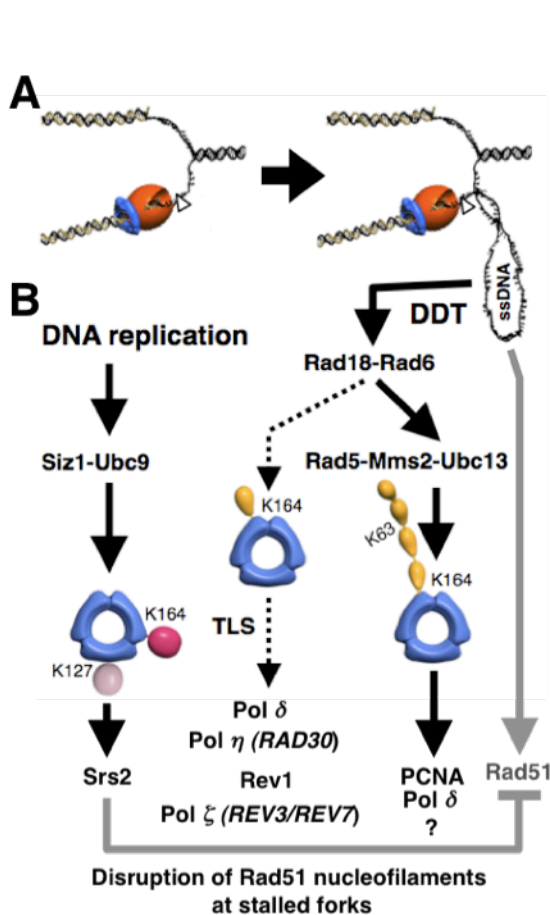


**Fig. 3: PCNA Modification by Ubiquitin and SUMO**

(A) DNA template lesions (arrowhead) block the replicative polymerases (upper left panel), resulting in the accumulation of single-stranded DNA at stalled forks (upper right panel). (B) ssDNA activates the *RAD6* DDT pathway by promoting the recruitment of Rad18 and Rad5 ubiquitin ligases to PCNA. Rad18 binds to ssDNA via a SAP domain. Monoubiquitylation of PCNA involves Rad6 and Rad18, and engages a complex of Pol δ and TLS polymerases in error-prone lesion bypass. Polyubiquitylation of PCNA by K63-linked ubiquitin chains requires the action of Rad6, Rad18, Mms2/Ubc13, and Rad5. Polyubiquitylated species trigger error-free bypass utilizing Pol δ. Both modifications occur on K164 of PCNA. On the contrary, PCNA SUMOylation occurs spontaneously during S-phase involving K164 and K127; only K164 modification involves an E3 (Siz1). These species recruit the translocase Srs2 to protect forks from engaging into error-prone recombination. PCNA is shown in blue, the replicative polymerase in orange, ubiquitin in light orange, and SUMO in crimson.

template (Courcelle and Hanawalt, 2003; Heller and Marians, 2006). Interestingly, both pro- and eukaryotes utilize two distinct DDT modes: an error-prone mechanism, which involves dedicated translesion polymerases (Friedberg et al., 2001; Prakash et al., 2005) that can bypass bulky DNA lesions by catalyzing DNA synthesis across the damaged template, and an error-free pathway that engages recombination proteins (Friedberg, 2005). As polymerases involved in translesion synthesis (TLS) can also incorporate an incorrect nucleotide across the damaged site, DDT is largely accountable for mutagenesis (Friedberg and Gerlach, 1999; Friedberg et al., 2002).

Distinctly different from the prokaryotic system, eukaryotic DDT essentially requires the ubiquitin protein modification pathway. Indeed, a large number of genes involved in eukaryotic DDT (called the *RAD6* pathway) encode enzymes of

this protein modification system (**Fig. 3B**) (Broomfield et al., 1998b; Jentsch et al., 1987; Ulrich and Jentsch, 2000). The crucial substrate of this pathway is the replicative polymerase processivity clamp PCNA (Hoege et al., 2002). Different types of ubiquitin modifications that become induced upon DNA damage dictate whether DDT proceeds via the error-prone or the error-free branch (**Fig. 3B**). Error-prone DDT is triggered by conjugation of a single ubiquitin moiety (monoubiquitylation) to PCNA at lysine-164 (K164), which involves the Rad6 ubiquitin-conjugating (E2) enzyme and Rad18, a RING-finger ubiquitin ligase (E3) that binds PCNA and the ssDNA-binding complex RPA (Davies et al., 2008; Hoege et al., 2002; Stelter and Ulrich, 2003). Monoubiquitylated PCNA in turn promotes TLS possibly through direct recruitment of TLS polymerases that possess ubiquitin-binding motifs (Bienko et al., 2005; Kannouche et al., 2004; Lehmann et al., 2007; Watanabe et al., 2004). By contrast, error-free DDT requires modification of the same residue of PCNA by a non-canonical polyubiquitin chain that is linked via K63 of ubiquitin (Hoege et al., 2002; Hofmann and Pickart, 1999). Synthesis of this polyubiquitin chain requires in addition to Rad6 and Rad18 the heterodimeric E2 Ubc13-Mms2, and the RING-finger E3 ubiquitin ligase Rad5, which binds PCNA and Rad18 (Hoege et al., 2002; Ulrich and Jentsch, 2000). Once modified by this polyubiquitin chain, PCNA triggers by a yet unknown mechanism lesion bypass involving the undamaged template (template switching) and specific repair proteins (Branzei et al., 2008; Giot et al., 1997; Zhang and Lawrence, 2005). Furthermore, PCNA can alternatively be modified at the same lysine residue (K164) by the ubiquitin-related modifier SUMO (Arakawa et al., 2006; Hoege et al., 2002; Leach and Michael, 2005). In *S. cerevisiae* this leads to the recruitment of Srs2, an anti-recombinogenic helicase, which helps to keep at check an alternative homology-dependent repair (HDR) error-free DDT mode that utilizes the Rad51 recombinase (**Fig. 3B**) (Papouli et al., 2005; Pfander et al., 2005).

Although after its discovery in the 1960s, DDT was initially coined “post-replicative repair” (Howard-Flanders, 1968; Rupp and Howard-Flanders, 1968),

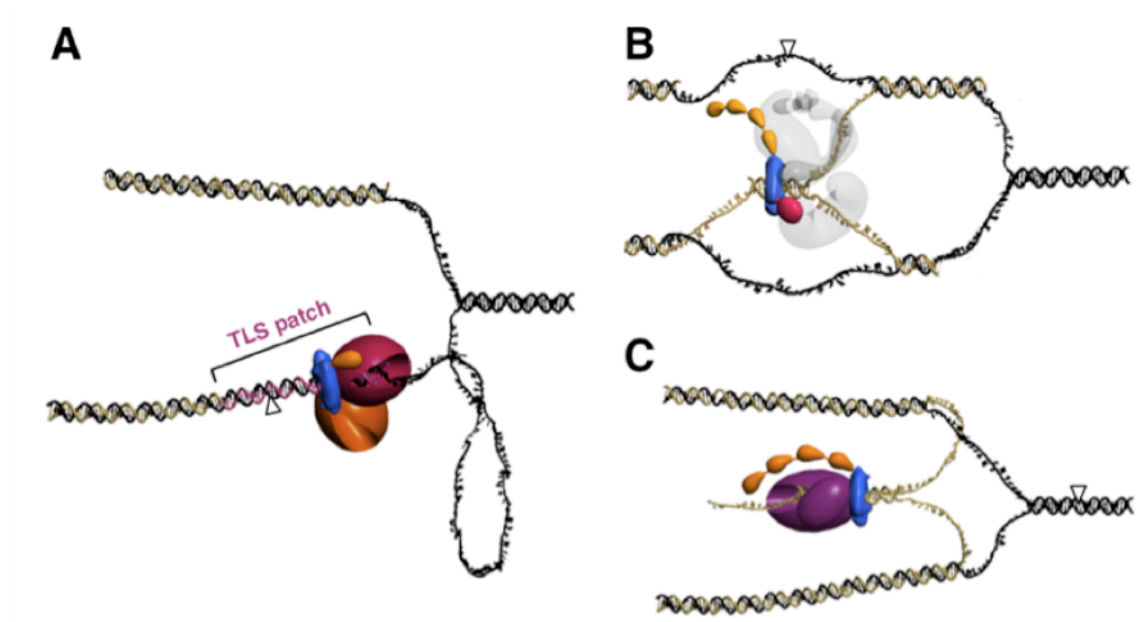


**Fig. 4: Model of *RAD6*-Mediated DDT Operating “on-the-fly”**

Three modes of DNA damage (arrowhead) bypass believed to be employed during *RAD6*-mediated DDT, all of which operate directly at stalled forks “on-the-fly” (coupled to the replication fork). Error-prone TLS (**A**) involves the recruitment of specialized polymerases (tyrian purple sphere) that directly recognize monoubiquitylated PCNA at the stalled fork. TLS polymerases engage only for short-track DNA synthesis (TLS patch). Error-free lesion bypass involves sister-chromatid recombination and is mediated by template switch formation (TS) (**B**) or fork regression (“chicken foot” structure) (**C**). PCNA is shown in blue, the replicative polymerase in orange, ubiquitin in light orange, and SUMO in crimson.

the prevailing view today is that DDT acts directly at the replication fork in S-phase (Andersen et al., 2008; Barbour and Xiao, 2003; Brnzei and Foiani, 2009; Budzowska and Kanaar, 2009; Chang and Cimprich, 2009; Lee and Myung, 2008; Prakash et al., 2005; Ulrich, 2009). In fact, PCNA ubiquitylation is believed to be physically coupled to the stalled fork (Davies et al., 2008; Ulrich, 2009; Yang and Zou, 2009), and PCNA modifications were reported to promote replication fork progression in frog egg extracts (Leach and Michael, 2005), yeast and humans (Bi et al., 2006; Vasquez et al., 2008). Moreover, since the helicase activity of yeast Rad5 appears to catalyze fork regression (also called reversal) *in vitro* (Blastyak et al., 2007), it was also suggested that Rad5 promotes template switching directly at the replication fork. These and several other studies led to the commonly accepted model that DDT is performed “on-the-fly”, employing TLS polymerases promoting “bypass replication” across the lesion (**Fig. 4A**), and the



error-free template-switching mode – either by sister chromatid junctions (SCJs; **Fig. 4B**) or fork regression leading to a DNA structure called “chicken foot” (**Fig. 4C**) – acting near the replication fork to promote replication restart similar to bacterial DDT.

The currently widely accepted model is at first glance appealing as it may superficially envision a swift rescuing mode for stalled forks. However, recent work has shown that a fraction of TLS can occur in the rear of the fork (Edmunds et al., 2008; Jansen et al., 2009a; Lopes et al., 2006) and that the *RAD6* pathway is not required for bulk DNA replication progression (Branzei et al., Nature 2008; Lopes et al., 2006). The issue of timing of DDT events is not only central from a mechanistic point of view, but also of singular general importance as DDT is highly crucial for cell survival upon DNA damage, genome stability and hence tumor biology (Myung and Smith, 2008).

### **II.3 Aim of this work**

Damaged DNA templates pose serious harm during replication and can be the cause of genome instability. In eukaryotes, tolerance of damaged DNA proceeds largely via the *RAD6* pathway, involving ubiquitylation of the DNA polymerase processivity factor PCNA. Whereas monoubiquitylation of PCNA mediates error-prone translesion synthesis (TLS), polyubiquitylation triggers an error-free recombination pathway.

For decades ongoing controversies about the timing, the DNA substrate, and the biological roles of DDT have dominated the field. On the one hand, the *RAD6* pathway was found essential for replication completion of damaged DNA, and on the other, there is evidence refuting any role for the *RAD6* pathway in fork progression in the presence of DNA damage. In parallel, DDT activation via PCNA ubiquitylation *per se* is believed to require proximal stalled forks and to occur at replication foci. Furthermore, the prominent *RAD6* component, Rad5 was shown to catalyze fork regression *in vitro*, suggesting it may also work

directly at stalled forks *in vivo*. This key issue remained unsettled, as it was thus far not directly tested when and in which phase of the cell cycle the *RAD6* DDT pathway has to operate.

The aim of this study was to address the timing and cell cycle specificity of *RAD6*-mediated DDT events in budding yeast and to attempt to identify new factors involved in error-free DDT. This information is anticipated to be helpful for the understanding of the DNA substrate and biological function of DDT throughout eukaryotes. Understanding the mechanistic actions and biological roles of DDT pathways is relevant for tumor biology, as well as evolution.

### III RESULTS

#### III.1 PCNA Ubiquitylation and DNA Replication

##### III.1.1 Role of Replication Forks in PCNA Ubiquitylation by the *RAD6* Pathway

DNA damage tolerance (DDT) mediated by the *RAD6* pathway is intrinsically connected to DNA replication. Indeed all DNA-damaging agents that trigger ubiquitylation of PCNA – despite their diverse chemistry – cause DNA replication stress during S-phase (Davies et al., 2008; Hoege et al., 2002). As replication stress is sensed in the form of ssDNA at stalled forks (Osborn et al., 2002) and the role of DDT is to promote replication completion (Branzei and Foiani, 2009), it is therefore believed that ubiquitylated PCNA is formed and must act directly at stalled replication forks near the site of the DNA damage (Ulrich, 2009). If proximal forks were indeed directly involved in PCNA modification, for example by docking or activating the PCNA ubiquitin ligases, there should exist fork components that when mutated result in reduced PCNA ubiquitylation in response to replication stress (Ulrich, 2009). A number of factors have been examined for a potential role in this modification. This led to the identification of DDK and RPA as essential replication fork components required for PCNA ubiquitylation (Davies et al., 2008), further suggesting DDT and DNA replication are physically linked.

However, several lines of evidence suggest that conclusions drawn from such approaches can easily be flawed. One major caveat is that mutation of replication factors may have secondary effects on PCNA modification, for instance by affecting global DNA replication. In fact, mutation of the DDK causes strong defects in the establishment of active replication forks (Bell and Dutta, 2002), which are indispensable for sensing replication stress (Byun et al., 2005), and thus for PCNA ubiquitylation (Brown et al., 2009). Moreover, a largely overlooked defect in replication progression caused by partial or complete

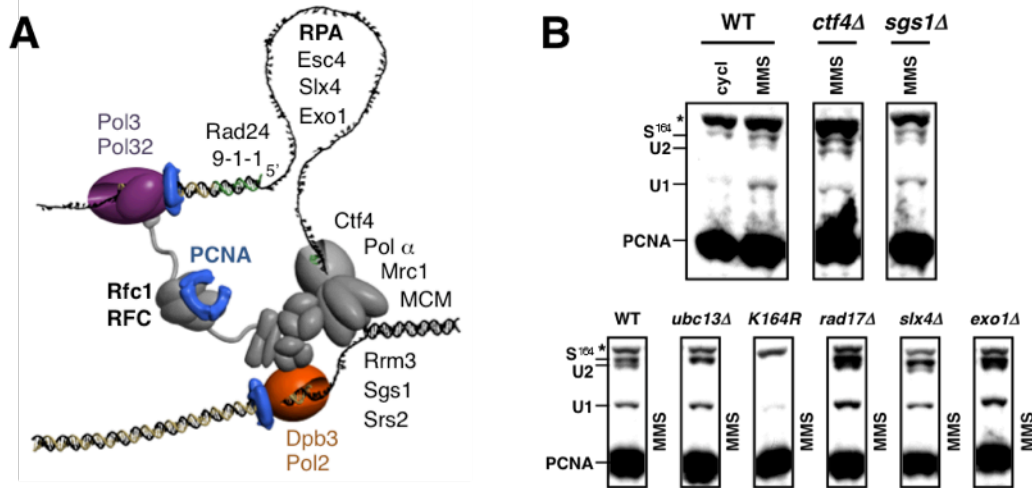


**Fig. 5: Summary of Replication Fork Components and their Role in PCNA Ubiquitylation**

**(A)** Replication factors in bold are physically required for PCNA ubiquitylation, while the rest are dispensable for this reaction (**B** and data not shown). Rfc1-RFC, required for loading of PCNA on chromatin; RPA, ssDNA-binding complex involved in lagging-strand synthesis and PCNA ubiquitylation; Dpb3, a subunit of DNA polymerase  $\epsilon$  that catalyzes leading-strand synthesis; Pol32, a subunit of DNA polymerase  $\delta$  (required for lagging-strand synthesis); MCM, replicative helicase complex essential for DNA replication, and functionally involved in PCNA modification (no evidence for a physical involvement) (Chang et al., 2006); Ctf4, an accessory factor of the priming DNA polymerase  $\alpha$ ; Mrc1, an MCM helicase regulatory cofactor and mediator of the replication checkpoint; Rrm3, Sgs1 and Srs2 are DNA helicases with functions at the fork; Esc4 chromatin silencing factor, 9-1-1 (Rad17, Mec3, Ddc1) clamp and its loader (Rad24-RFC), and Slx4 and Exo1 nucleases, involved in checkpoint signaling. RNA/iDNA primers catalyzed by the primase-Pol  $\alpha$  complex are depicted in green at the 5' end of each Okazaki fragment (upper strand).

**(B)** Examples of replication fork components and the effect of their deletion upon PCNA modification via ubiquitin and SUMO. Cultures of the indicated mutants were grown to mid-exponential phase, and aliquots were isolated for protein precipitation by the TCA method. The remaining cultures were treated with 0.02% MMS for 2 h before TCA protein precipitation. Cell extracts were run on 4-12% Bis-Tris NuPAGE gels and proteins were blotted on a PVDF membrane. PCNA modifications were visualized by Western blot using an anti-PCNA antibody (Hoege et al., 2002). Upper and lower panels originate from separate gels. Equal loading is verified by the cross-reactive band indicated by the asterisk (\*). S<sup>164</sup>- Mono-SUMOylated PCNA; U2- Di-ubiquitylated PCNA; U1- Mono-ubiquitylated PCNA on K164. K164R represents strains expressing the PCNA allele *pol30-K164R*.

depletion of RPA in yeast or humans (Davies et al., 2008; Niimi et al., 2008) is expected to result in reduced numbers of forks that encounter DNA damage at any time, possibly explaining why RPA appears to promote PCNA ubiquitylation *in vivo*, yet has no effect *in vitro* (Ulrich, 2009). Thus, it is reasonable to assume that the involvement of DDK and RPA in PCNA ubiquitylation (Bi et al., 2006;

Davies et al., 2008; Niimi et al., 2008) most likely reflects their crucial roles in DNA replication, and not a direct requirement of proximal forks or fork components for PCNA ubiquitylation.

Another enzymatic issue is the definition of a fork component. Repair proteins often operate at the fork in the presence of DNA damage (Herzberg et al., 2006; Moriel-Carretero and Aguilera, 2010), and replication core components participate in repair (Courcelle and Hanawalt, 2001; Hubscher, 2009; Ogi and Lehmann, 2006). Because there is no way to distinguish functions at the fork from those that act far from the fork, it is currently impossible to attribute the mechanics of PCNA ubiquitylation to events taking place directly at stalled forks.

Interestingly, from a large number of core and associated fork components (**Fig. 5A**) we found that most are actually dispensable for PCNA ubiquitylation upon MMS treatment (**Fig. 5B**, and data not shown). Even proteins that are seemingly important for this modification in humans and *X.laevis* (Gohler et al., 2008; Yang et al., 2008) apparently play a minor role in this reaction in budding yeast ((Ulrich, 2009) and data not shown). Replication factors that affect PCNA ubiquitylation seem to be rare, which challenges the investigation of the roles *RAD6* pathway at the fork.

### III.1.2 Loss of The Replication Fork Protein Pol32 Results in Spontaneous PCNA Ubiquitylation

Interestingly, we could find replication mutants inducing PCNA ubiquitylation in the absence of any exogenous DNA damage. This was surprising considering a potential requirement of stable forks for the reaction; therefore we decided to examine these mutants.

Deletion of Pol32, a subunit of the replicative DNA Pol  $\delta$  that is believed to synthesize the lagging-strand (Kunkel and Burgers, 2008; Stillman, 2008), results in the spontaneous appearance of slower migrating PCNA species (**Fig. 6**). To verify the identity of those species we analyzed PCNA modifications in cells

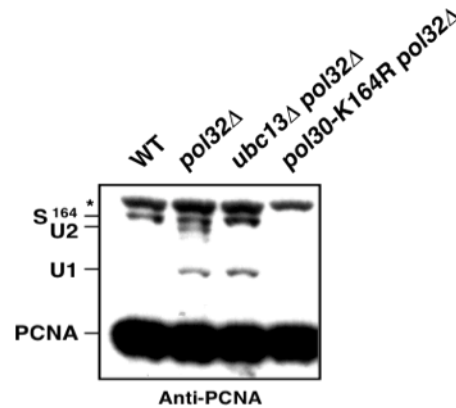


**Fig. 6: Activation of DDT in the Absence of Exogenous DNA Damage in Cells Lacking Pol32**

Cultures of the indicated mutants were grown at 30°C to the mid-exponential phase and samples were collected for protein precipitation by the TCA method. Cell extracts were probed with the anti-PCNA antibody. U2 band was lost by deletion of *UBC13*, while all visible modifications were eliminated by replacement of the endogenous gene for PCNA (*POL30*) with the *pol30-K164R* allele, encoding a PCNA variant that cannot be modified in a *RAD6*-dependent manner (Hoege et al., 2002). Equal loading was verified by the cross-reactive band indicated by the asterisk (\*).

lacking Pol32 in addition to various components of the *RAD6* pathway. We found the di-ubiquitylated PCNA “U2” species is lost upon deletion of *UBC13* (**Fig. 6**), encoding the Ubc enzyme, Ubc13, that is essential for the formation of K63-ubiquitin chains (Hofmann and Pickart, 1999). Furthermore, all detected PCNA modifications (ubiquitylated “U1”, “U2”, and SUMOylated “S<sup>164</sup>” species) required lysine 164 (K164) of PCNA (**Fig. 6**). Because PCNA is ubiquitylated on chromatin (Pfander, 2005) this suggests that in *pol32*Δ cells the Rad18-Rad6 and Rad5-Ubc13-Mms2 complexes localize on chromatin. Understanding the underlying defect that leads to this unusual phenotype in *pol32*Δ cells could provide valuable insights into the mechanism of PCNA modification and DDT activation in yeast.

### III.1.3 Pol32 Does Not Function as an Enzymatic Inhibitor of PCNA Ubiquitylation

A possible explanation for the spontaneous PCNA ubiquitylation in *pol32*Δ is that Pol32 may function as an enzymatic inhibitor of the *RAD6* ubiquitylation machinery. The idea for this hypothesis stems from the observation that the

human cell cycle inhibitor p21<sup>Cip1/Waf1</sup> is able to sterically inhibit PCNA monoubiquitylation through its PCNA-interacting protein (PIP-box) motif (Soria et al., 2006). Pol  $\delta$  in budding yeast consists of three subunits: two essential Pol3/Cdc2 and Pol31/Hys2, and a non-essential subunit Pol32 (Gerik et al., 1998) – at least two of which (Pol3 and Pol32) bear characteristic PIP-box motifs (Johansson et al., 2004). Association between Pol32 and PCNA could prevent the modification of the latter via occlusion of the Rad18 and Rad5 docking sites on PCNA.

If the above mechanism were true, then overproduction of Pol32 should impair PCNA ubiquitylation in response to replication stress. However, this is not the case *in vivo*, as cells overproducing Pol32 (>10-fold) exhibit efficient mono and polyubiquitylation of PCNA after MMS treatment (**Fig. 7A**; compare U1 and U2 bands between lanes 1 and 2). Furthermore, Pol32 overproduction does not affect the interaction between PCNA and Rad18 or Rad5 in yeast two-hybrid (**Fig. 7B**). Thus, Pol32 may not sterically inhibit ubiquitylation of PCNA. On the contrary, Pol32 overproduction appears to stabilize ubiquitylated PCNA with a strong preference towards the monoubiquitylated species (**Fig. 7A**; compare U1 band among lanes 1 and 2), which becomes visible even in the absence of MMS treatment (**Fig. 7A**; lanes 3 and 4). Because, overproduction of the anti-recombinogenic helicase Srs2 stabilizes the SUMOylated form of PCNA by binding to it (Pfander et al., 2005), the effects of Pol32 overproduction may be – in analogy to Srs2 – caused by coexistence of Pol32 and monoubiquitylated PCNA in the same complex. In support of this view, Pol32 is functionally linked to monoubiquitylated PCNA, both of which are required for error-prone DDT (Huang et al., 2000; Huang et al., 2002). Furthermore, overproduction of the TLS polymerase Rad30, which is also involved in error-prone DDT, induces PCNA monoubiquitylation as well (**Fig. 7C**). These results bring forward two conclusions. First, Pol32 is not an enzymatic inhibitor of PCNA ubiquitylation, although its overproduction was sufficiently high to have an effect. Second, Pol32 is a component of the active TLS polymerase “effector” that contains Rad30 and

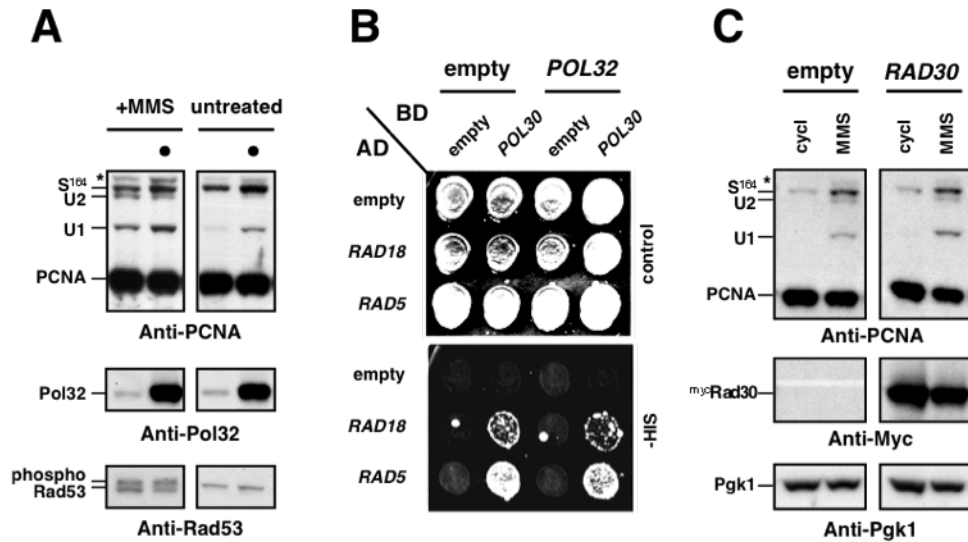


**Fig. 7: Pol32 Does Not Function as an Enzymatic Inhibitor of PCNA Ubiquitin Conjugation.**

(A) Overproduction of Pol32 does not block PCNA ubiquitylation. The effect of Pol32 dose on PCNA modifications was assessed in the presence (left panel) or absence of 0.02% MMS (right panel). Ylp211-empty (strain YGK1544) or containing *POL32* under the control of *ADH1* promoter were integrated at the *URA3* genomic locus, and strains with high levels of Pol32 (•), detected by a specific antibody against the endogenous protein (Lucian Moldovan PhD Thesis) were selected (strain YGK1545). The signal corresponding to phosphorylated Rad53 (Phospho) was used to control for MMS treatment and loading.

(B) Yeast two-hybrid interactions between PCNA and the ubiquitin ligases of the *RAD6* pathway remain unaffected by high levels of Pol32. Strains YGK1544 (empty) and YGK1545 (*POL32*) were transformed with the indicated vectors and spotted on SC-Trp-Leu (control) or SC-Trp-Leu-His plates (-HIS). Plates were scanned after 4 days at 30°C.

(C) Overproduction of Rad30 induces mono- but not poly-ubiquitylation of PCNA. *mycRad30* was expressed under the *GAL* promoter by growth of strains YGK1544 and YGK797 in YP media supplemented with 2% galactose. MMS treatment was done as in (A). Pgk1 signal was used as loading control.

monoubiquitylated PCNA (Acharya et al., 2009). Undoubtedly, Pol32 cannot be envisioned as a steric inhibitor of *RAD6*-mediated DDT in cells.

#### III.1.4 Defects in DNA Replication Trigger PCNA Ubiquitylation in *pol32Δ* Cells

An alternative explanation for the increased PCNA ubiquitylation in the absence of Pol32 is that loss of this protein results in replication defects that resemble those induced by DNA lesions. Notably, Pol32 is found associated with Pol  $\delta$  (Gerik et al., 1998). To test whether spontaneous PCNA ubiquitylation in



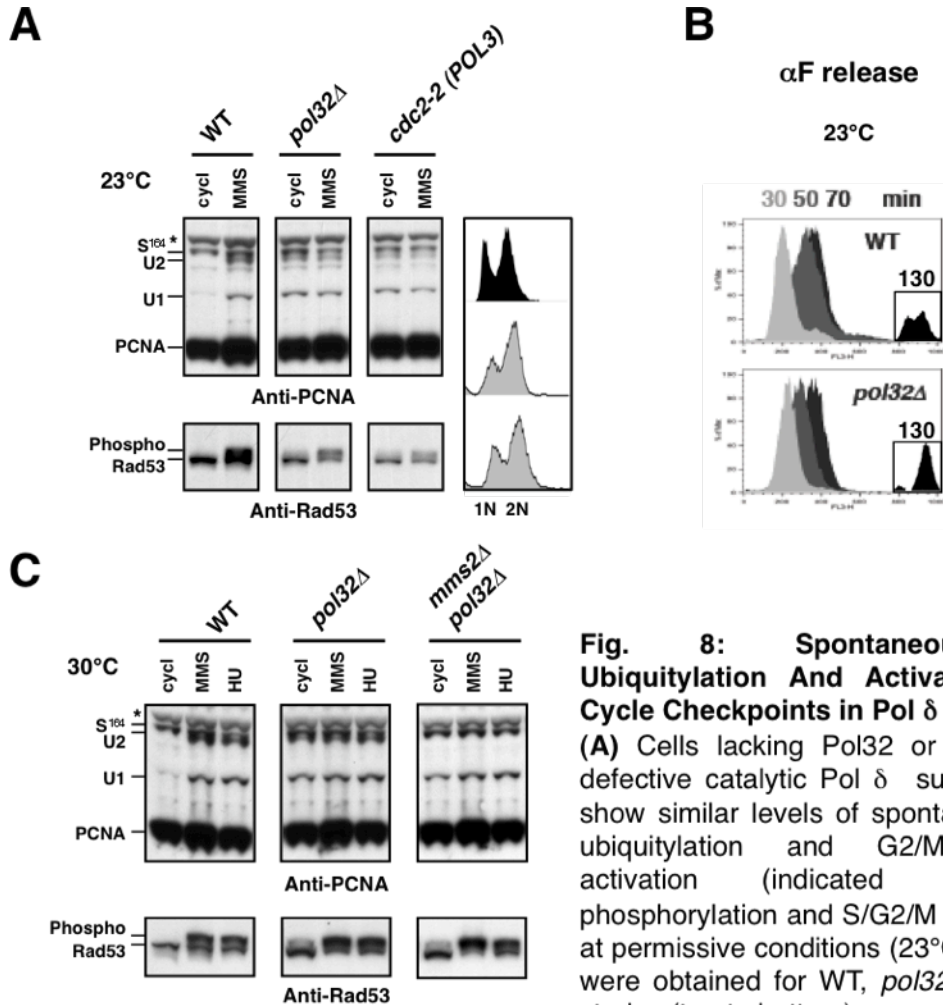


**Fig. 8: Spontaneous PCNA Ubiquitylation And Activation of Cell Cycle Checkpoints in Pol  $\delta$  Mutants**

(A) Cells lacking Pol32 or expressing a defective catalytic Pol  $\delta$  subunit (*cdc2-2*) show similar levels of spontaneous PCNA ubiquitylation and G2/M checkpoint activation (indicated by Rad53 phosphorylation and S/G2/M delay) already at permissive conditions (23°C). FACS data were obtained for WT, *pol32Δ* and *cdc2-2* strains (top to bottom).

(B) Replication in the absence of Pol32 triggers the S- and G2/M phase checkpoints. Early-exponential Cultures were arrested by a-factor in G1 and released at 23°C (see Experimental Procedures). *pol32Δ* cells exhibit distinct S-phase (50 min post-release) and G2/M (130 min post-release; lower right panels) delays. For (A) and (B) cells were stained for DNA content with propidium iodide (PI).

(C) Exogenous replication stress does not further induce ubiquitylation of PCNA in *pol32Δ*. Cultures at the mid-exponential phase (cycl; 30°C) were treated with 0,02% MMS (MMS) or 200mM hydroxyurea (HU) for 2 h, and whole cell extracts were analyzed by Western blot against PCNA and Rad53. PCNA ubiquitylation levels that accumulate spontaneously in *pol32Δ* (lane 7) are comparable to those induced in WT cells by MMS (lane 2) or HU (lane 3). PCNA SUMOylation (at K164; S<sup>164</sup>) is not affected by the absence of *POL32*.

*pol32Δ* can be attributed to the functionality of the Pol  $\delta$  holoenzyme, we assessed PCNA modifications in cells expressing Pol  $\delta$  mutants. The functionally compromised *cdc2-2* allele encodes a temperature sensitive mutant of the

catalytic subunit of Pol  $\delta$ , Pol3/Cdc2 (Blank et al., 1994; Blank and Loeb, 1991; Hartwell and Smith, 1985). We found *cdc2-2* mutants – containing an intact *POL32* locus – induced PCNA mono and polyubiquitylation spontaneously already growing at permissive conditions, similarly to *pol32 $\Delta$*  cells (**Fig. 8A**; compare lanes 1, 3 and 5). We observed the same effect in a strain harboring the catalytic site mutation Y708A on Pol3/Cdc2 (data not shown), recently reported to induce PCNA monoubiquitylation in budding yeast (Northam et al., 2006). Thus we conclude that faulty Pol  $\delta$  activity, rather than the loss of a polymerase subunit, is the cause for spontaneous PCNA ubiquitylation in Pol  $\delta$  mutants.

Pol  $\delta$  is an essential component of the replication fork with a prominent role in DNA replication (Nick McElhinny et al., 2008; Waga and Stillman, 1998). Defects during DNA synthesis are sensed by the components of cellular checkpoint pathways that delay the cell cycle, thereby assisting in the correct completion of chromosomal replication (Branzei and Foiani, 2010). In support of the view that Okazaki fragment synthesis is encumbered in *pol32 $\Delta$*  and *cdc2-2*, both mutant strains have a prolonged S/G2/M phase (**Fig. 8A**; right panel). Moreover, *pol32 $\Delta$*  cells progress slowly through S-phase (**Fig. 8B**; compare the time-point 50 min after synchronous release). In addition, both *pol32 $\Delta$*  and *cdc2-2* mutants exhibit spontaneous phosphorylation of the checkpoint kinase Rad53 (**Fig. 8A**; lower panels, compare lanes 1, 3 and 5, and **Fig. 8C**; compare lanes 1 and 4) accompanied by a strong delay in G2/M (**Fig. 8B**; lower right corner), indicative of an activated G2/M checkpoint. These observations indicate that both S-phase and G2/M checkpoints are activated due to defective DNA synthesis by Pol  $\delta$ .

In agreement with this conclusion, defective Pol  $\delta$  activity was shown to provoke the accumulation of ssDNA *in vivo* (Fukui et al., 2004), and PCNA-Pol  $\delta$  complexes lacking Pol32 (PCNA-Pol  $\delta^*$ ) are far less stable or processive *in vitro* than normal (Burgers and Gerik, 1998; Johansson et al., 2004; Masuda et al., 2007). Along those lines, PCNA ubiquitylation in *pol32 $\Delta$*  was similar to wild-type

cells that had been challenged by exogenous DNA damage, and could not be further enhanced by MMS or hydroxyurea (HU), a drug that induces fork stalling (**Fig. 8A and 8C**). This indicates that the underlying defect is neither sporadic nor restricted to specific genomic loci, but rather concerns a large majority of replication forks (or Okazaki fragments). Importantly, loss of *RAD6*-mediated DDT in *pol32Δ* did not affect spontaneous G2/M checkpoint activation (**Fig. 8C**; compare Rad53 phosphorylation in lanes 4 and 7, and data not shown), in support of the current model that checkpoint activation and modification of PCNA proceed uncoupled from and parallel to each other (Chang and Cimprich, 2009; Ulrich, 2009). Taken together, these findings strongly suggest that *pol32Δ* cells accumulate un-replicated ss-gaps during Okazaki fragment synthesis in S-phase, which directly trigger PCNA ubiquitylation and S/G2/M checkpoint activation.

Thus, DNA replication in the absence of Pol32 becomes discontinuous and triggers DDT in a manner very similar to the presence of replication-blocking agents, possibly involving the accumulation of stalled forks.

### **III. 2 PCNA Ubiquitylation And The Cell Cycle**

#### **III.2.1 Role of Pol32 in Error-Free DDT Becomes Prominent at Low Temperatures**

Although loss of Pol32 is comparable to treatment with high doses of DNA damaging agents, it has surprisingly minor effects on cell viability. Yet, it has been noted previously that conditional mutants of several essential DNA replication components arrest in late-S or G2/M at restrictive conditions (Amin and Holm, 1996). Although *POL32* is not essential, *pol32Δ* cells stop growing at low temperatures (12-18°C) and accumulate in late-S/G2/M with non-segregated chromosomes (**Fig. 9A**; 14°C, and (Gerik et al., 1998; Huang et al., 1997; Huang et al., 2000)). This cold-sensitivity is accompanied by a dramatic increase of phosphorylated Rad53 (**Fig. 9B**), suggesting that Pol δ\* (Pol δ lacking Pol32) is further compromised at low temperatures.

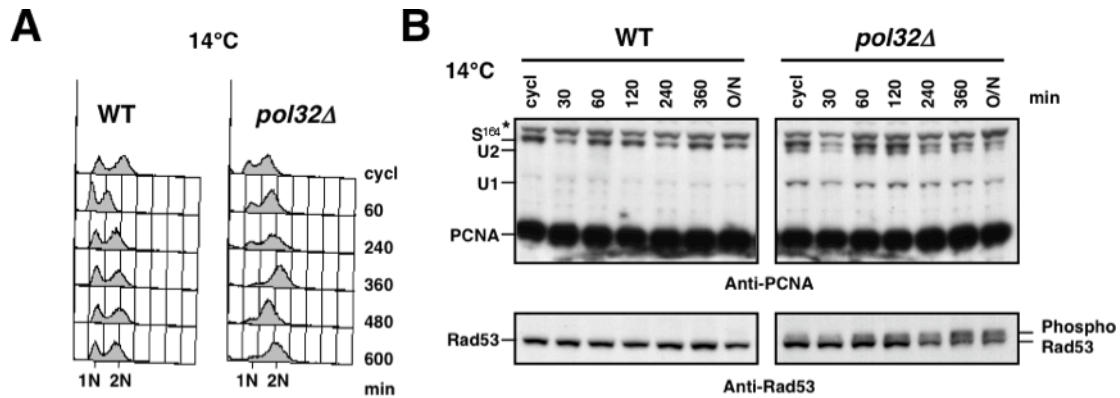


**Fig. 9: G2/M Checkpoint Activation in *pol32Δ* Mutants at Restrictive Temperatures**

**(A)** *pol32Δ* cells accumulate in G2/M at restrictive temperatures. Cultures were grown at permissive conditions (30°C; cycl) and were subsequently shifted to 14°C. At the indicated time-points (O/N = over night) samples were collected and analyzed by FACS using PI staining.

**(B)** Phosphorylated Rad53 accumulates at restrictive temperatures in *pol32Δ*. Cultures were treated as in (A) and analyzed by Western blot using antibodies specific for PCNA and Rad53. Cells lacking *POL32* show increased PCNA ubiquitylation (U1, U2) and Rad53 phosphorylation (30%; see Experimental Procedures) already at non-restrictive temperatures. Note that more than half of the Rad53 population is in the phosphorylated form (Phospho) after 360 min at 14°C, while the level of SUMOylated PCNA (at K164; S<sup>164</sup>) dropped to 50% of the initial value but the level of di-ubiquitylated PCNA (U2) remained essentially unaffected.

Interestingly, the heat sensitivity of certain Pol  $\delta$  mutants partially depends on modification of PCNA by ubiquitin (Branzei et al., 2004; Branzei et al., 2002; Giot et al., 1997; Vije Motlagh et al., 2006). We thus examined whether the cold-sensitivity of *pol32Δ* cells can also be attributed to PCNA modification. Interestingly, we found that deletion of *RAD6* pathway members involved in PCNA ubiquitylation, or altered K164 on PCNA efficiently suppressed the cold-sensitivity of *pol32Δ* (**Fig. 10A**; two rightmost panels). This rescue effect is also reflected at the reduced levels of phosphorylated Rad53 in *ubc13Δ pol32Δ* cells that lack the ability to polyubiquitylate PCNA (**Fig. 10B**). We therefore conclude that the cold-sensitivity of *pol32Δ* cells largely depends on PCNA polyubiquitylation. This finding provides us with a useful genetic tool to study the timing and function of polyubiquitylated PCNA.

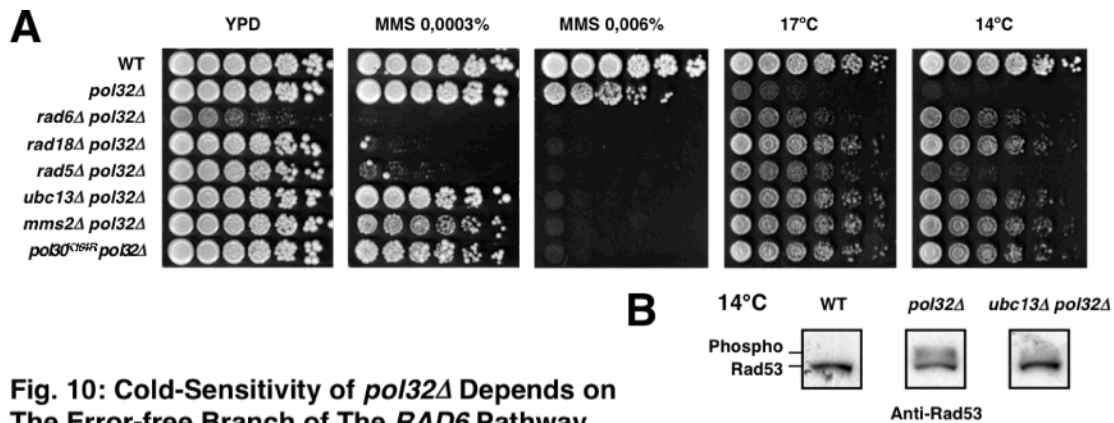


**Fig. 10: Cold-Sensitivity of *pol32Δ* Depends on The Error-free Branch of The *RAD6* Pathway**

**(A)** Deletion of *RAD6* pathway members (*rad6Δ*, *rad18Δ*, *rad5Δ*, *ubc13Δ*, *mms2Δ*) or elimination of the ubiquitylation site of PCNA (*pol30<sup>K164R</sup>*) suppresses the cold-sensitivity of *pol32Δ* cells. Serial 1:5 dilutions of the indicated strains were spotted on YPD-agar plates with or without the indicated amounts of MMS and scanned after incubation at 30°C (for 2,5 days), 17°C (5 days), or 14°C (16 days). Mutants lacking *POL32* require the *RAD6* pathway for resistance to MMS (second and third panels) and for reduced growth at low temperatures (last two panels). Note that deletion of *RAD6* leads to a synthetic slow growth defect of *pol32Δ*. On the other hand, *rad6Δ* is a better suppressor of the cold-sensitivity of *pol32Δ* than *rad5Δ* (14°C panel; compare rows 2, 3 and 5 from the top), indicating that Rad5 may additionally contribute to the rescue.

**(B)** Polyubiquitylated PCNA potentiates the G2/M checkpoint in *pol32Δ* at restrictive temperatures. Cells were grown at 30°C to early-logarithmic phase and shifted to 14°C in the presence of nocodazole for 7 h before TCA sample collection. G2/M arrest by nocodazole was verified microscopically, and was used in order to keep populations into a comparable cell cycle phase. Total cell extracts were probed with anti-Rad53.

### III.2.2 Ubiquitylated PCNA Persists Beyond S-Phase

By using the cold-sensitivity of *pol32Δ* cells we could now address when during the cell cycle polyubiquitylated PCNA normally operates. Because ubiquitylated PCNA is believed to act at stalled replication forks, we expected to find that this phenotype would be coupled to S-phase. For this purpose, we arrested *pol32Δ* cells in metaphase/early anaphase using the microtubule poison nocodazole at permissive conditions, and allowed them to complete the cell cycle at restrictive temperatures by removal of the drug. We noticed that full activation of the G2/M checkpoint (used as a measure of cold-sensitivity) occurred with a very long delay (4-6 hours, **Fig. 11**; lanes 2-4), suggesting the cause of the cold-sensitivity may not originate in G2/M. Indeed, releasing a parallel culture from



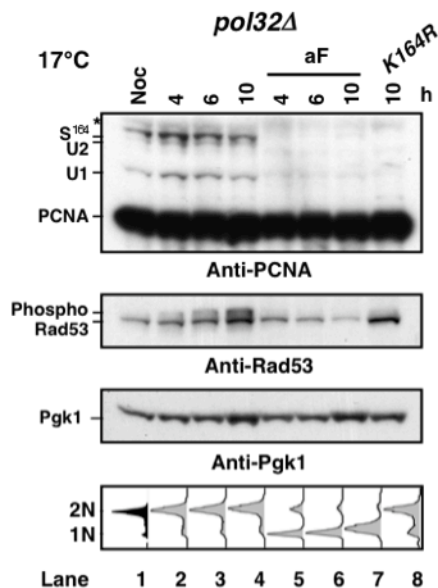


**Fig. 11: *RAD6*-Dependent Checkpoint Activation in *pol32Δ* Requires Passage Through S-phase**

Cells arrested in G2/M by nocodazole treatment were rapidly released and grown at 17°C in the absence (lanes 2-4) or presence of 10 $\mu$ M  $\alpha$ -factor (lanes 5-7). Samples were withdrawn after 4, 6 or 10 h and analyzed by Western blot (Pgk1 used for loading control) and FACS (lower panel). Unlike PCNA ubiquitylation (lane 1), full activation of the DNA damage checkpoint (Rad53 phosphorylation and G2/M arrest) occurred only 4-6 h after release at 17°C (lanes 2-4). Release into  $\alpha$ -factor-containing medium (lanes 5-7) arrested the majority of *pol32Δ* cells in G1 (FACS, bottom panel) before checkpoint activation could occur, indicating that cells have to engage in DNA replication at restrictive temperatures to trigger a full checkpoint response. Cells defective in PCNA ubiquitylation (*pol30<sup>K164R</sup>*) did not trigger a full checkpoint response even though they passed through S-phase (lane 8). DNA was stained with SYTOX.

nocodazole arrest in the presence of the mating pheromone  $\alpha$ -factor resulted in G1 arrest at restrictive conditions (**Fig. 11**; lanes 5-7). This indicates that *pol32Δ* cells must pass through S-phase at non-permissive temperatures in order to trigger a full checkpoint response. As expected, mutation of K164 of PCNA abolished full checkpoint activation, even when cells lacking *POL32* were allowed to pass through S-phase (**Fig. 11**; lane 8). These results suggest that the function of polyubiquitylated PCNA is likely responsible for exacerbating the processivity defects of Pol  $\delta^*$  at restrictive temperatures, a function that appears to be largely S-phase-coupled. In agreement with this interpretation, both mono and polyubiquitylated PCNA appear already early during S-phase in *pol32Δ* cells synchronously growing at low temperatures (**Fig. 12A**; lane 4).

Surprisingly, the levels of ubiquitylated PCNA in synchronous *pol32Δ* cells do not correlate with the measured DNA replication activity. Although, in budding yeast most of DNA is replicated early in S-phase (Raghuraman et al., 2001), ubiquitylated PCNA peaks late in S-phase (as judged by FACS analysis and Clb2

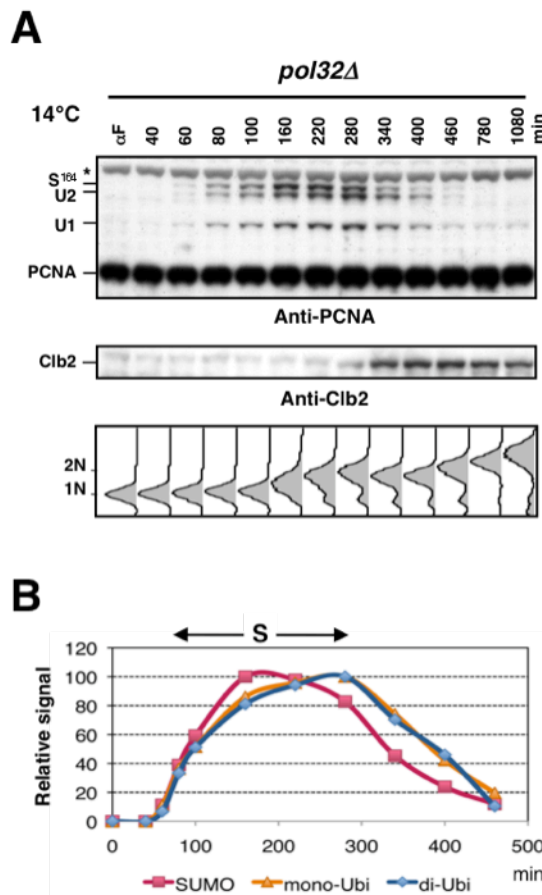


**Fig. 12: Ubiquitylated PCNA Persists Until G2/M in *pol32Δ* Cells**

(A and B) Exponentially growing cultures were arrested in G1 with  $\alpha$ -factor, released from the arrest for synchronous growth and grown at 14°C (see Experimental Procedures). At the indicated time-points samples were prepared for Western blot (two upper panels; anti-PCNA and anti-Clb2), and FACS (bottom panel of (A)). First time-point ( $\alpha$ F) was collected immediately after release from  $\alpha$ -factor. (A) Cells lacking Pol32 exhibit spontaneous PCNA ubiquitylation during S-phase (80-280 min; determined by FACS analysis), which peaks late in S-phase (280 min) and persists until G2/M (340-400 min post-release; determined by Clb2 accumulation). (B) Fluctuation of mono-SUMOylated PCNA on K164 (crimson squares), mono- (orange triangles) and di-ubiquitylated (blue diamonds) PCNA species during the cell cycle of *pol32Δ* cells growing at restrictive conditions. Values were derived from quantification of (A) (see Experimental Procedures). The cross-reactive band indicated by the asterisk was used as loading-control. Note that levels of SUMOylated PCNA decay faster than those of ubiquitylated PCNA. DNA was stained with PI.

accumulation) at restrictive temperatures (**Fig. 12A**; 280 min post-release from  $\alpha$ -factor). Interestingly, a substantial fraction of ubiquitylated PCNA (70% of time-point 280 min post-release) persisted in G2/M at 14°C (**Fig. 12A and 12B**). However, because S-phase completion was not directly measured, we needed other assays to verify our conclusion. In order to determine S-phase completion more directly, we utilized the property of S-phase chromosomes to be irresolvable by pulse-field gel electrophoresis (PFGE) (Lengronne et al., 2001), a property attributed to the conformation of actively replicating chromosomes. Indeed, we found that *pol32Δ* cells had largely completed bulk DNA replication by the time that cells still accommodate ubiquitylated PCNA in G2/M (**Fig. 13**). We obtained support for this conclusion when we analyzed by 2D gel electrophoresis

replication intermediates at the late-replicating rDNA locus (Brewer et al., 1980). We observed that bulk DNA replication was efficiently completed (> 80%) in *pol32Δ* cells at restrictive conditions (**Fig. 14A**; upper panel). Notably, we could also detect persistent ubiquitylated PCNA in G2/M at permissive temperatures (**Fig. 11**; lane 1), as well as in wild-type cells that initiated synchronous DNA replication after short exposure to HU or MMS (data not shown and see section III.5). Although SUMOylated PCNA initially accumulated in parallel to ubiquitylated PCNA in S-phase, it vanished much faster (**Fig. 12A and 12B**), in agreement with the notion that PCNA SUMOylation may primarily act near replication forks (Pfander et al., 2005). By contrast, the observed persistence of ubiquitylated PCNA beyond S-phase suggests that if these molecules are not simple byproducts of completed DDT reactions, they may play active roles far behind or even fully uncoupled of advancing replication forks.

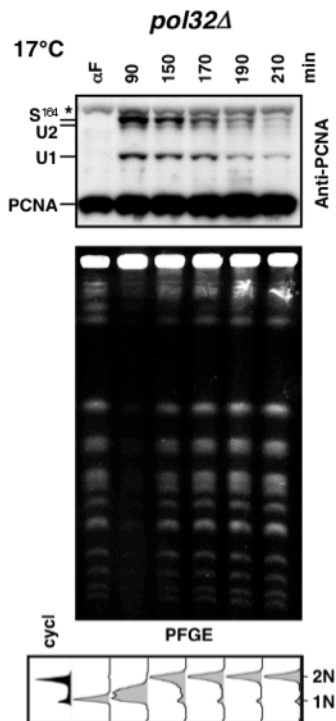


**Fig. 13: Ubiquitylated PCNA Persists Beyond S-Phase in *pol32Δ* Cells**

Exponentially growing cells arrested by  $\alpha$ -factor and released in YPD at 17°C were collected for Western blot, PFGE, and FACS analysis. *pol32Δ* cells show significant PCNA ubiquitylation still 190 min after  $\alpha$ -factor release (top panel) at a time when chromosomes have already been replicated (PFGE, middle panel) and passed S-phase (FACS, bottom panel). Note that replicating chromosomes (at 90 min post release) cannot enter the PFGE gel (Lengronne et al., 2001). DNA was stained with SYTOX.



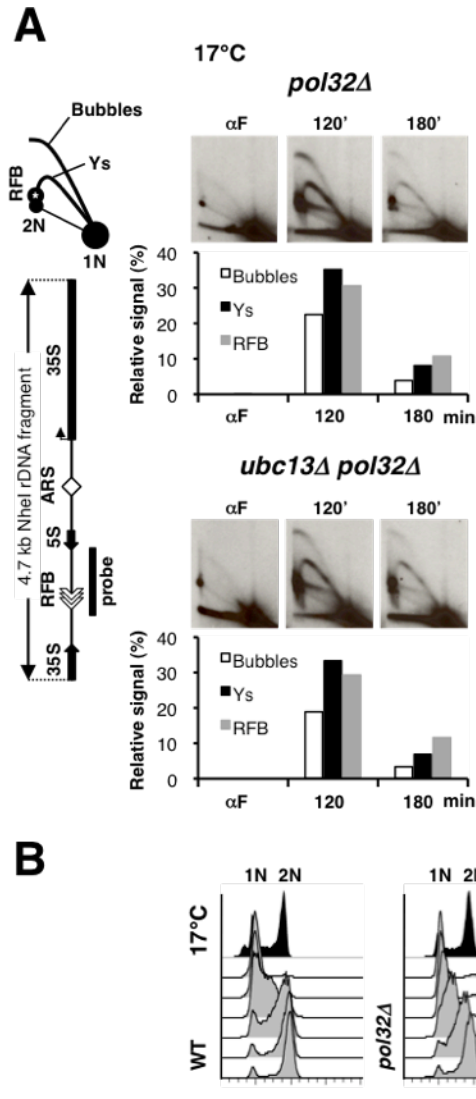


**Fig. 14: Ubiquitylated PCNA Is Not Required for The Progression of Replication Forks in *pol32Δ***

**(A and B)** Exponentially growing cells arrested by  $\alpha$ -factor and released in YPD at 17°C were collected for FACS, and 2D gel analysis. **(A)** Replication of a late-replicating locus in *pol32Δ* cells is not affected by loss of PCNA polyubiquitylation. Genomic DNA was isolated from strains YGK1295 (*bar1Δ pol32Δ*) and YGK1297 (*bar1Δ ubc13Δ pol32Δ*), digested with *NheI*, and analyzed by 2D gel with a probe specific for the rDNA locus. Definitions of quantified signals and probe genomic location are depicted in the schematic *NheI* restriction digest on the left. Asterisk indicates the replication fork barrier (RFB). **(B)** S-phase delay (assayed by FACS) of *pol32Δ* and *pol32Δ* cells additionally defective in PCNA ubiquitylation (*pol32Δ ubc13Δ*, *pol32Δ pol30<sup>K164R</sup>*). Note that the S-phase delay is not affected by the loss of PCNA ubiquitylation. DNA was stained with SYTOX.

### III.2.3 Ubiquitylated PCNA Is Not Required for S-Phase Progression in The Presence of DNA Damage

Although the *RAD6* pathway is currently believed to facilitate replication progression by promoting the restart of stalled forks (Barbour and Xiao, 2003), the evidence for this conclusion is not compelling. In addition, since our findings point to a role of PCNA ubiquitylation beyond S-phase, we decided to revisit this issue.

We first addressed this question by using the *pol32Δ* mutation to induce faulty replication. As we described above, *pol32Δ* cells experience spontaneous

replication stress and progress slowly through S-phase. If the *RAD6* pathway had a role in bulk S-phase completion in these cells, then *RAD6* mutants would be expected to accumulate replication intermediates. However, deletion of *UBC13* (required for PCNA polyubiquitylation) did not affect the levels of replication intermediates in late-S or G2 in *pol32Δ* cells growing at non-permissive conditions (eg. the “Y” structures that represent Y-shaped replication forks measured at the rDNA locus **Fig. 14A**), as shown by 2D gel analysis (**Fig. 14A**; compare upper with lower panels). Moreover, S-phase progression remained apparently unaffected in *pol32Δ* cells additionally defective in PCNA ubiquitylation (**Fig. 14B**). These findings clearly indicate that a functional *RAD6* pathway is not needed for normal S-phase progression in the presence of *pol32Δ*-induced replication stress, and that the cause of the cold-sensitivity of these cells is not an enhanced accumulation of stalled forks.

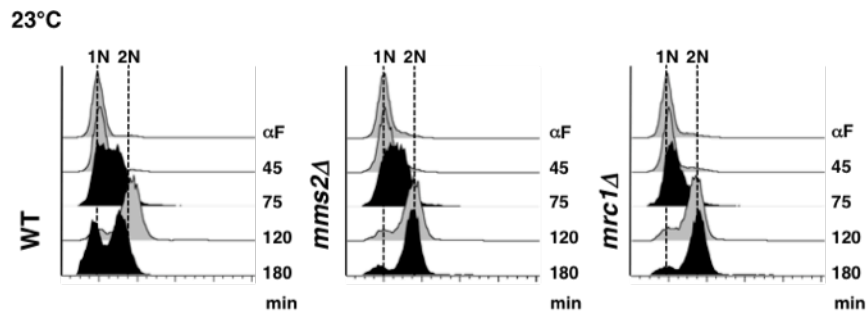


**Fig. 15: DDT Is Not Involved in Bulk DNA Replication Completion of Damaged Chromatin**

Polyubiquitylated PCNA is not required S-phase progression of MMS-treated cells. Synchronously growing cultures of the indicated strains were released from  $\alpha$ -factor after treatment with 0,02% MMS for 1 h at 23°C (see scheme at the top and Experimental Procedures). Samples were collected and analyzed by FACS (PI staining). Cells lacking *MMS2* progress through S-phase indistinguishably from WT cells, but exhibit a G2/M delay. Cells lacking *MRC1*, a non-essential component of the replication fork, exhibit both S-phase (Szyjka et al., 2005) and G2/M delays and were chosen as positive control.

Because DNA replication in the absence of Pol32 may be distinct from DNA replication in the presence of MMS or HU (Komata et al., 2009), we addressed the role of the *RAD6* pathway in DNA replication challenged by these chemicals. In fact, ubiquitylated PCNA was not important for replication of chromatin containing MMS-induced lesions (**Fig. 15** and see Section III.5). We

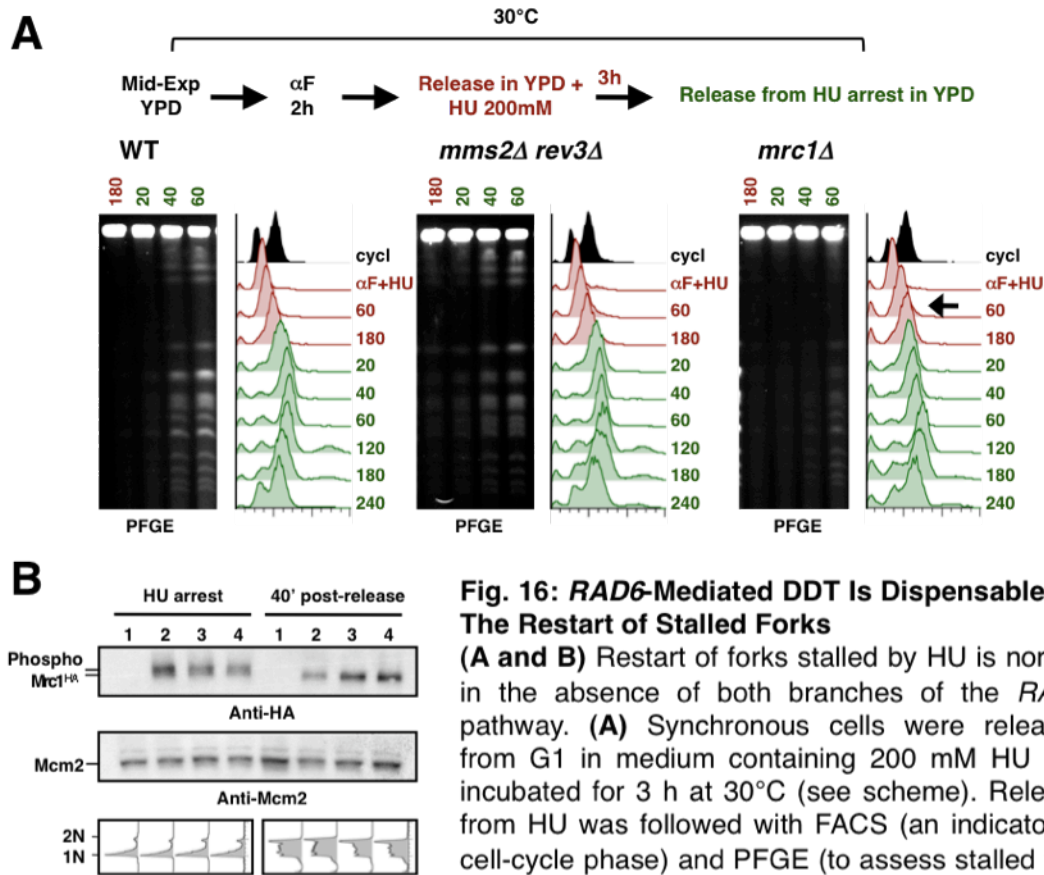


**Fig. 16: *RAD6*-Mediated DDT Is Dispensable for The Restart of Stalled Forks**

**(A and B)** Restart of forks stalled by HU is normal in the absence of both branches of the *RAD6* pathway. **(A)** Synchronous cells were released from G1 in medium containing 200 mM HU and incubated for 3 h at 30°C (see scheme). Release from HU was followed with FACS (an indicator of cell-cycle phase) and PFGE (to assess stalled fork restart). Note that cells that lack Mrc1, which are deficient in S-phase checkpoint signaling, progress faster through S-phase in the presence of HU (arrow), but are unable to complete replication in a time. **(B)** Mrc1 phosphorylation, a marker for stalled forks, decays normally in DDT mutants. Exponentially growing cells expressing Mrc1<sup>HA</sup> (lanes 2 (WT), 3 (*ubc13Δ*) and 4 (*pol30<sup>K164R</sup>*)) were arrested in early S-phase by HU (75 mM for 1 h at 30°C), washed in YPD and then allowed to recover at 30°C for 40 minutes. Cell extracts were run on 6% Tris-glycine gels and analyzed by Western blot against the anti-HA and anti-Mcm2 antibodies (used as loading control). Lower panel shows FACS results for the same samples. DNA was stained with PI in (A) and SYTOX in (B).

also addressed this issue in cells challenged with HU. For this purpose we released synchronous cultures from G1 arrest into HU-containing medium to induce maximal accumulation of stalled forks. Subsequently we removed the HU washing the cells in fresh medium and allowed them to recover (**Fig. 16A**; see scheme). Using PFGE we could assess the time needed for replication completion (see section III.2.2), and found that it was 40 minutes in wild-type cells under our conditions (**Fig. 16A**). Cells lacking the non-essential replication factor Mrc1 showed a delay in the appearance of replicated chromosomes by

PFGE (Tourriere et al., 2005), but DDT-deficient cells (*mms2Δ rev3Δ*) behaved like wild-type cells (**Fig. 16A**). Furthermore, attenuation of phosphorylated Mrc1, a marker of stalled forks (Osborn and Elledge, 2003), and S-phase progression (visualized with FACS) occurred normally after HU-release of cells unable to polyubiquitylate (*ubc13Δ*) or at all ubiquitylate PCNA at K164 (*pol30-K164R*) (**Fig. 16B**). These findings are directly in contrast to the standing view that ubiquitylated PCNA operates at stalled forks in order to promote their restart.

In line with our finding that the *RAD6* pathway is not required for the restart of stalled forks and S-phase progression, TLS polymerases were found dispensable for replication of UV-damaged chromatin in yeast, and TLS mutants are known to leave ss-gaps behind the advancing forks (Lopes et al., 2006). Moreover, deletion of *RAD18* does not cause the accumulation of replication intermediates in MMS treated cells (Branzei et al., 2008), but instead triggers the G2/M checkpoint (Hishida et al., 2009). We could also observe increased G2/M checkpoint activation in cells lacking *RAD5* (see Section III.5) or *MMS2* (**Fig. 15**). Altogether these data strongly suggest that *RAD6*-mediated DDT does not promote S-phase progression or stalled fork restart, but rather controls the sealing of ss-gaps (gap-filling) left behind active forks.

### III. 3 Error-Prone DDT Proceeds Uncoupled From The Replication Fork

#### III.3.1 The G2 tag

Although we now know that ubiquitylated PCNA does not promote restart of stalled forks, this does not mean that ubiquitylated PCNA may not operate at or near stalled forks (Ulrich, 2009). In fact, the standing view is that PCNA is ubiquitylated directly at stalled forks (Ulrich, 2009), and there is strong evidence that ss-gaps and SCJs accumulate in proximity to the replication fork (Lopes et al., 2003; Lopes et al., 2006).

These findings suggest that DDT may be directly coupled to the replication

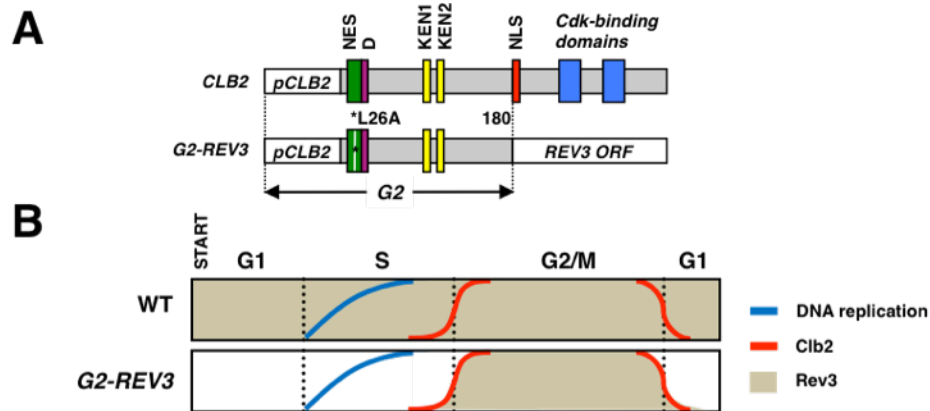


**Fig. 17: Genetic Tool for The Restriction of Target Nuclear Proteins to G2/M**

**(A)** Elements of the Clb2 protein and gene (upper panel) and the *G2-REV3* chimera. D (violet) and KEN boxes (yellow), nuclear export (NES, green) and nuclear localization (NLS, red) sequences, and two CYCLIN Cdk-binding domains (blue) are indicated. The *REV3* gene (and other DDT genes used in this study) was fused to the “G2-tag”, a DNA sequence that carries the *CLB2* promoter (*pCLB2*; which is activated at G2/M) and sequences encoding the N-terminal 180 amino acids of Clb2 harboring the D- and KEN box degrons (the NES is mutated; L26A, indicated by an asterisk). The G2-tag encoded peptide also reacts with the Clb2 antibody.

**(B)** Cell cycle phase durations are represented schematically in context of DNA replication timing (blue curve) and Clb2 expression (red curve). The predicted levels of Rev3 and *G2-REV3* proteins in WT and *G2-REV3* cells, respectively, is represented by the shaded area.

fork. However, if this were true, specific loss of the *RAD6* components from the replication fork would be expected to render cells unable to tolerate DNA damage. Because the mode of recruitment of the *RAD6* pathway specifically to the replication fork still remains elusive, we decided to exclude the *RAD6* components from S-phase instead. For this purpose, we designed a genetic tool that allows the restriction of proteins to the G2/M phase of the cell cycle. This system utilizes the N-terminal domain of cyclin B2 (Clb2), which contains D-box and KEN boxes (**Fig. 17A**), responsible for the ubiquitylation and degradation of Clb2 in an APC/C-dependent manner. Thus the corresponding chimeras would get depleted in late-M/G1 phase of the cell cycle (Amon et al., 1994; Hendrickson et al., 2001; Maher et al., 1995; Schwab et al., 1997; Wasch and Cross, 2002). To ensure correct localization of the fusion protein, we introduced a nuclear



export signal (NES) mutation L26A, which has no effect on Clb2 degradation (Hood et al., 2001). Finally, to restrict the expression of our targets to G2/M, we placed the constructs under the control of the G2/M-specific promoter of *CLB2* (Maher et al., 1995). The combination of these elements – together termed the G2 tag – creates novel APC/C substrates that should follow the expression and degradation pattern of Clb2 during the cell cycle (**Fig. 17B**).

Indeed, the G2 tag specifically and efficiently restricts the abundance of proteins it is fused to, to the G2/M. Cells bearing a single copy of the corresponding G2 tagged ORFs at their endogenous genomic loci, expressed the tagged protein as visualized by Western blot analysis, showing a unique band corresponding to the expected size of the chimeras (**Fig. 18**). We verified the correct expression of the construct by using additional C-terminal tags (data not shown), showing that the fusions were correctly expressed. G2 tagged strains also showed no traces of the respective chimeras in G1 by  $\alpha$ -factor arrest (**Fig. 19A**; left and right panels lane 1, and data not shown), indicative of the high efficiency of the system. Synchronous release of such cells into DNA replication

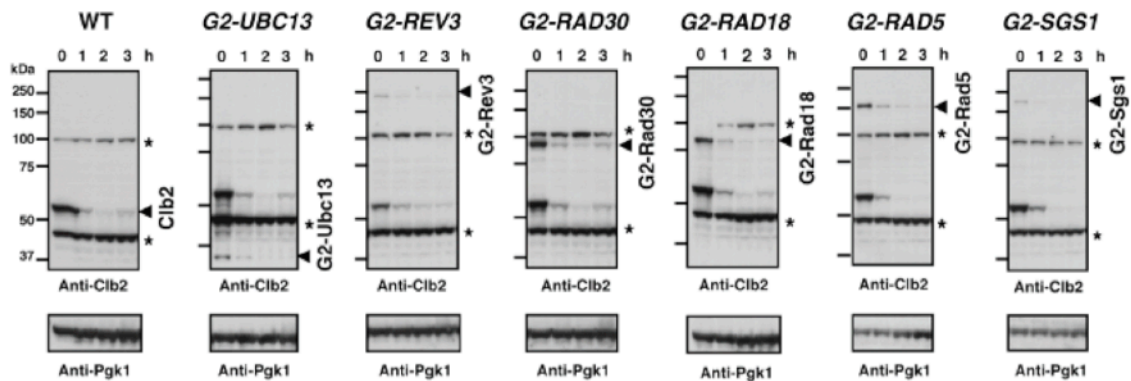


**Fig. 18: G2-Fusion Proteins are Readily Degraded After Release from Nocodazole-induced G2/M Arrest**

Cultures were arrested in G2/M by nocodazole (as in Fig. 1B; see Experimental Procedures), and released in YPD containing 17  $\mu$ g/ml  $\alpha$ -factor. After 2.5 h, additional  $\alpha$ -factor (17  $\mu$ g/ml) was added to maintain the G1 arrest. Samples were withdrawn at 0, 1, 2 or 3 h post-release as indicated. Respective G2-fusion protein levels (corresponding to the expected molar masses and detected by anti-Clb2 antibodies) are indicated by arrowheads. Endogenous Clb2 is labeled in the first panel. The asterisks denote cross-reactive bands. Pgk1 signals (bottom panels) were used for loading control.

resulted in expression of the G2-fusions in parallel to *CLB2*, specifically in the G2/M phase of the cell cycle, after the bulk of chromosomal DNA had been replicated (**Fig. 19A** for *G2-REV3* and *G2-RAD30*; lower panels, sections III.4 for *G2-SGS1* and III.5 for *G2-RAD5*, and data not shown). Therefore, the presence of DNA damage – known to delay S-phase progression and G2-onset and **Fig. 19B** – delayed the expression of the G2-chimeras (**Fig. 19A and 19B**; compare time-points 40-50 min post-release among the panels), indicating the system is not leaky. Most importantly, the levels of G2-Rev3 and G2-Rad30 dropped drastically by completion of mitosis, and the remaining signal can be explained by the inability to retain cell synchrony for time periods longer than one cell cycle

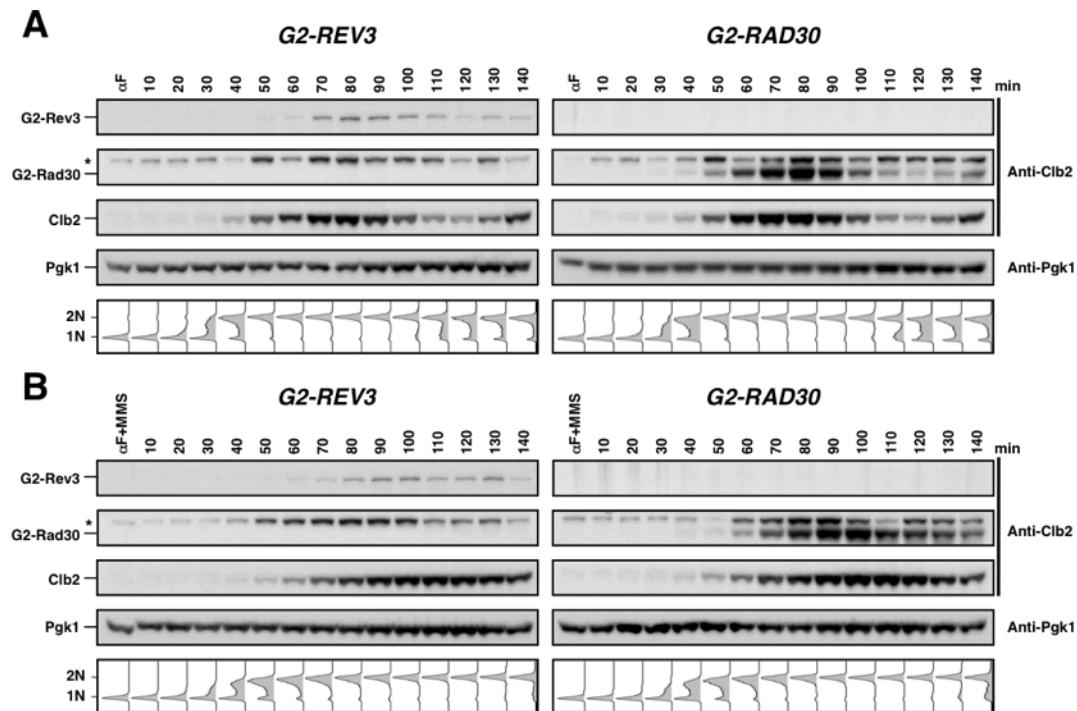


**Fig. 19: Cell Cycle Expression Profiles for G2-TLS Polymerases**

**(A and B)** Exponentially growing cultures were arrested in G1 by  $\alpha$ -factor, incubated at 23°C, followed by treatment with 0,033% MMS **(A)** or without MMS **(B)** for control. Subsequently 5% w/v sodium thiosulfate was added to all cultures and release from  $\alpha$ -factor was conducted by washing in YPD at 23°C. Samples were withdrawn at the indicated time-points and were analyzed by Western blot and FACS (lower panels; SYTOX). Regions without a signal represent the control blot area to allow the identification of background signal. Asterisk indicates a cross-reactive band. Note that S-phase (FACS) and G2-onset (Clb2 and G2 fusion expression) are delayed in the presence of DNA damage.

(**Fig. 19A**). Indeed, release from nocodazole arrest in G2/M resulted in complete depletion of all the G2-chimeras analyzed in this study (**Fig. 18**). Importantly, we also found that the presence of the new APC/C substrates did not overload APC/C activity, as judged by the normal degradation of Clb2 (**Fig. 18**).

The most important advantage of the G2 tag is that it alleviates the need for cell synchronization, which is the major disadvantage of most former systems for studying cell cycle associated events. Thus, the G2 tag facilitates the assessment of drug resistance and mutagenesis in asynchronous populations. Having constructed yeast strains that specifically express members of the *RAD6* pathway in G2/M, we used them in the following to differentiate this crucial branch of DDT from DNA replication and examine their ability to deal with replication stress and drive mutagenesis.

### III.3.2 Efficient and Specific Tolerance to DNA Damage by TLS Polymerases in G2/M

Mutagenesis is a largely catalytic process that can either occur “spontaneously” or be “induced” by DNA damage (Hastings et al., 1976; Lawrence and Christensen, 1976; Morrison et al., 1989). Its activity relies on the utilization of specialized polymerases that can replicate damaged DNA templates due to their distorted active sites (Friedberg, 2005; Pages and Fuchs, 2002; Yang and Woodgate, 2007). This damage bypass mechanism is known as trans-lesion synthesis (TLS) and is usually (but not always) error-prone (Kunkel et al., 2003; Waters et al., 2009). PCNA modification is crucial for DDT via TLS in eukaryotes, which in budding yeast involves the enzymatic activity of two TLS polymerases, Pol  $\zeta$  and Pol  $\eta$  (Hoege et al., 2002; Kunz et al., 2000; Lehmann et al., 2007; Stelter and Ulrich, 2003). However, any potential requirement for a specific cell cycle phase has not yet been discovered.

To address whether TLS can occur in G2/M, we restricted the catalytic subunit of Pol  $\zeta$  (Rev3) and Pol  $\eta$  (Rad30) to the G2/M phase using the G2 tag.



Both Rev3 and Rad30 are normally stable during the cell cycle (Waters and Walker, 2006) and both contribute to cellular resistance to DNA damaging agents ((Lemontt, 1971) and **Fig. 20A**). Importantly, restricting the expression of the polymerases to the G2/M phase did not affect resistance to UV, MMS or 4NQO (**Fig. 20A**). It is notable that *rad30Δ* cells are not sensitive to the UV-mimicking agent 4NQO although they are sensitive to UV (**Fig. 20A**), conditions known to result in subtly different DNA lesions (Fronza et al., 1992), in agreement with the view these polymerases are specialized for different types of DNA lesions (Bresson and Fuchs, 2002; de Padula et al., 2004). Apparently, the G2/M-restricted TLS polymerases display high DDT efficiency, as they fully uphold DNA damage resistance even in the absence of error-free branch of the *RAD6* (*mms2Δ*; **Fig. 20B**), where loss of TLS polymerases synergistically reduces

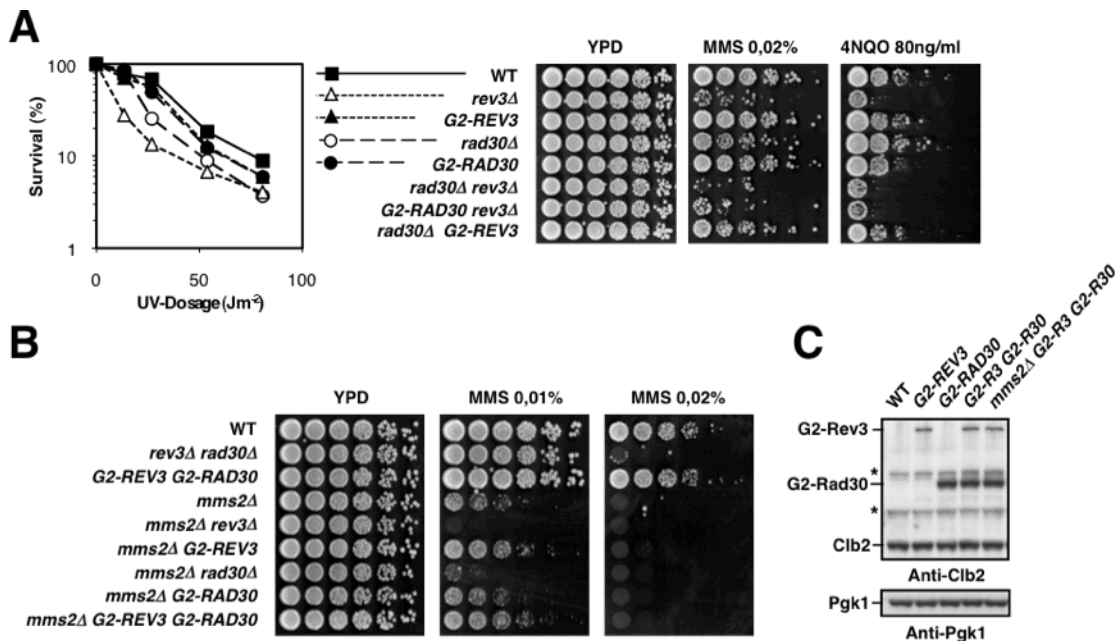


**Fig. 20: TLS Polymerases Restricted to G2/M Support Efficient DDT**

**(A and B)** Survival to DNA damage assays. Spotting of 1:5 serial dilutions on YPD plates supplemented with MMS or 4NQO, where indicated. **(A)** G2-TLS polymerase fusions complement the sensitivities of their corresponding deletion mutants to UV-light (left panel), MMS and 4NQO (right panel). **(B)** G2-TLS polymerases are proficient in DDT even in the absence of *MMS2*. **(C)** Strains expressing the G2-restricted TLS polymerase(s) were verified by Western blot using anti-Clb2 and anti-Pgk1 antibodies. *R3-* *REV3*; *R30-* *RAD30*.

survival to DNA damage (Broomfield et al., 1998a; Torres-Ramos et al., 2002). Moreover, cells expressing both TLS polymerases as G2-fusions simultaneously also exhibited wild-type sensitivity to DNA damaging agents (**Fig. 20B**). Importantly, expression of both G2-TLS polymerases in the same strain had no impact on Clb2 levels (**Fig. 20C**), in agreement with the high robustness of the APC/C-ubiquitin-proteasome system (Carroll and Morgan, 2002; Rape et al., 2006).

For a quantitative assessment of TLS in cells expressing G2-TLS polymerases, we estimated forward mutation rates at the *CAN1* genomic locus (Cassier-Chauvat and Fabre, 1991). We initially focused on spontaneous mutagenesis, which involves PCNA SUMOylation (but not monoubiquitylation) in budding yeast (Hoege et al., Nature 2002; Stelter and Ulrich, Nature 2003). Very low levels of mutations accumulate spontaneously in wild-type cells, yet mutation rates rise by 4-7 fold in error-free DDT mutants (eg. *mms2Δ*) (Broomfield et al., 1998a; Liefshitz et al., 1998; Xiao et al., 1999). This increase requires error-prone DNA synthesis catalyzed by Pol  $\zeta$ , as deletion of its catalytic subunit, Rev3, reduces spontaneous mutagenesis to wild-type levels (Broomfield et al., PNAS 1998; and **Fig. 21A**). However, restriction of Rev3 to G2/M in *mms2Δ* cells did not affect the increased mutation rates of this strain (**Fig. 21A**). Importantly, expression of G2-Rev3 in wild-type cells did not impose any increase in mutagenesis (**Fig. 21A**), indicating that mutagenesis by G2-Rev3 is not the result of overproduction of the chimera. Furthermore, G2-Rev3 induces spontaneous mutagenesis in a specific manner, as all increased mutation rates were abolished by deletion of the Siz1 SUMO ligase (**Fig. 21A**), responsible for PCNA SUMOylation (Hoege et al., Nature 2002). Thus, we concluded that spontaneous TLS can efficiently and specifically take place in G2/M.

By employing DNA damaging agents, we could reach the same conclusion for induced-TLS. Similar to spontaneous, also induced-mutagenesis requires the Pol  $\zeta$  subunit Rev3 (Lawrence and Christensen, 1976; Morrison et al., 1989). In fact, loss of Rev3 rendered cells immutable in response to UV irradiation (**Fig.**

**21B).** Expression of Rev3 in G2/M was sufficient to recover mutability (**Fig. 21B**). Enhanced Rev3-dependent mutagenesis occurs in the absence of Pol  $\eta$  /Rad30 (*rad30 $\Delta$* ; **Fig. 21B**), a TLS polymerase that promotes tolerance of UV lesions in and error-free manner (McDonald et al., 1997; McCulloch et al., Nature 2004;

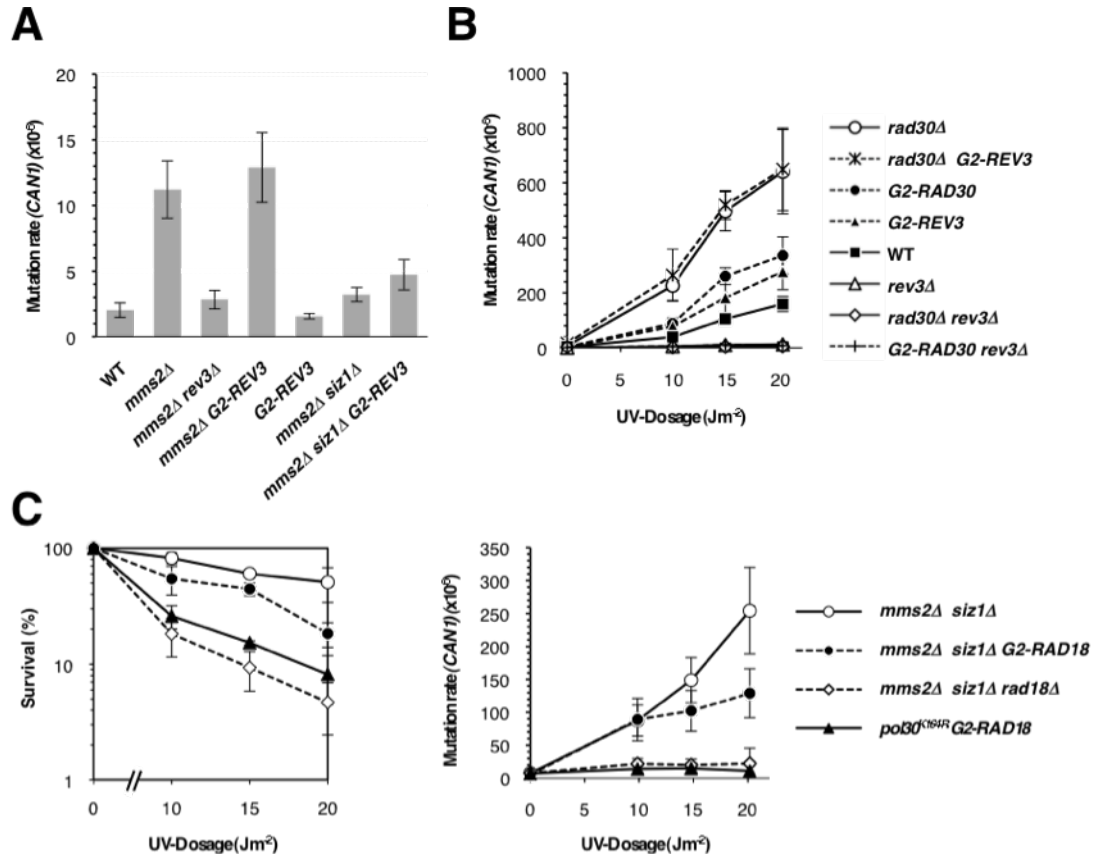


**Fig. 21: Mutagenesis via TLS in G2/M Is Specific**

**(A and B)** G2-TLS component fusions are proficient in catalyzing TLS-mediated mutagenesis. Rates of spontaneous **(A)**, and UV-induced forward mutagenesis **(B)** are shown for the *CAN1* locus. Cell suspensions of appropriate dilutions were plated on YPD or SC-Arg plates supplemented with 60  $\mu$ g/mL canavanine, a toxic Arginine analogue. Loss of function mutations on the basic-amino-acid-permease, Can1, block canavanine uptake (these strains retain a functional Arginine biosynthesis pathway), and are detected as viable colonies on SC-Arg+CAN plates.

**(C)** G2-restricted Rad18 is proficient in promoting DDT specifically via PCNA monoubiquitylation. Strains lacking the ability to polyubiquitylate and SUMOylate PCNA on K164 (*mms2 $\Delta$  siz1 $\Delta$* ), expressing WT *RAD18* (open circles), *G2-RAD18* (closed circles), or carrying a *RAD18* deletion (*rad18 $\Delta$* , open diamonds) were UV-irradiated as indicated and their survival (left panel) and induced mutation rates (right panel) were estimated and compared to a *G2-RAD18* strain defective for PCNA modification (*pol30<sup>K164R</sup>*, closed triangles). Values and associated error bars represent averages and their standard deviations from 3-7 independent experiments.

Johnson et al., 1999; Masutani et al., 1999). Moreover, restriction of Rad30 to G2/M was also able to suppress mutagenesis almost to wild-type rates (**Fig. 21B**), strongly suggesting that both error-prone and error-free induced-TLS can take place efficiently in G2/M. Importantly, induced-TLS requires monoubiquitylation of PCNA by Rad18 ubiquitin ligase (Hoege et al 2002; Ulrich and Stelter 2003). Indeed, expression of Rad18 in G2/M was also proficient in promoting DDT and induced-mutagenesis in UV-irradiated cells incapable of PCNA polyubiquitylation and SUMOylation (*mms2Δ siz1Δ*) (**Fig. 21C**). Furthermore, abolishment of monoubiquitylated PCNA by mutation of K164 in these cells resulted in immutability (**Fig. 21C**). So, we conclude that induced-TLS catalyzed during the G2/M phase of the cell cycle is both specific and efficient, strongly suggesting it initiates and proceeds uncoupled from the replication fork.

### **III. 4 Error-Free DDT Involves Sgs1 Functions Behind The Replication Fork**

#### **III.4.1 A Genetic Screen For Components of Error-Free DDT**

Above we showed that the effectors of error-prone DDT, TLS polymerases, operate efficiently when they are restricted to the G2/M. We have tried to address whether this also holds true for the error-free branch of *RAD6*-mediated DDT. However, because effectors of the error-free branch of DDT were to date unknown, we designed a genetic screen to identify error-free components of the *RAD6* pathway. For this purpose, we took advantage of our finding that the cold-sensitivity of *pol32Δ* cells involves polyubiquitylation of PCNA (**Fig. 10**).

It remains a puzzling question why cells lacking this polymerase subunit (Pol32) are viable at optimal temperatures. We envisioned the existence of repair pathways that specifically promote ss-gap filling under these conditions. Indeed, a surprisingly large number of genes are essential for growth in *pol32Δ* or other Pol  $\delta$  mutants. We identified approximately 400 essential genes, encoding transcription factors, repair enzymes, sister-chromatid cohesion components, cell

cycle checkpoint members, RNA-processing factors, metabolic regulators, membrane sorting proteins and other uncharacterized proteins (data not shown), which will not be described here. Among the uncovered interactors are the genes of the *RAD52* epistasis group (Hanna et al., 2007) (including *RAD52*, *RAD51*, *RAD55*, *RAD57* and *RAD54*), indicating the importance of homologous recombination (HR) in dealing with ss-gaps (Merrill and Holm, 1998). However, some other genes, like the checkpoint kinase Dun1, the mismatch-repair factor, Msh2, and the endonuclease Rad27 required for proper Okazaki fragment maturation, might rather not be directly involved in ss-gap filling.

In order to identify components required for ss-gap filling directed by polyubiquitylated PCNA, we screened for synthetic lethal genetic interactions that are alleviated by the deletion of *MMS2*. We deleted the *MMS2* gene using the *URA3* cassette, which is counter-selectable by use of the drug 5'-fluoroorotic acid (5'-FOA). Following mating to a library of non-essential deletion mutants, sporulation and specific killing of diploids on a robot-based platform (Tong et al., 2001, and see methods), we selected haploid cells that had inherited either all three or only two deletions, on media lacking uracil or supplemented with 5'-FOA, respectively (**Fig. 22**). This allowed us to conveniently isolate those genetic interactions that occurred exclusively in a manner dependent on PCNA polyubiquitylation. Intriguingly, only few hits were recovered using this approach, indicating that our screening strategy was highly specific.

#### III.4.2 Sgs1 Helicase Operates Downstream of Polyubiquitylated PCNA

The most prominent genetic interaction was *SGS1* (**Fig. 22B**), encoding a DNA helicase mainly known for its roles in the stabilization of stalled forks and promoting non-reciprocal (not involving the exchange of genetic information between recombining sequences) homologous recombination, as well as its requirement for genome stability in yeast and cancer prevention in humans

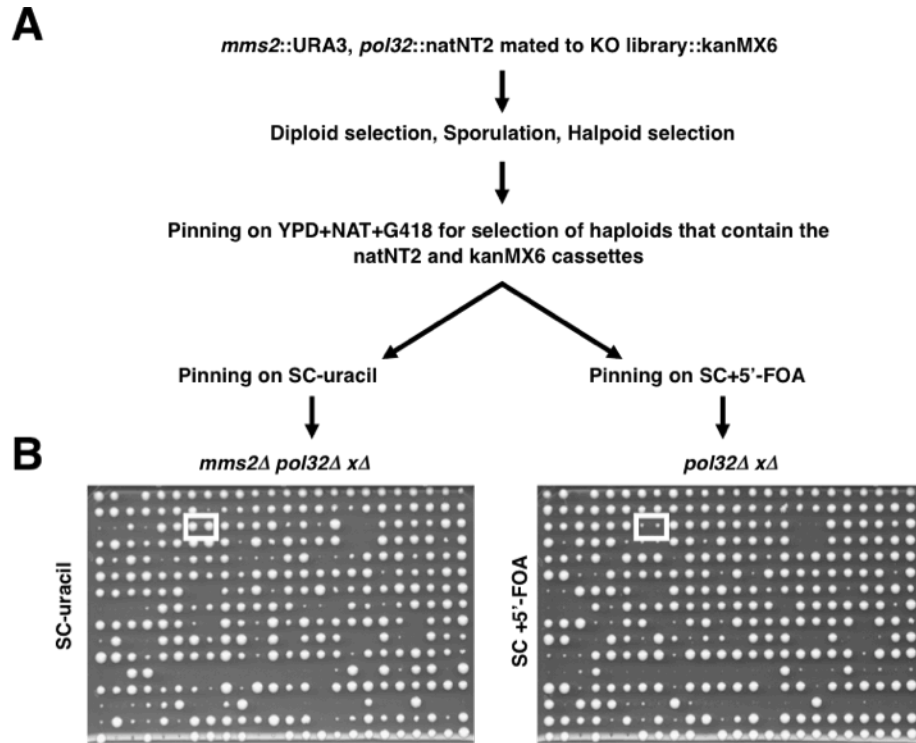


**Fig. 22: A Synthetic Lethal Rescue Screen Identifies Downstream Components of Error-free DDT**

**(A-B)** Robot-based synthetic lethal (SL) analysis was performed with a strain bearing *mms2Δ* and *pol32Δ* deletions. The basic layout of the screen is summarized (see also Experimental Procedures). Final pinning was performed on SC plates that lack uracil but contain G418 and NAT to specifically select for viable triple mutants (*mms2Δ pol32Δ xΔ*; x = deletion mutant of the library), and on SC plates containing G418 and NAT and supplemented with 0,1% w/v 5'-FOA (to select against the *mms2Δ* mutant inactivated by the *URA3* marker) to select for viable double mutants that contain the WT *MMS2* gene (*pol32Δ xΔ*). Comparing the growth of colonies selected by the two screens done in parallel identifies mutants that can exacerbate the phenotype of *pol32Δ* in a manner dependent on PCNA polyubiquitylation. **(B)** Synthetic lethality between *pol32Δ* and *sgs1Δ* depends on *MMS2*. Plates, containing *sgs1Δ* deletion (white box) were photographed 3 days after final pinning at 23 °C .

(Rossi et al., 2010). We verified our finding by two strategies. We initially used tetrad analysis in two different genetic backgrounds (data not shown). We then expressed *SGS1* under a truncated *GAL10* promoter that is galactose-inducible and strongly glucose-suppressible (Janke et al., 2004). Plating *GAL-SGS1* expressing cells on glucose resulted in terminal growth arrest only in the absence of *POL32* (**Fig. 23A**). Importantly, this phenotype depended on the PCNA polyubiquitylation machinery as well as the acceptor lysine of PCNA (**Fig. 23A**),



indicating that the interaction is indeed mediated via the error-free branch of the *RAD6* pathway for DDT. We demonstrated the DDT-dependent arrest also quantitatively, calculating colony formation efficiency of viable cells, after plating on glucose-containing media (**Fig. 23B**; compare the first three strains from the top). Importantly, epistatic behavior between the error-free branch of the *RAD6* pathway (*MMS2*) and *SGS1* in response to replication stress due to DNA alkylation damage, in cells containing an intact *POL32* gene (Branzei et al., 2008, and **Fig. 23C**). The role of Sgs1 in error-free DDT is likely the catalysis of a rather late step, based on the extensive accumulation of joint sister chromatids (sister-chromatid junctions; SCJs) in its absence (Branzei et al., 2008).

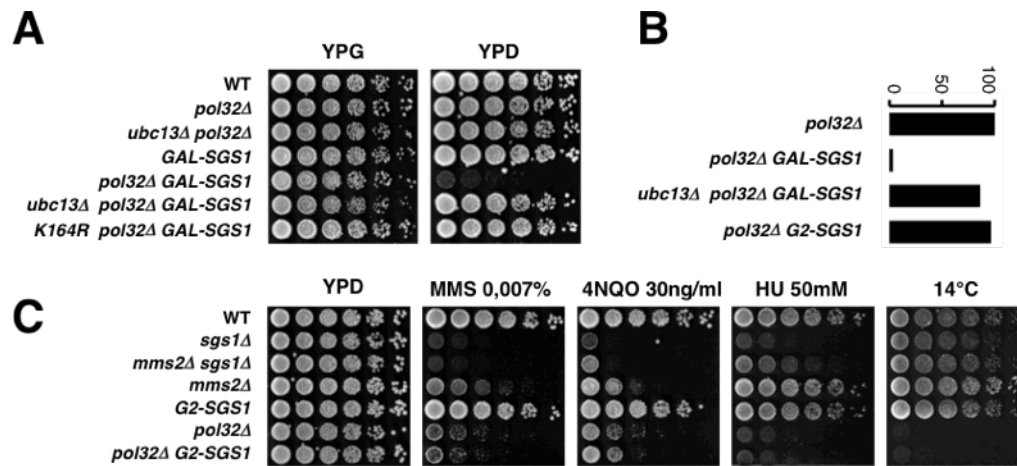


**Fig. 23: Sgs1 Operates in *RAD6*-Mediated Error-Free DDT**

**(A)** Synthetic lethality of the *pol32Δ sgs1Δ* strain depends on PCNA polyubiquitylation. *SGS1* (tagged with HA epitope) driven by the *GAL* promoter (*GAL-SGS1*) was integrated at its genomic locus and turned off by plating on glucose-containing media (right panel). Whereas *pol32Δ GAL-SGS1* cells are inviable on glucose, mutants defective in polyubiquitylation (*ubc13Δ*, *pol30<sup>K164R</sup>*) can grow. Serial 1:5 dilutions were spotted on plates and incubated at 23°C for 2,5 days.

**(B)** Restriction of Sgs1 to G2 (*G2-SGS1*), but not Sgs1 depletion (*GAL-SGS1*), supports viability in the absence of *POL32*. Cells from cultures grown to logarithmic phase (YP medium, 0,5% galactose 1,5% raffinose) were plated on galactose (YP, 2% galactose) or glucose (YP, 2% glucose)-containing plates, incubated at 30°C for 3 days, and counted. Reduced colony formation efficiency of *pol32Δ GAL-SGS1* on glucose plates can be rescued by deletion of *UBC13*.

**(C)** Sgs1 promotes PCNA polyubiquitylation-dependent DDT effectively at G2/M. *MMS2* is epistatic to *SGS1* as *sgs1Δ* and the *sgs1Δ mms2Δ* double mutant have the same MMS sensitivity, whereas the double mutant is less sensitive to 4NQO and HU. *G2-SGS1* is able to complement the DNA damage sensitivities of the *sgs1Δ* mutant to MMS, 4NQO, or HU, in the presence or absence of *POL32*.

In agreement with the view that the role of Sgs1 in DDT is late and may not involve the stabilization of stalled forks, *SGS1* deletion causes *UBC13*-dependent G2/M arrest and Rad53 phosphorylation in *pol32Δ* (**Fig. 24A**) without affecting PCNA ubiquitylation (**Fig. 24A**) or DNA replication (as judged by FACS

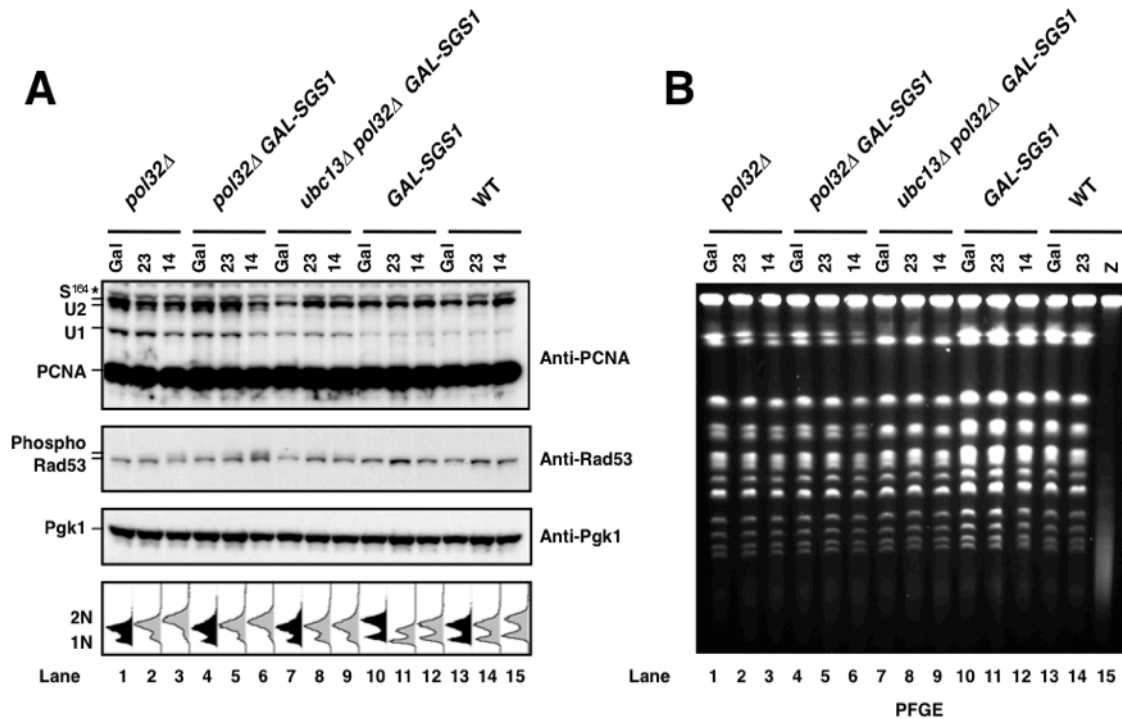


**Fig. 24: Sgs1 Lowers the Restrictive Temperature of *pol32Δ***

**(A and B)** *SGS1* is not required for DNA damage checkpoint activation or PCNA modification by ubiquitin and SUMO in *pol32Δ*, yet *sgs1Δ* enhances the cold-sensitivity of *pol32Δ* cells without inducing a measurable accumulation of DSBs. Glucose-shut-off for Sgs1 expression (under the control of the *GAL* promoter) (see Fig. 4 and Experimental Procedures). **(A)** Exponentially growing cultures (YP rich media containing 0,2% galactose and 1,8% raffinose) (lanes labeled Gal) were shifted from 30°C to either 23°C (for 6 h; lanes labeled 23) or 14°C (for 10 h; lanes labeled 14) after glucose (2% final concentration) addition. Samples were withdrawn at the indicated time-points and analyzed by FACS (bottom panel; PI). *pol32Δ* cells depleted for Sgs1 show increased DNA damage checkpoint activation (indicated by high phospho-Rad53 levels; phospho) in comparison to *pol32Δ* cells, already at 23°C (compare lanes 2 and 5). Sgs1 is not required for checkpoint activation or PCNA ubiquitylation in *pol32Δ* (compare lanes 3 and 6). Pgk1 levels were used as loading control. **(B)** No apparent replication defects or DSBs are induced in *pol32Δ* or Sgs1-deprived *pol32Δ* cells at permissive or restrictive conditions, as judged by PFGE. PFGE analysis of chromosomes from WT cells treated with 0,1% zeocine for 2 h at 30°C (Z) serves as a positive control for the visualization of broken chromosomes (lane 15). Samples for (A) and (B) were collected in parallel.



analysis and PFGE; **Fig. 24A and 24B**), or inducing any DSBs (**Fig. 24B**) through potential fork collapse. Moreover, *SGS1* overproduction in *sgs1Δ* cells arrested in the presence of MMS reduced aberrant SCJ accumulation (Liberi et al., 2005). These results suggest that the inability to resolve (or most likely “dissolve”) recombination intermediates is the reason for the lethality of *pol32Δ sgs1Δ* as well as the cold-sensitivity of *pol32Δ*.

Interestingly, when we assessed the sensitivity to 4NQO and HU, treatments that are well characterized and involve the accumulation of ssDNA (Mirzayans et al., 1985; Sogo et al., 2002), we observed partial rescue of the sensitivities of *sgs1Δ* by deletion of *MMS2* (**Fig. 23C**). We found this rescue requires an intact HR pathway, as deletion of any member of the *RAD52* epistasis group alleviated the rescuing effect of *MMS2* deletion to *sgs1Δ* (data not shown). Altogether, our findings imply that polyubiquitylated PCNA controls a recombination mode and may be required for the stabilization or induction of deleterious recombination intermediates that are normally detoxified by the action of the Sgs1/Top3/Rmi complex.

#### III.4.3 Restriction of Sgs1 to G2/M Supports DDT, But Not its Functions at The Fork

At this point we had identified Sgs1 as a crucial mediator of *RAD6*-mediated error-free DDT, and had indications it promotes a late recombination event. To prove that the role of Sgs1 in DDT is uncoupled to the replication fork, we asked whether the helicase is operational when restricted to G2/M. Indeed, G2-fusions of *SGS1* (*G2-SGS1*) expressed as the only source of Sgs1 in *pol32Δ* cells, fully supported the viability of *pol32Δ* cells (**Fig. 23B**). Moreover, *G2-SGS1*-expressing cells exhibited no hypersensitivity towards DNA-damaging agents compared to WT even in the absence of *POL32* (**Fig. 23C**).

We next compared cell cycle progression and checkpoint activation of *pol32Δ* cells grown at (semi-permissive) 20°C with *pol32Δ G2-SGS1* cells, and

with *pol32Δ* cells depleted for Sgs1 (*GAL-SGS1*). We monitored synchronous cell cycle progression in glucose (to block the expression of *GAL-SGS1*) after G1 arrest in the presence of galactose (to ensure equal growth rates for all three strains) (**Fig. 25**, top). We found that DNA damage checkpoint activation (monitored by Rad53 phosphorylation) was evidently higher in Sgs1-depleted *pol32Δ* cells compared to *pol32Δ* and *pol32Δ G2-SGS1* cells (**Fig. 25**; compare

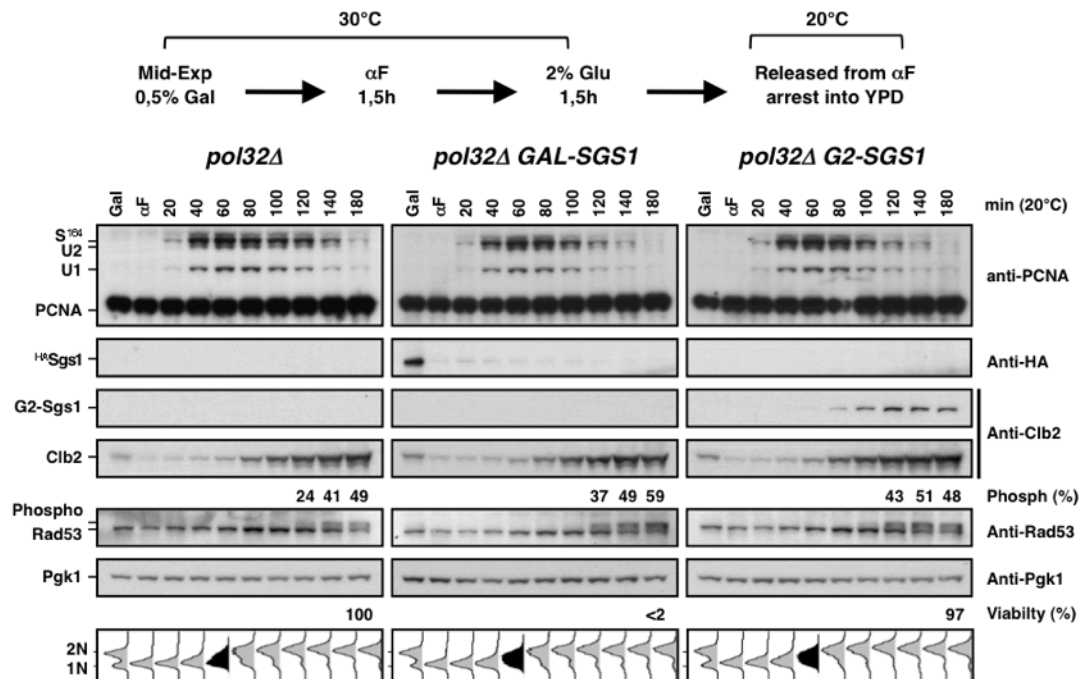


**Fig. 25: Sgs1 Contributes to the S-Phase Delay of *pol32Δ* Cells**

Scheme depicts a summary of the following procedure. Cells were grown to the early exponential phase in the presence of 0.5% galactose and 1.5% raffinose, arrested in G1 with  $\alpha$ -factor (1.5 h, 30°C) (Gal) and subsequently supplemented with 2% glucose (to shut off *GAL-SGS1* expression). After additional 1.5 h incubation, cultures were washed and grown (released) in YPD (2% glucose) at 20°C. Depletion of Sgs1 from S-phase results in faster progression through S-phase in *pol32Δ*. Samples withdrawn at different time-points post-release (20°C) were probed by Western analysis for the indicated proteins. Protein profiles of *pol32Δ* cells, *pol32Δ* cells depleted for Sgs1 (*GAL-SGS1*), and *pol32Δ* cells expressing Sgs1 in G2/M (*G2-SGS1*). Lower panel shows FACS profiles for the same samples, and (above the panel) cell survival after plating on 2% glucose YP-plates. In *pol32Δ* cells in the absence of Sgs1 or when Sgs1 is restricted to G2/M, S-phase is shortened (60 min post-release; highlighted in black; PI staining) and PCNA modifications decay faster and Rad53 phosphorylation appears earlier. Note that plating efficiency on glucose is reduced and phospho-Rad53 is enriched in Sgs1-depleted *pol32Δ* cells, as compared to WT Sgs1 or *G2-SGS1*-expressing *pol32Δ* cells (180 min post-release).

the 180 min lanes), which paralleled their inability to form colonies on plates (**Fig. 24B and 25**). Thus, G2-Sgs1 indeed represses *pol32Δ*-induced DNA damage checkpoint activation in a manner similar to that of WT Sgs1.

Although G2-Sgs1 is as efficient as Sgs1 in supporting DDT, it does not seem to uphold all Sgs1 functions. In fact, we noticed that Rad53 phosphorylation in *pol32Δ GAL-SGS1* and *pol32Δ G2-SGS1* cells occurred about 20 min earlier than in *pol32Δ* cells (**Fig. 25**). This was due to a faster progression as determined by FACS analysis (**Fig. 25**). Faster S-phase progression was shown before for *sgs1Δ* cells grown in the presence of the HU (Frei and Gasser, 2000), which suggested that Sgs1 plays a role in promoting the S-phase checkpoint. Thus we assume that the complete absence of Sgs1, or its restriction to G2/M, also weakens S-phase checkpoint activation in *pol32Δ*, thereby causing the observed faster S-phase progression. Notably, this defect in S-phase checkpoint activation resulted in no increased MMS or HU sensitivities (**Fig. 23C**), in agreement with the absence of a phenotype from the checkpoint-specific mutant, *mrc1<sup>AQ</sup>* (Tourriere et al., Mol Cell 2005). In conclusion, while G2/M-restricted Sgs1 fully supports its vital role in error-free DDT, it does not support an S-phase specific, fork-coupled role, the promotion of the S-phase checkpoint. Importantly, this finding demonstrates that G2-Sgs1 is completely excluded from S-phase, and hence shows that the G2 tag is not leaky, but highly efficient.

### **III. 5 *RAD6*-Dependent Error-Free DDT Proceeds Uncoupled From The Replication Fork**

#### **III.5.1 Restriction of the *RAD6* Pathway to G2/M Has No Impact on DDT**

Having established the efficiency and cell cycle specificity of the G2 tag we could now assess the activity of DDT in all G2 tagged *RAD6* pathway members. Indeed, *G2-UBC13*, *G2-RAD5*, or even *G2-RAD18*-expressing cells complemented the UV, MMS and 4NQO sensitivities of the corresponding

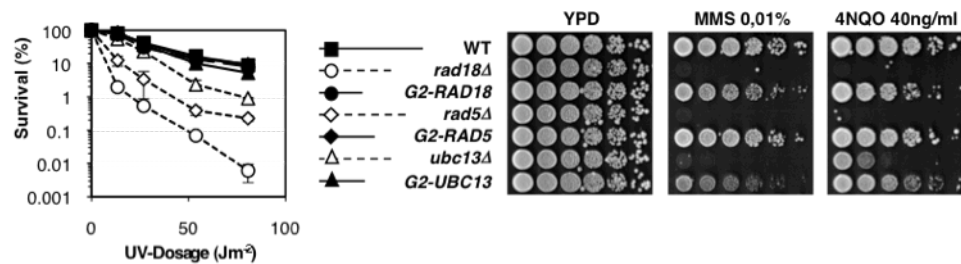


**Fig. 26: Restriction of The PCNA Ubiquitin Conjugation Machinery to G2/M Supports DDT**

G2-fusions of Rad18, Rad5, and Ubc13 complement the sensitivity of their respective deletion mutants to UV light (left panel), and DNA-damaging agents (1:5 serial dilutions on YPD containing MMS, HU, or 4NQO; right panel). Error bars represent standard deviations from 2 independent experiments.

deletion strains almost completely (**Fig. 26**). Thus, the entire *RAD6* pathway, with both the error-free and the error-prone branches, are fully functional during G2/M. In particular, our finding that Rad5 can support resistance to DNA damage when restricted to G2/M is surprising, for it is currently believed that Rad5 is the ideal DDT factor to foster the restart of stalled replication forks. The RING domain of Rad5, responsible for PCNA polyubiquitylation, is embedded inside an SWI/SNF2 ssDNA-dependent ATPase domain, found to catalyze regression of fork-like DNA structures *in vitro* with unprecedented specificity and efficiency (Blastyak et al., 2007). Although the ATPase domain of Rad5 is important for DDT *in vivo* (Gangavarapu 2006), there is no evidence supporting the existence of a DDT mechanism involving fork regression *in vivo*, though such a mechanism was proposed more than thirty years ago (Higgins et al., 1976). If G2-Rad5 supported DDT in a specific manner, then our results would strongly suggest that the ATPase activity of Rad5 proceeds uncoupled from the replication fork.

In contrast to the TLS polymerases, the Sgs1 helicase, and the ubiquitin-conjugating enzyme Ubc13, Rad5 is a very complex protein. Rad5 promotes DDT via three mechanisms: PCNA polyubiquitylation, TLS, and the unknown function of its enigmatic ATPase activity (Gangavarapu et al., 2006). It is possible that the levels of Rad5 required for one of its functions are much lower than for promoting the other two. It is also possible that even small overproduction of

Rad5 might result in unspecific rescue of an error-free DDT defect by channeling tolerance to more error-prone mechanisms, or vice versa. We focused on studying the *G2-RAD5* strain in order to address those concerns on the specificity of G2-Rad5 in DDT.

### III.5.2 Restricting Rad5 to G2/M Postpones DDT, Without Affecting S-Phase Progression

We arrived at the conclusion that the ATPase activity of Rad5 is not involved in fork-restart *in vivo*, by following S-phase progression in synchronous cells that had received a pulse of MMS during G1 (**Fig. 27A**). In fact, cells lacking *RAD5* reached G2/M (Cib2 accumulation; **Fig. 28B**) and progressed through S-phase with identical to wild-type kinetics (**Fig. 27B**; lower panel). The major defect *rad5Δ* cells exhibited is that they could not enter into a new cell cycle in a timely manner (as judged by the loss of SUMOylated PCNA originating from the following S-phase; compare time-points 120-180 min to wild-type, **Fig. 27B**; upper panel) and arrested in G2/M with hyper-phosphorylated Rad53 kinase (**Fig. 27B and 27C**). The G2/M arrest was terminal, since a large fraction of the population did not survive to form colonies (**Fig. 27D**), and even the surviving fraction formed micro-colonies (data not shown). This dramatic defect is due to loss of the DDT functions of Rad5, and correlates with the inability of *rad5Δ* cells to deal with MMS-induced DNA lesions already during S-phase (measured as residual phosphorylated Rad53; **Fig. 27B and 27C**), indicating that Rad5 operates also in S-phase in wild-type cells. We also detected a marked accumulation of DSBs using PFGE in *rad5Δ* (**Fig. 27E**). MMS-induced DSBs are actually not present *in vivo*, but rather form *in vitro* during PFGE sample preparation due to the heat-lability of MMS-treated chromosomes (Lundin et al., 2005), a property that is quantifiable (Ma et al., 2008). In this manner, we can conveniently estimate the total amount of DNA damage the culture has received, as well as follow its repair. In fact, lesion density in this setup reached

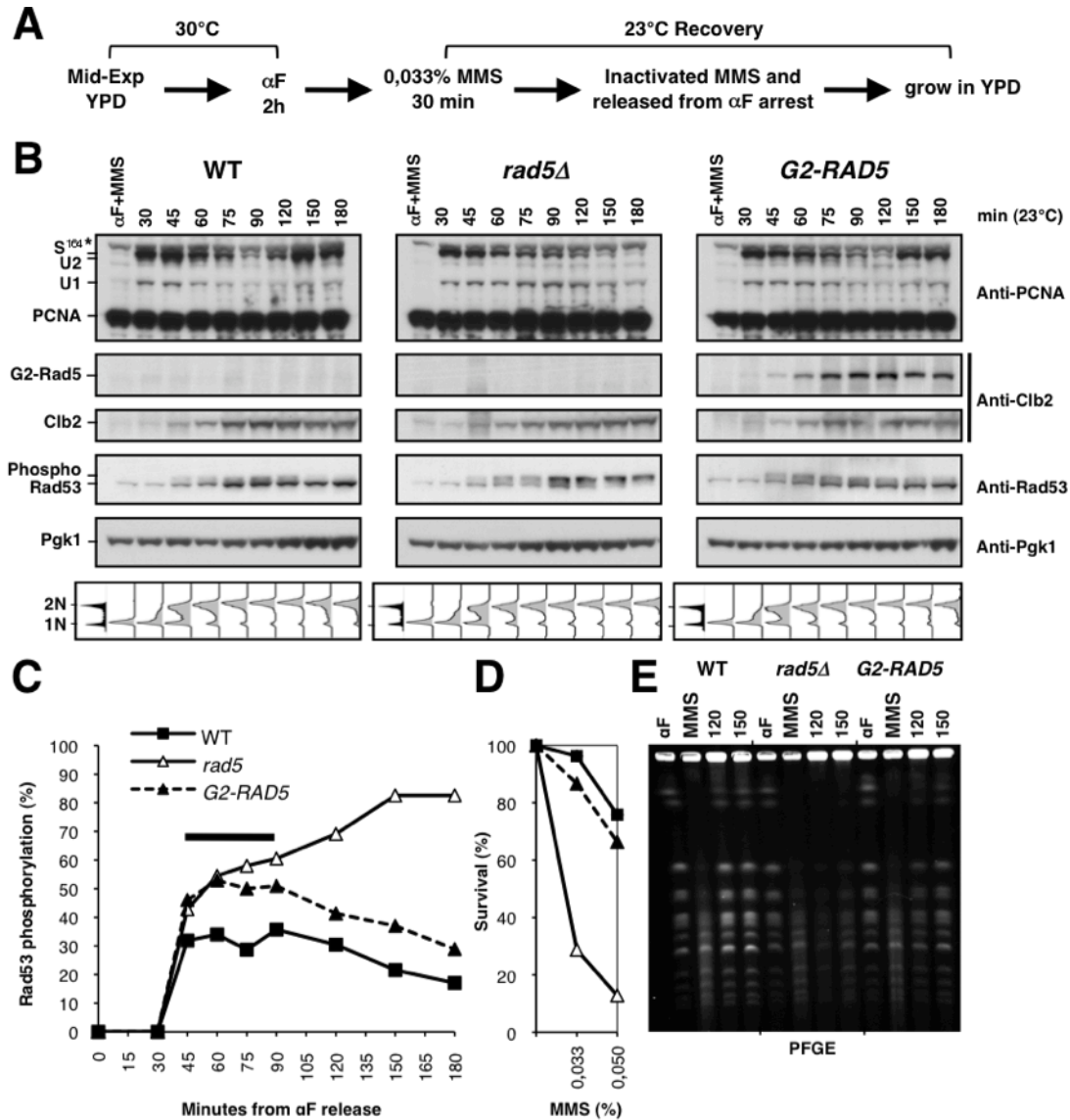


**Fig. 27: PCNA Polyubiquitylation in G2/M Supports DDT**

(A-E) WT, *rad5Δ* and *G2-RAD5*-expressing cells were arrested in G1 ( $\alpha$ -factor, 30°C), transferred to 23°C and treated with MMS (0,033%; additionally 0,05% for Fig. 27D) for 30 minutes(A). Subsequently, MMS was inactivated by Na-thiosulfate (5%) and cells were synchronously released from G1 arrest by transfer into YPD medium. Samples before ( $\alpha$ -factor) and after release were withdrawn at the indicated time-points and analyzed by Western blots, FACS, and PFGE. (B) G2-Rad5 (detected with Cln2 antibody; *G2-RAD5*) accumulates parallel to Cln2 in G2/M (time-points 60-180 min), after S-phase completion (FACS; lower panel; SYTOX staining) and supports PCNA polyubiquitylation during G2/M (time-points 60-90 min; see enlargement of the anti-PCNA blot in Fig. 28). In addition, G2-Rad5 is required for re-entry into the cell cycle, as indicated by increased PCNA SUMOylation levels (compare 150 and 180 min lanes). (B and C) Phosphorylated Rad53 increasingly accumulates in *rad5Δ* cells in G2/M (anti-Rad53 blot; 45-180 min). Although *G2-RAD5*-expressing cells reach similar phospho-Rad53 levels during S-G2 (45-60 min), they drop to almost WT levels yet delayed by about 30 min (bar). Quantification (C) of the phospho-Rad53 levels detected by Western blots.



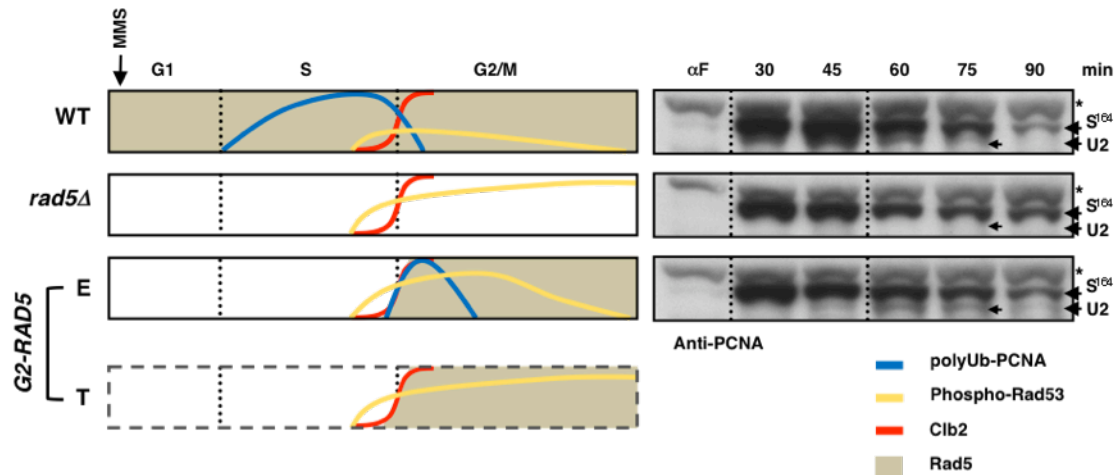


**Fig. 28: Comparison Of Experimental And Predicted Results**

Schematic representation of PCNA polyubiquitylation and Rad53 phosphorylation in synchronously growing populations in response to a pulse of MMS in G1 (see **Fig. 26A**). The top three panels (framed) show the profiles of polyubiquitylated PCNA and phospho-Rad53 obtained experimentally in WT, *rad5Δ* and *G2-RAD5*-expressing cells. The panels on the right show the corresponding PCNA ubiquitylation levels (enlargements of the data shown in **Fig. 27B**; U2, polyubiquitylated PCNA; S164, SUMOylated PCNA at K164). According to the prevailing model, if Rad5 had to function at stalled forks to promote replication restart, then *G2-RAD5*-expressing cells would exhibit the same checkpoint activation pattern (increasing levels of phospho-Rad53) as *rad5Δ* cells (theoretical curves, **T**). However, *G2-RAD5*-expressing cells exhibit a drop of phospho-Rad53 levels in G2/M (experimental curves, **E**), suggesting that the construct effectively complemented MMS-induced checkpoint activation (Rad53 phosphorylation) later during G2/M phase (where the fusion is expressed). Because MMS treatment was able to induce PCNA polyubiquitylation in *G2-RAD5*-expressing cells (in G2/M; right panel, bottom row), ss-gaps, which originate during S-phase, are apparently recognized and processed efficiently post S-phase.

#### continued Fig. 27 legend

(D) Survival of cells from the same experiment before or after MMS addition (plated on YPD and colonies were counted after 2 days at 30°). (E) PFGE analysis of the same samples before (a-factor) and after MMS treatment (MMS), and 120 and 150 min after G1 release. Chromosomes from MMS-treated cultures are labile upon heat treatment *in vitro* and appear fragmented after PFGE (Lundin et al., 2005), serving as control for the equal amount of MMS used for all three cultures. Note that during recovery, chromosomes of WT and *G2-RAD5*-expressing cells become less labile than those from *rad5Δ* cells, indicating that Rad5, even when restricted to G2/M, can handle damage induced by replication of MMS-modified templates.

approximately 1 adduct per 20kb (according to Ma et al, 2008), which is high enough to affect most replication forks. Although, *rad5Δ* cells progress through S-phase normally in these conditions, they are unable to repair the genome-wide DNA lesions induced by MMS (**Fig. 27E**). This strongly suggests that instead of stalled forks, by retaining a robust ability to promote fork restart downstream of the DNA lesion, *rad5Δ* cells rather accumulate ss-gaps containing the DNA adduct (that are heat-labile for the case of MMS damage).

Using the above setup we followed repair in cells expressing *G2-RAD5*. In agreement with our finding that G2-Rad5 fully supports DDT (**Fig. 26**), we found *G2-RAD5* cells were capable of entering into the following cell cycle and normally engaged into a second round of DNA replication after MMS treatment (PCNA SUMOylation accumulation in time-points 120-180 min; **Fig. 27B**), supporting the formation of viable colonies (**Fig. 27D**). Importantly, G2-Rad5 catalyzed similar to wild-type levels of PCNA polyubiquitylation, yet with a 30-minute delay (**Fig. 27B and 28**), indicating G2-Rad5 is absent from S-phase. Interestingly, phosphorylation of Rad53 followed identical kinetics to *rad5Δ* during S-phase and early G2/M (time-points 45-75; **Fig. 27B and 27C**), but quickly dropped to near wild-type levels following further recovery (time-points 90-120; **Fig. 27B and 27C**). Moreover, efficient repair of MMS-induced lesions also occurred with a visible delay (**Fig. 27E**), suggesting no unspecific DNA repair had taken place during S-phase in *G2-RAD5* cells. These results independently establish that G2-Rad5 is indeed excluded from S-phase, and that this exclusion only postpones DDT. Thus, the roles of Rad5 in DDT start already early in S-phase, but need not be limited to this phase of the cell cycle. Therefore we conclude that Rad5 has no essential role in DDT that is directly coupled to stalled forks.

### III.5.3 The *RAD6* Pathway Supports DDT in G2/M Specifically

As we described previously (paragraph III.5.1) the fact that Rad5 participates in so many diverse activities raises a question about the specificity of DDT



observed in *G2-RAD5* cells. Moreover, we were able to provide strong evidence that G2-Rad5 promotes DDT in a highly specific manner. We found that the cold-sensitivity of *pol32Δ* mutants, which depends on the *RAD6* pathway including Rad5; **Fig. 10A**), was supported by G2-Rad5 (**Fig. 29A**). Furthermore, G2-Rad5 promoted resistance to MMS in a manner dependent on *UBC13* (**Fig. 29B**), suggesting that G2-Rad5 specifically promotes error-free DDT. This result also implies that *G2-RAD5* is not favoring TLS over error-free DDT; *RAD5* over-expression can suppress the MMS sensitivity of *ubc13Δ* in a TLS-dependent manner (data not shown). To verify that G2-Rad5 is not affecting the regulation of

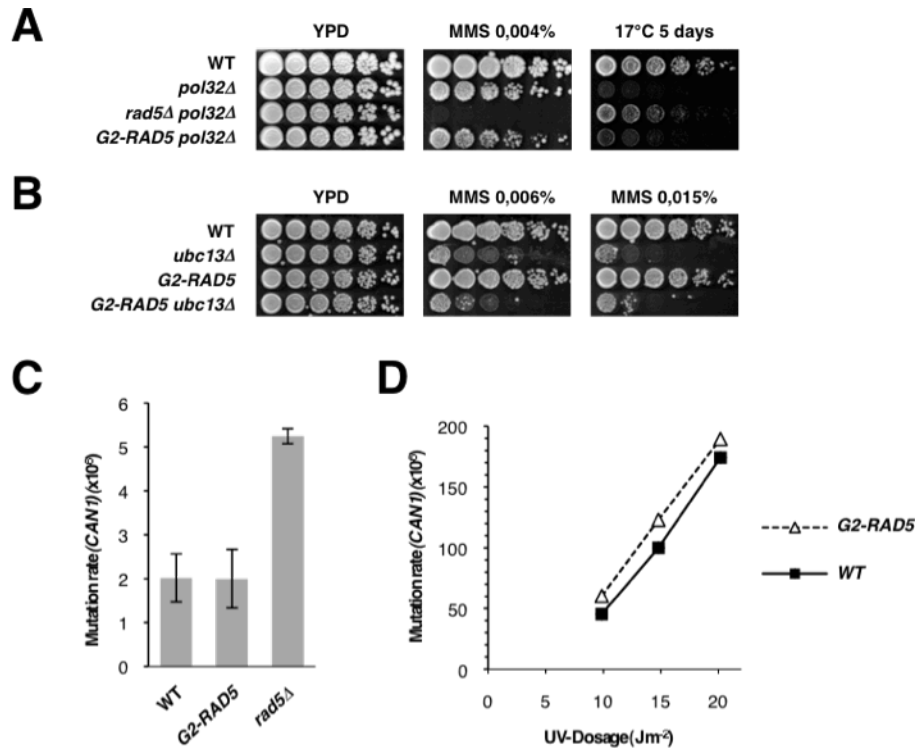


**Fig. 29: G2-Rad5 Specifically Induces Both Branches of The *RAD6* Pathway**

**(A)** Error-free DDT is fully supported by G2-Rad5 in cells lacking *POL32*. The critical contribution of *RAD5* to resistance to MMS and the cold-sensitivity of *pol32Δ* cells are unaltered by restriction of Rad5 to G2/M. Spotting of 1:5 serial dilutions on YPD agar at the indicated conditions. Plates were incubated for 2,5 days at 30°C or 5 days at 17°C.

**(B-C)** G2-Rad5 specifically mediates error-free DDT via PCNA polyubiquitylation. **(B)** Epistasis of *UBC13* over *G2-RAD5* in the presence of DNA MMS. Spotting of serial dilutions as in A. **(C)** Spontaneous mutagenesis is unaffected by restriction of Rad5 to G2/M. Plotted values represent averages and standard deviations from 2-7 independent experiments.

**(D)** G2-Rad5 supports its role in UV-induced TLS

TLS, we estimated mutation rates in its presence. Indeed, expression of *G2-RAD5* supports error-free DDT preventing the accumulation of spontaneous errors (**Fig. 29C**), and is capable of inducing error-prone DDT mutagenesis in response to UV-irradiation similarly to wild-type *RAD5* (**Fig. 29D**). From these findings we conclude that the *G2*-construct specifically promotes bona-fide error-free DDT via PCNA polyubiquitylation, and induced error-prone TLS. Thus, MMS- and *pol32Δ*-caused DNA defects, although they originate in S-phase, can be sensed and processed by Rad5-dependent DDT post S-phase. In conclusion, our data strongly suggest that all functions of Rad5, both error-free and error-prone DDT, including its ATPase activity are fully functional outside S-phase, and therefore not coupled to the replication fork.

## IV DISCUSSION

Since the discovery of DDT in the 60ies a large body of data has accumulated on the genetics and biochemistry of this pathway. We now appreciate the roles of many of the factors of DDT in securing genome stability and controlling mutagenesis. However, the actual DNA substrate on which DDT operates remains an issue of controversy in the field. Initially bacterial DDT was called post-replication repair (PRR), as was suggested to operate on ss-gaps left behind the two bacterial forks (Rupp and Howard-Flanders, 1968). 50 years later, the prevalent model rather suggests the opposing view that DDT operates directly at stalled forks to promote their recovery (“on-the-fly”) (**Fig. 30**).

Although the standing model is well-rooted textbook knowledge, “on-the-fly” DDT has not been firmly proven in any model organism. It can be assumed that a number of misconceptions may have led to the current view. The first wrong assumption is that DDT in eukaryotes must resemble that of prokaryotes. However, besides other important differences, eukaryotes employ two major pathways for DDT, governed by the *RAD52* and the *RAD6* epistasis groups, respectively. These pathways are genetically non-redundant and therefore may possibly operate on DNA intermediates of distinct size and/or structure. Thus, tolerance of replication stress in eukaryotes may not involve a single DNA substrate. Another issue is related to the approaches used for the study of fork stalling. In particular, DNA synthesis rates are often mistaken for fork progression rates, although DNA synthesis can also occur behind and uncoupled from the fork. Moreover, microscopy studies largely interpret replication stress-induced foci (eg. of PCNA, Rad18 or Pol  $\eta$ ) as sites of stalled replication, although the radius of these foci is large enough to accommodate DNA beyond the fork junctions. The third misconception is that proteins are often expected to “function” *in vitro* exactly as they do *in vivo*.

Considering these experiments, it became clear to us that the DNA substrate and thus the biological role of DDT remains an open question. Settling

this issue would significantly extend our understanding on replication stress tolerance, somatic hypermutation (Arakawa et al., 2006), genetic variation, evolution, and carcinogenesis (Friedberg, 2005).

#### IV.1 The G2 tag

To investigate the connection between DDT and the stalled fork one would require DDT mutants that have lost their ability to localize at stalled replication forks, but retain localization capacity to the rest of the genome. A simple survival assay for such mutants would directly address whether DDT necessarily has to operate at stalled forks or not (**Fig. 30**). To expel DDT from the fork experimentally, we developed a genetic tool, we named the “G2 tag”, to exclude components of the *RAD6* pathway from S-phase and restrict them to the G2/M-phase of the cell cycle. With this system we expected to uncouple *RAD6*-mediated DDT execution from DNA replication in a non-invasive manner.

##### IV.1.1 Evidence for the Validity and Efficiency of the G2 tag Strategy

The “G2 tag” approach employs the tagging of endogenous target ORFs with a sequence encoding the N-terminal domain of Clb2 and the characterized G2-specific promoter of *CLB2*. This combination is expected to restrict protein abundance to the G2/M phase of the cell cycle (**Fig. 17**). Importantly, characteristic activities that need to function during S-phase were not supported when the chimeras were expressed in this system, demonstrating that the G2 tag is not “leaky” but accurate for expression in G2/M. For example, Sgs1 besides its roles in homologous recombination also has activities that are coupled to the replication fork. We were able to fully dissect those functions by restricting Sgs1 to G2/M, demonstrating that G2-Sgs1 is defective in the S-phase checkpoint in *pol32Δ* cells (see section III.4.3). Moreover, G2/M-restricted Rad5 was unable to promote DDT during S-phase, as shown by the increased accumulation of DNA

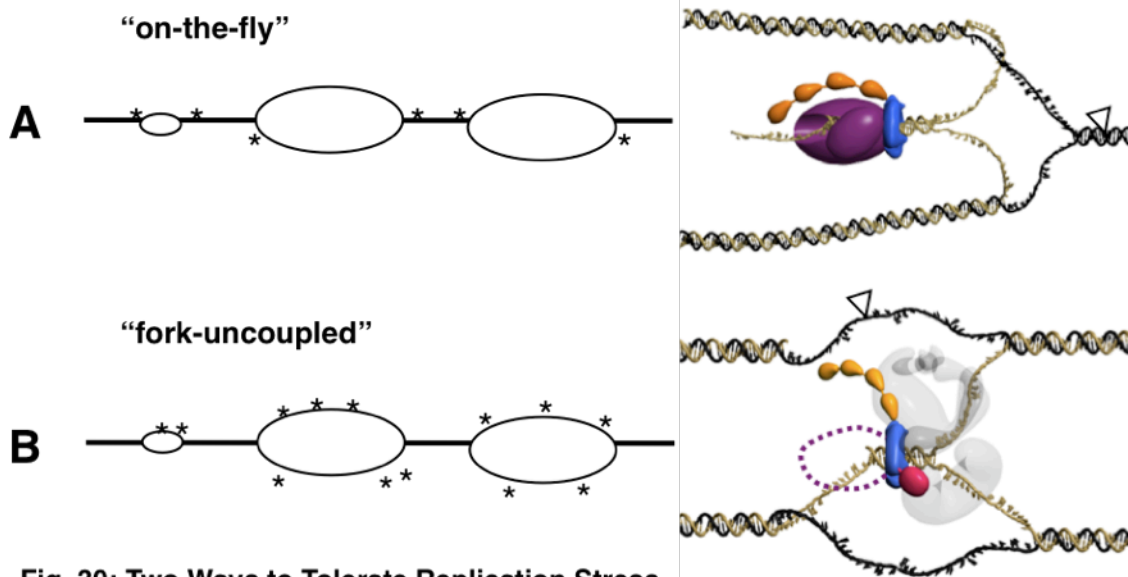


**Fig. 30: Two Ways to Tolerate Replication Stress**

Comparison between "on-the-fly" and "fork-uncoupled" DDT modes. Both mechanisms respond to replication blockade involving the accumulation of RPA-decorated ssDNA. On the left genome replication in the presence of replication stress is depicted, where asterisks (\*) indicate discrete tolerance events. On the right a hypothetical structure of the respective recombination intermediates of error-free DDT is shown. Arrowheads represent replication-blocking DNA lesions.

**(A)** "on-the-fly" DDT is co-replicative, and thus must take place directly at stalled forks. Error-free DDT may involve fork reversal (right), bypassing the requirement for the damaged template in DNA replication, by switching it to the likely intact nascent strand of the sister chromatid (DNA intermediate often referred as "chicken-foot"). Two eukaryotic error-free DDT factors, Rad5 and Sgs1, were shown to regulate the formation of this topologically very unstable DNA structure *in vitro* (see introduction). Error-prone DDT involves switching the replicative polymerase at the stalled fork to a complex of specialized polymerases ("mutagenic replication bypass") that can bypass the DNA lesion (TLS).

**(B)** "fork-uncoupled" DDT is post-replicative, involving ss-gaps containing the DNA lesion left behind restarted forks, where error-free recombination involving the sister-chromatid ("template switch" (TS); right) or mutagenic lesion bypass (TLS) can occur.

PCNA is shown in blue, the replicative polymerase in orange, ubiquitin in light orange, and SUMO in crimson.

damage and phosphorylated Rad53 (see section III.5.2). This behavior was reproducible at different MMS doses (0,02%- 0,05%), as well as using strains expressing *G2-RAD18* or *G2-UBC13* (data not shown). Therefore these results establish that the G2 tag depletes target proteins by confirming their absence from S-phase.

Despite the high efficiency of the G2 tag, tolerance to DNA damage in G2/M may theoretically still take place on forks that possibly have escaped S-

phase and persisted until G2/M (Weinert, 2007). However, the number of residual forks already in late S is apparently very low ( $\ll 10\%$ ) in unchallenged cells (Raghuraman et al., 2001; D. Collingwood, M. Raghuraman, and B. Brewer, personal communication published with permission from the authors). The same we observed even at a late-replicating DNA locus under conditions of replication stress (see section III.2.2), which are expected to have no impact on the timing of the genome replication program (Alvino et al., 2007). But even if a few forks could have escaped the S-phase surveillance mechanisms in these conditions, it seems unlikely that a diminutive fraction of forks in G2 can account for all DDT events (resistance to DNA damage and mutagenesis) triggered at hundreds of stalled forks throughout S-phase (Feng et al., 2006). Furthermore, we do not expect any increase in the number of forks entering G2 in DDT mutants and thus also not in cells expressing G2/M-restricted DDT components. It is important to note that the *RAD6* pathway operates on lesions in a genome-wide fashion (TLS: (Lawrence et al., 1974); *pol32Δ*: section III.1.4; MMS-lesions: section III.5.2). So if *RAD6* promoted stalled fork restart, then *RAD6* mutants would be expected to exhibit strong S-phase delays in the presence of replication stress. However, even in the presence of high-densities of uniformly distributed genomic DNA lesions (see *pol32Δ*: section III.1.4; MMS-lesions: section III.5.2) no S-phase delay, fork progression and stalled fork restart defects could be observed for cells deficient for PCNA ubiquitylation or Rad5 functions (see section III.2.3), or Rad18 and TLS polymerase functions (Branzei et al., 2008; Lopes et al., 2006).

Thus we conclude that applying the G2 tag on DDT components evidently uncouples DDT from DNA replication in an efficient and non-invasive manner.

#### IV.1.2 Advantages of the G2 tag

There are several major advantages associated with the G2 tag over conventional cell cycle analysis. First, it allows bypassing the requirement for cell synchronization for the study of events coupled to certain cell cycle phases.

Therefore we were able to quantitatively assess cell cycle specific mutagenesis and DNA damage tolerance in cycling cells, which is impossible using inducible promoters. Another important advantage is that the G2 tag alleviates the need for controlling the expression of our gene chimeras. Inducible expression, for example by galactose addition, at a certain level and stage during the cell cycle can only be very arbitrarily selected, and thus is extremely difficult to reproduce. Moreover, due to the imperfect synchronization of any population, every cell is at a different stage at the time of induction. On the contrary, the *CLB2* promoter is always and in every cell expressed at the same level and stage in the cell cycle, reducing the complexity of result interpretation while increasing reproducibility. A third advantage is that any protein can be subjected to G2 tagging as soon as it is at least to a certain extent nuclear (like the complete *RAD6* pathway). This limitation is based on the fact that APC/C-dependent ubiquitylation of Clb2 requires nuclear localization (Eluere et al., 2007; Hood et al., 2001).

## **IV.2 The DNA Substrate of *RAD6*-Mediated DDT**

### **IV.2.1 The *RAD6* Pathway Proceeds Uncoupled From The Replication Fork**

With this powerful tool in hand we could test the validity of the model that *RAD6* necessarily acts during S-phase. We found that the otherwise metabolically stable TLS polymerases Pol  $\eta$ /Rad30, and Rev3 (Waters and Walker, 2006) were fully capable of supporting survival in the presence of DNA damaging agents and mutagenesis when restricted to the G2/M phase of the cell cycle (see section III.3.2). This indeed suggests that TLS acts predominantly on DNA lesions that stay behind the moving fork. This conclusion is in line with previous findings in yeast showing that TLS polymerases do not facilitate fork progression (Lopes et al., 2006) and that Rev1 is strongly enriched during G2/M (Waters and Walker, 2006). Thus, it seems that at least yeast TLS polymerases operate usually outside bulk replication and that switching from replicative to TLS

polymerases may not normally function at stalled replication forks. An important exception may be repair of interstrand crosslinks (ICL) in S-phase, which requires replication fork-coupled TLS polymerase activities (Raschle et al., 2008). Such fork-coupled activities of TLS polymerases appear more pronounced in higher eukaryotes, with Rev1 and Pol  $\zeta$  participating in the restart of stalled forks (Edmunds et al., 2008; Jansen et al., 2009a; Jansen et al., 2009b).

Our genetic screen and previous work (Branzei et al., 2008) identified the RecQ-type helicase Sgs1 as an essential down-stream component of the error-free branch of DDT. Sgs1 is closely related to the human BLM, WRN, and RECQ4 RecQ-family helicases (mutation of which results in Bloom, Werner, and Rothmund-Thomson syndromes, respectively) and functions to dissolve topological DNA structures such as supercoils and catenanes and in the restart of stalled forks. We found that also Sgs1 and polyubiquitylated PCNA support error-free DDT if restricted to G2 (see sections III.4 and III.5). These findings directly challenge the view that Rad5 and/or Sgs1 promote DDT mediating fork regression. Moreover, establish the conclusion that proximal stalled or active forks are dispensable for PCNA ubiquitylation, explaining our difficulty to identify fork components required for this modification (see section III.1.1). Altogether these results provide strong support to the model that error-free DDT operates via template switching, involving SCJs, apparently across lesions that stay behind the moving replication fork (Branzei et al., 2008; Liberi et al., 2005; Lopes et al., 2006).

#### IV.2.2 The DNA substrate(s) of the *RAD6* Pathway

Our findings strongly suggest that stalled forks are able to restart leaving the polymerase-blocking lesions behind. Therefore tolerance mechanisms that promote fork restart must exist, involving re-priming at the discontinued nascent strand (**Fig. 31**). It is important to note that re-priming can occur on both lagging and leading strands (Lehmann and Fuchs, 2006), which suggests that such



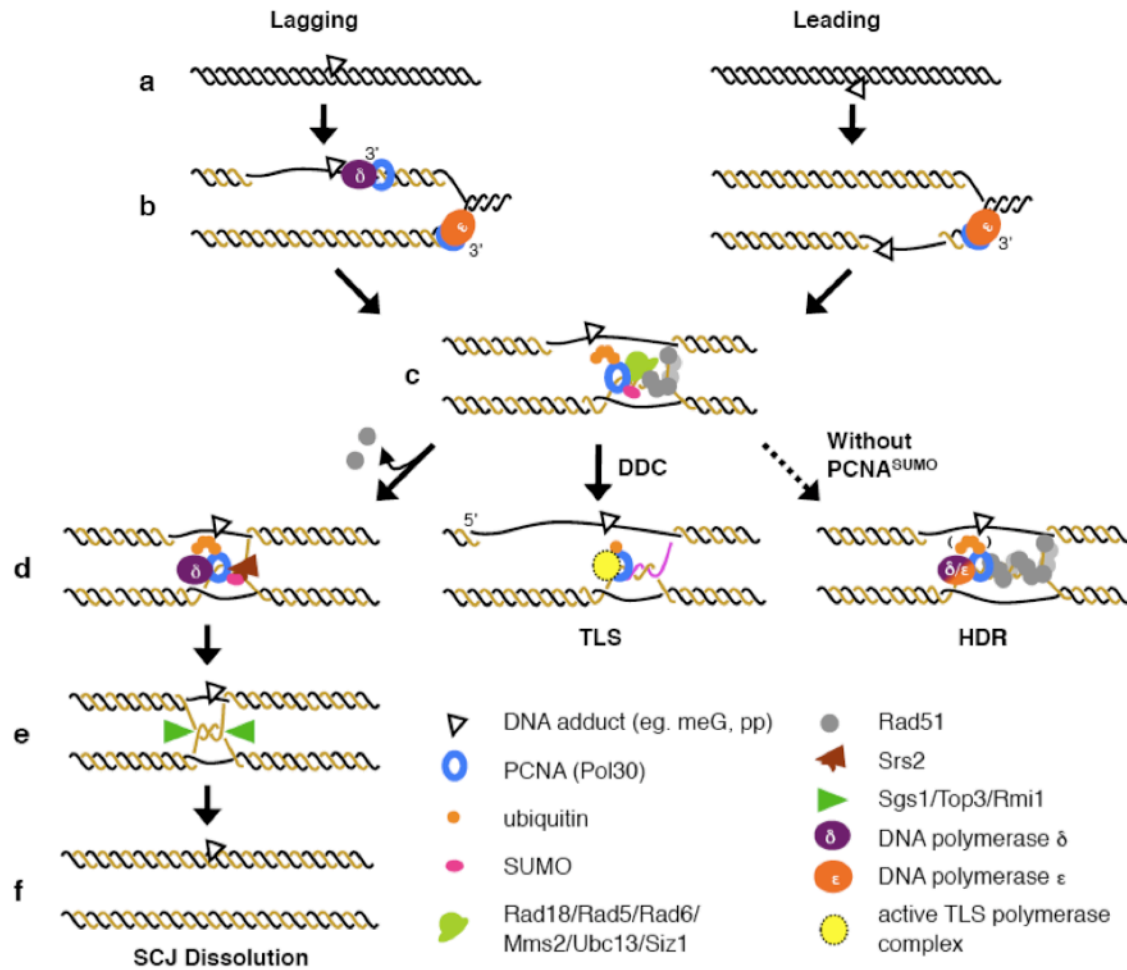


**Fig. 31: Hypothetical Model of Tolerance to Replication-Blocking DNA Lesions**

Bulky DNA adducts (eg. methylated bases and photoproducts) on the template strand (black) block DNA synthesis by the replicative polymerases (a). DDT is activated in an identical manner by lesions blocking the lagging-strand (b, left; Pol  $\delta$ ) or the leading-strand polymerases (b, right; Pol  $\epsilon$ ). Leading strand synthesis (yellow) stalling promotes re-priming downstream of the lesion, thereby leaving a ssDNA stretch (ss-gap) that contains the lesion behind. Similarly, ss-gaps are formed by lagging strand stalling (incomplete Okazaki fragments). The ss-gaps participate in D-loop formation (c; boxed Fig.), which are resolved by three different mechanisms. Modification of PCNA (blue ring) by SUMO (crimson) triggers recruitment of the helicase Srs2 (brown triangle), which removes the recombinase Rad51 (gray) from chromatin. The first mechanism (left row; d-g) involves polyubiquitylated (light orange) PCNA and sister chromatid junctions (SCJs), which are dissolved by the Sgs1-Top3-Rmi1 complex (green triangles). The second mechanism (middle row) is activated by the DNA damage checkpoint (DDC) and involves PCNA monoubiquitylation, which triggers the recruitment of specific TLS polymerases for induced TLS. The third mechanism (right row) is activated in the absence of PCNA SUMOylation (without PCNA<sup>SUMO</sup>). This pathway involves Rad51-dependent recombination and the resolution of double Holliday junctions (dHJ) involving the Sgs1-Top3-Rmi1 complex (green) or specific nucleases.

replication-coupled events would result in the formation of ss-gaps containing the DNA lesions. In fact, this is exactly the situation in cells lacking the Pol  $\delta$  subunit, Pol32, with the exception that these ss-gaps are unlikely to contain DNA adducts. These damages are capable of triggering PCNA ubiquitylation (see section III.1.4), suggesting they are key to *RAD6*-mediated DDT. Moreover, in DDT mutants, heat-labile MMS-induced DNA lesions persist in G2/M (see section III.5.2), supporting the view they occur on fork-uncoupled ss-gaps. Furthermore, TLS polymerases were shown to counteract the accumulation of ss-gaps behind replication forks (Lopes et al., 2006). The above findings suggest the ss-gap or a derivative ss-gap processing intermediate is the DNA structure that recruits the *RAD6* pathway.

Indeed it is currently difficult to tell whether *RAD6*-mediated DDT may actually gain access to the unreplicated ssDNA stretch directly or only after certain steps of ss-gap processing have occurred. In our model, the formation of a D-loop, which engages the undamaged sister duplex and the free 3'-end of a ss-gap, is crucial for all branches of DDT. In the absence of PCNA SUMOylation, this structure is the substrate for Rad51-mediated sister chromatid recombination (Papouli et al., 2005; Pfander et al., 2005). This is avoided by the anti-recombinogenic translocase activity towards the Rad51 nucleofilaments of the Srs2 helicase (Krejci et al., 2004; Pfander et al., 2005; Veaute et al., 2003). Polyubiquitylated PCNA may promote gap filling at D-loops and the subsequent formation of SCJs that will be finally dissolved by the Sgs1/Top3/Rmi1 complex. By contrast, monoubiquitylated PCNA promotes TLS through recruitment of TLS polymerases that bypass the lesion post-replicatively in an error-free or error-prone manner (**Fig. 31**).

On the other hand, the enigmatic helicase activity of Rad5 may operate on even more exotic DNA structures. Notably, epistasis between Rad5 and H2B (*htb-1*) has been observed (Martini et al., 2002), pointing towards a role for Rad5 in chromatin remodeling. In line with this view, the ATPase domain of Rad5 resembles that of the remodeler Rad54. It would be interesting to test whether

Rad5 can engage during recombination, and in a manner analogous to Rad54 promote remodeling of recombination intermediates (Heyer et al., 2006). Based on our results that restricting Rad5 to G2/M does not impact on the efficiency of DDT, it appears that the *in vitro* observed fork regression activity of its helicase domain could be an *in vitro* artefact. Nevertheless, torsional stress on fork-like structures may indeed lead to regression of naked DNA *in vitro*, but not of protein-coated forks *in vivo*. Clearly, addressing these questions would be important for the understanding of the roles of Rad5 in DDT.

It is intriguing to speculate that DDT of a single DNA lesion may involve several discreet steps, harboring the progressive remodeling of the damaged DNA substrate from a stalled fork into a ss-gap, and subsequently into recombination intermediates, reactions that may occur with distinct kinetics and at different times within the cell cycle.

### IV.3 Timing of DDT

Indeed, consecutive events during DDT can be observed. Although it has been proposed that polyubiquitylation of PCNA may follow its monoubiquitylation (Andersen et al., 2008), our data suggest that error-free DDT normally precedes any mutagenic event. A crucial argument comes from the finding that in the absence of Rad5 or Ubc13 we observed increased checkpoint activation for the same amount of exogenous DNA damage already during S and early G2 phases (see section III.5.2). This suggests that, although not necessarily coupled to replication, error-free DDT may usually commence during S-phase and continues (if necessary) during G2/M. These findings are in agreement with the kinetics of PCNA ubiquitylation (see section III.2.2) and the accumulation of SCJs during S-phase (Lopes et al., 2003). Moreover, by restricting the PCNA polyubiquitylation enzyme Rad5 to G2/M, we observed that the ability of newly polyubiquitylated PCNA to hold back MMS-induced checkpoint activation was further delayed (**Fig. 27C and 28**; in *G2-RAD5* expressing cells recovery of wild-type levels of

phosphorylated Rad53 is reached 30-60 min after the appearance of polyubiquitylated PCNA). This result may suggest that error-free DDT preferentially starts immediately after ss-gap formation in S-phase because it is a slow procedure.

The scenario is markedly different for TLS; although monoubiquitylated PCNA is equally abundant to its polyubiquitylated form, spontaneous or induced mutagenesis are very rare events, and cannot out-compete error-free DDT even after restriction of error-free DDT (Rad5) to G2/M (**Fig. 29C and 29D**). This implies that TLS-mediated DDT cannot start in S-phase, for it may require in addition to PCNA monoubiquitylation a second signal. In fact, the crucial component required for error-prone DDT, the DNA polymerase Rev1, is expressed largely during G2/M (Waters and Walker, 2006). The question is whether this cell cycle regulation of *RAD6*-mediated mutagenesis, or more generally, the fork-uncoupled mode of DDT, is of any relevance to the handling of replication stress.

#### **IV.4 The Biological Role of Fork-Uncoupled DDT**

Our findings suggest that the primary *raison d'être* for a post-replicative DDT mode is the ability to uncouple chromosomal replication from means that take care of DNA synthesis-blocking lesions. In fact, if all DDT (including the slow *RAD6* pathway; see section IV.3) had to initiate and complete DDT directly at stalled forks ("on-the-fly" model; **Fig. 30A**), it would delay replication, and thus potentially also induce genome instability (Cox et al., 2000). This might be especially relevant for eukaryotes, as replication of their genomes involves a very large number of forks. However, at least for budding yeast the detrimental effects of stalled fork accumulation do not appear to have been the driving force behind the evolution of fork-uncoupled DDT; even arrest in early S-phase due to the accumulation of hundreds of stalled forks in hydroxyurea (Feng et al., 2006)

results in a minor increase of the already low wild-type gross-chromosomal rearrangement (GCR) rate by 2-3-fold (Cobb et al., 2005).

On the other hand, fork-uncoupled tolerance to DNA damage may facilitate decision-making between error-free or error-prone modes. Mutagenesis is usually detrimental and thus many mechanisms have evolved to keep it restricted. The *RAD6* pathway offers an additional layer of control by introducing as a requirement for error-prone DDT monoubiquitylation of PCNA. However, as the abundance of monoubiquitylated PCNA does not correlate well with the activation of error-prone TLS even during G2/M when Rev1 is present (see section IV.3), there must exist mechanisms that control mutagenesis in a manner dependent on the total DNA damage load. A strong indication that cells indeed are able to “contemplate” on the DNA damage load is the multiphasic nature of induced mutagenesis. Results obtained from several organisms suggest that for a certain window of DNA damage doses the mutation rates increase exponentially (quadratic (Q) component; **Fig. 32** and (Abdulovic and Jinks-Robertson, 2006)), despite the fact that the number of DNA adducts increases linearly (Lawrence and Christensen, 1976). Intriguingly, mutagenesis is stimulated by the Mec1/ATR-dependent checkpoint response (Pages et al., 2009; Paulovich et al., 1998; Sabbioneda et al., 2007; Sabbioneda et al., 2005). A corollary of our conclusion is that the checkpoint pathway in question is not the conventional S-phase checkpoint, but rather the G2/M checkpoint that becomes activated by ss-gaps behind the replication fork. Indeed, the DNA damage checkpoint mediator Rad9 (homologue of the tumor suppressor BRCA1) facilitates error-prone DDT (Paulovich et al., 1998), and might be contributing to the quadratic kinetics of mutagenesis (**Fig. 32**). Importantly, “on-the-fly” tolerance to DNA damage does not allow total assessment of the DNA damage involved, as repair coincides with sensing (**Fig. 31**). In contrast, fork-uncoupled tolerance gives an opportunity to the cell to reflect on the total amount of DNA damage it has received and decide whether induction of mutagenesis is essential. The DNA damage threshold would have likely also evolved.

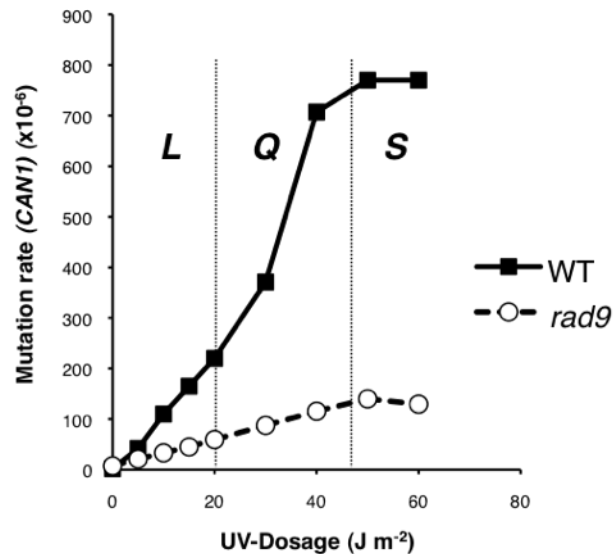


**Fig. 32: Hypothetic Biological Role of Post-Replicative DDT**

Fitting DNA damage induced mutagenesis to a multiphasic curve. The linear (L) and quadratic (exponential; Q) components are often followed by a super-linear (shoulder; S) when mutation rates decline. Because of the Q component it appears that cells know how much damage they received. This suggests “fork-uncoupled” DDT may not only control but also facilitate decision-making in collaboration with checkpoints or other pathways that are responsive to DNA damage. According to this model mutation of such mechanisms (eg. *rad9Δ*) is predicted to result in linearization of the quadratic component. Closed symbols represent data obtained from Abdulovic and Jinks-Robertson, 2006, and open are hypothetical data.

The molecular mechanism of the induction of mutagenesis still remains obscure, but it can be envisioned that is perhaps guided by the sizes of the ss-gaps located opposite of D-loops. It is therefore interesting to speculate that by evolving fork-uncoupled DDT mechanisms, eukaryotes may have acquired more effective means to control mutagenesis for desired hypermutation (eg. at the IgG locus), genetic adaptation, and speciation, while protecting their genome from “unscheduled instability” that can be detrimental and lead to pathology and cancer.

## V MATERIALS AND METHODS

Standard procedures for the following microbiological, molecular biological and biochemical techniques were followed (Ausubel and Struhl., 1994; Sambrock, 1989) based on the manufacturer's instruction where applied. For all methods described, deionized sterile water, sterile solutions and sterile flasks were used. Unless otherwise mentioned, chemicals and reagents were obtained from Amersham-Pharmacia, Applied Biosystems, Biomol, Biorad, Difco, Fluka, Invitrogen, Kodak, Merck, New England Biolabs, Promega, Roth, Roche, Serva, or Sigma.

### V.1 Computational analyses

For database searches (sequence search and comparison, literature research) electronic services provided by Saccharomyces Genome Database (<http://www.yeastgenome.org/>) and National Center for Biotechnology Information (<http://www.ncbi.nlm.nih.gov/>) were used. DNA and protein sequence analyses (DNA restriction enzyme maps, DNA sequencing analyses, DNA primer design, protein sequence comparison) were done with the DNA-Star software (DNA Star Inc.). Western-Blot films were digitalized with a scanner (AGFA Arcus II) and processed with the Adobe Photoshop software (Adobe Systems Inc.). For quantification of immunoblots and radiograms, the chemiluminescence and radioactivity signals were detected on film, scanned, and processed with the program Image Gauge V4.1 (Fujifilm). The percentage of Rad53 phosphorylation was calculated by dividing the level of (slower migrating) phospho-Rad53 by the level of total Rad53 (unmodified plus modified) for each time-point. The quantification shown in **Fig. 13A** gives values of band intensities (normalized to a loading-control) in relation to their maximum values. For the presentation of texts, tables, graphs and figures, the Microsoft Office software package 2008 (Microsoft Corp.) was used.

### V.2 Microbiological and genetic techniques

#### V.2.1 *E. coli* techniques

##### *E. coli* strains

XL1-Blue: hsd R17 rec A1 end A1 gyrA46 thi-1 sup E44 relA1  
lac [F' pro AB lacI<sup>q</sup>Δ M15 Tn10 (Tet<sup>r</sup>)] (Stratagene)  
BL21 (DE3)/RIL: B F<sup>-</sup> ompT hsdS (rB<sup>-</sup>mB<sup>-</sup>) dcm+ Tet<sup>r</sup> galλ (DE3) EndA  
Hte [argU ileY leuW Cam<sup>r</sup>] (Stratagene)

##### *E. coli* media

LB-medium / (plates): 1% Trypton (Difco)



0,5% yeast extract (Difco)  
1% NaCl  
(1,5% agar)  
sterilized by autoclaving

### **Cultivation and storage of *E. coli***

Liquid cultures were grown in LB media at 37°C with shaking at 200rpm. Solid cultures were grown on agar plates at 37°C. The selection of transformed bacteria was done by adding ampicillin (50µg/ml) to the media. The culture density was determined by measuring the absorbance at a wavelength of 600 nm (OD<sub>600</sub>). Cultures on solid media were stored at 4°C up to 7 days. For long-term storage, stationary cultures were frozen in 15% (v/v) glycerol solutions at –80°C.

### **Preparation of competent bacteria**

*E. coli* vectors were transformed into competent cells either by calcium chloride transformation or by electroporation. For the preparation of competent cells, 1L liquid LB medium was inoculated with 10ml of an overnight culture derived from a single *E. coli* colony and grown to an OD<sub>600</sub> of 0.6-0.8 at 37°C. The cultures were chilled in ice-cold water for 1h and cells were harvested by centrifugation (15 min, 5000g, 4°C). All following steps were performed at 4°C, with prechilled sterile materials and solutions. For the preparation of electrocompetent bacteria, sedimented cells were washed once with 1L water centrifuged and a second time with 0,5l water containing 10% (v/v) glycerol. After another centrifugation step, cells were resuspended in 3ml 10% (v/v) glycerol and stored in 100µl aliquots at –80°C. For the preparation of chemically competent cells, sedimented cells were carefully resuspended in 200ml MgCl<sub>2</sub> solution (100mM). The cells were repelleted by centrifugation, resuspended in 400ml CaCl<sub>2</sub> solution (100mM) and incubated in ice-cold water for 20 min. Finally, the competent cells were pelleted again by centrifugation, resuspended in 20ml 100mM CaCl<sub>2</sub> solution containing 10% (v/v) glycerol and stored in 100µl aliquots at –80°C.

### **Transformation of plasmid DNA into bacteria cells**

Shortly before transformation, competent cells were thawed on ice. For electroporation, 20-25µl competent cells were mixed with 10ng plasmid DNA or 2µl ligation sample dialyzed against water. The suspension was electroporated in a pre-chilled cuvette (0,1cm electrode gap) with a pulse of 1,8kV and 25µF at a resistance of 200W. Cells were recovered in 1ml LB medium, incubated on a shaker at 37°C for 1h and plated on antibiotic-containing LB agar plates overnight at 37°C. For chemical transformation, 50µl competent cells were mixed with 10ng plasmid DNA and incubated on ice for 30 min. A 42°C heat shock was performed for 45s, followed by a 2min incubation on ice. For recovery, 1ml pre-warmed LB medium without antibiotics was added, and cells were incubated on a shaker at 37°C for 1h. Transformed cells were selected by plating the cell suspension on antibiotic-containing LB agar plates and incubating the plates over-night at 37°C.

## V.2.2 *S. cerevisiae* techniques

### Yeast plasmids

pYIplac211 (V0009)	(Gietz and Sugino, 1988)
pYM-N32	( <i>EUROSCARF</i> )
pGAL- <sup>myc</sup> RAD30 (D2501)	(Lucian Moldovan unpublished plasmid)
pYIplac211 <i>pADH<sup>HIS</sup>POL32-tADH</i> (D2503)	(Moldovan, 2006)
pGBT9, pGAD424	(Bartel et al., 1993)
pGBT9-Pol30	(Hoege et al., 2002)
pGAD424-Rad18	(Ulrich and Jentsch, 2000)
pGAD424-Rad5	(Ulrich and Jentsch, 2000)
pGIK43 (D3218)	(this study)

### Yeast plasmid construction

Plasmid pGIK43 was constructed in two steps. First, the *GAL* promoter of plasmid pYM-N31 (*EUROSCARF*) was replaced (by digestion with *SacI* and *XbaI*) by a 1,4 kb PCR product containing the promoter (886 bp upstream) and 540 bp downstream of the start codon of the *CLB2* gene amplified using purified genomic DNA as template. Subsequently, the L26A alteration was created by site-directed mutagenesis. Phusion High-Fidelity polymerase was used for all PCR reactions and restriction enzymes were purchased from *NEB*.

### Yeast strains

*S. cerevisiae* yeast strains used in this study are listed below. All strains are haploid and isogenic to DF5, unless indicated otherwise.

### *S. cerevisiae* strains

Strain	Relevant Genotype	Reference
DF5/Y0003	<i>MATa trp1-1 ura3-52 his3Δ200 leu2-3,11 lys2-801 CAN1 BAR1</i>	(Ulrich and Jentsch, 2000)
Y0618	<i>mms2::HIS3MX6</i>	(Ulrich and Jentsch, 2000)
Y0720	<i>mms2::HIS3MX6 rad30::HIS3MX6</i>	SJ strain collection library
Y0797	<i>YCplac211 pGAL<sup>myc3</sup>RAD30</i>	This study
YGK211	<i>rad5::natNT2</i>	This study
YGK381	<i>sgs1::kanMX6</i>	This study
YGK431	<i>mms2::HIS3MX6 sgs1::kanMX6</i>	This study
YGK569	<i>pol32::kITRP1</i>	This study
YGK571	<i>mms2::HIS3MX6 pol32::kITRP1</i>	This study
YGK599	<i>mms2::HIS3MX6 siz1::kanMX6</i>	This study
YGK761(SL)	<i>mms2::URA3 pol32::natNT2</i>	This study
YGK771	<i>pol30-K164R::kanMX6 pol32::kITRP1</i>	This study
YGK797	<i>YCplac211 pGAL<sup>myc3</sup>RAD30</i>	This study

YGK877	<i>rad17::HIS3MX6</i>	This study
YGK893	<i>rad24::HIS3MX6</i>	This study
YGK960	<i>rad9::URA3</i>	This study
YGK1076	<i>ubc13::hphNT1</i>	This study
YGK1078	<i>ubc13::hphNT1 pol32::kITRP1</i>	This study
YGK1119	<i>mrc1::HIS3MX6</i>	This study
YGK1125	<i>MRC1<sup>HA3</sup>::HIS3MX6</i>	This study
YGK1127	<i>ubc13::hphNT1 MRC1<sup>HA3</sup>::HIS3MX6</i>	This study
YGK1195	<i>pGAL-<sup>HA3</sup>SGS1::natNT2</i>	This study
YGK1197	<i>pol32::kITRP1 pGAL-<sup>HA3</sup>SGS1::natNT2</i>	This study
YGK1198	<i>ubc13::hphNT1 pol32::kITRP1 pGAL-<sup>HA3</sup>SGS1::natNT2</i>	This study
YGK1199	<i>rad30::HIS3MX6</i>	This study
YGK1234	<i>cdc2-2</i>	This study
YGK1295	<i>bar1::HIS3MX6 pol32::kITRP1</i>	This study
YGK1297	<i>bar1::HIS3MX6 ubc13::hphNT1 pol32::kITRP1</i>	This study
YGK1353	<i>G2-SGS1::natNT2</i>	This study
YGK1354	<i>rev3::kITRP1</i>	This study
YGK1356	<i>mms2::HIS3MX6 rev3::kITRP1</i>	This study
YGK1362	<i>pol30-K164R::kanMX6</i>	This study
YGK1366	<i>bar1::HIS3MX6 pol30-K164R::kanMX6 pol32::kITRP1</i>	This study
YGK1378	<i>G2-UBC13::natNT2</i>	This study
YGK1398	<i>G2-RAD30::natNT2</i>	This study
YGK1407	<i>mms2::HIS3MX6 G2-REV3::natNT2</i>	This study
YGK1434	<i>G2-RAD5::natNT2</i>	This study
YGK1435	<i>ubc13::hphNT1 G2-RAD5::natNT2</i>	This study
YGK1436	<i>pol32::kITRP1 G2-RAD5::natNT2</i>	This study
YGK1460	<i>G2-RAD18::natNT2</i>	This study
YGK1494	<i>pol32::kITRP1 G2-SGS1::natNT2</i>	This study
YGK1499	<i>rev3::kITRP1 rad30::HIS3MX6</i>	This study
YGK1512	<i>rad30::HIS3MX6 G2-REV3::natNT2</i>	This study
YGK1513	<i>pol30-K164R::kanMX6 pol32::kITRP1 pGAL-<sup>HA3</sup>SGS1::natNT2</i>	This study
YGK1514	<i>rad18::kITRP1</i>	This study
YGK1515	<i>mms2::HIS3MX6 siz1::kanMX6 rad18::kITRP1</i>	This study
YGK1520	<i>mms2::HIS3MX6 siz1::kanMX6 G2-RAD18::natNT2</i>	This study
YGK1522	<i>mms2::HIS3MX6 siz1::kanMX6 G2-REV3::natNT2</i>	This study
YGK1523	<i>pol30-K164R::kanMX6 G2-RAD18::natNT2</i>	This study
YGK1536	<i>rev3::kITRP1 G2-RAD30::natNT2</i>	This study
YGK1537	<i>mms2::HIS3MX6 G2-RAD30::natNT2</i>	This study
YGK1541	<i>G2-REV3::natNT2</i>	This study
YGK1544(2H)	<i>YCplac211</i>	This study
YGK1545(2H)	<i>YCplac211 pADH-<sup>HIS</sup>POL32</i>	This study
YGK1562	<i>rad6::HIS3MX6 pol32::kITRP1</i>	This study
YGK1563	<i>rad5::natNT2 pol32::kITRP1</i>	This study

YGK1564	<i>rad18::klTRP1 pol32::hphNT1</i>	This study
YGK1613	<i>pol30-K164R::kanMX6 MRC1<sup>HA3</sup>::HIS3MX6</i>	This study
YGK1614	<i>mms2::HIS3MX6 G2-REV3::natNT2 G2-RAD30::natNT2</i>	This study
YGK1615	<i>G2-REV3::natNT2 G2-RAD30::natNT2</i>	This study
YGK1597 (E134)	<i>WT</i>	Pavlov, 2001
YGK1598 (E134)	<i>pol1-Y869A pms1D::LEU2</i>	Pavlov, 2001
YGK1599 (E134)	<i>pol2-Y831A</i>	Pavlov, 2001
YGK1600 (E134)	<i>pol3-Y708A</i>	Pavlov, 2001

**(SL)** Strain YGK761 is a derivative of BY5563 (S288C background) (Tong et al., 2001)

**(2H)** strains derived from pj69-7A (genotype; reference) by integration of the indicated vectors.

**(E134)** Strains isogenic to E134 (YGK1597) described in (Pavlov et al., 2001).

Strains were prepared by genetic crosses and standard techniques (Janke et al., 2004; Knop et al., 1999). Strain YGK761 was derived from strain BY5563 (*EUROSCARF*) by two consecutive PCR disruptions (Lorenz et al., 1995). *GAL-SGS1* harbors a short version of the *GAL* promoter (*GALs*), which exhibits reduced leakiness in glucose (Janke et al., 2004) (vector pYM-N32 *EUROSCARF*). For tagging genes with the G2-tag, plasmid pGIK43 was used. Strains bearing complete deletion of the ORF of *SLX4*, *ESC4* or *CTF4* were obtained from *EUROSCARF*.

### ***S. cerevisiae* media and solutions**

YPD / YPGal [plates]:      1% (10 mg/ml) yeast extract (Difco)  
    2% (20 mg/ml) bacto-peptone (Difco)  
    2% (20 mg/ml) D-(+)-glucose or galactose  
    [2% (20 mg/ml) agar]  
    sterilized by autoclaving

YPD G418/NAT plates:      After autoclaving, YPD medium with 2% agar was cooled to 50°C, and G418 (geneticine disulphate; Sigma) to 250 mg/L or NAT (nourseothricin, HKI Jena) to 100mg/L was added.

SC-media [plates]:            0,67% (6,7 mg/ml) yeast nitrogen base (Difco)  
    0,2% (2 mg/ml) drop out amino acid mix (according to the requirements)  
    2% (20 mg/ml) carbon source (glucose, raffinose, or galactose)  
    [2% (20 mg/ml) agar]

SC-5'FOA plates: 0,67% (6,7 mg/ml) yeast nitrogen base (Difco)  
0,2% (2 mg/ml) drop out amino acid mix  
(according to the requirements)  
3% (30 mg/ml) adenine  
3% (30 mg/ml) uracil  
2% (20 mg/ml) glucose  
2% (20 mg/ml) agar  
After autoclaving, the mixture was cooled to 50°C,  
and 5'FOA was added to the final concentration of  
0,1% (1mg/ml).

drop out amino acid mix: 20 mg Ade, Ura, Trp, His  
30 mg Arg, Tyr, Leu, Lys  
50 mg Phe  
100 mg Glu, Asp  
150 mg Val  
200 mg Thr  
400 mg Ser

Sporulation medium: 2% (w/v) potassium acetate (in sterile water)

SORB: 100 mM LiOAc  
10 mM Tris-HCl, pH 8,0  
1 mM EDTA, pH 8,0  
1 M sorbitol  
sterilized by filtration

PEG: 100 mM LiOAc  
10 mM Tris-HCl, pH 8,0  
1 mM EDTA, pH 8,0  
40 % (w/v) PEG-3350  
sterilized by filtration, stored at 4°C

Zymolase 100T solution: 0,9 M sorbitol  
0,1 M Tris-HCl, pH 8,0  
0,2 M EDTA, pH 8,0  
50 mM DTT  
0,5 mg/ml zymolase 100T (ICN Biochemicals)

### **Cultivation and storage of *S. cerevisiae***

Liquid cultures were inoculated with a single yeast colony from freshly streaked plates and grown overnight. In general, the main culture was inoculated with this starter culture at a dilution of 1:100 – 1:1000 and grown until the culture had reached the mid-log phase growth ( $1-3 \times 10^7$  cells/ml). Liquid cultures were grown

at 30°C (temperature sensitive strains at 23°C), in an incubator with shaking at 150-250rpm. The culture density was determined photometrically (OD<sub>600</sub> of 1 is equal to 1,5x10<sup>7</sup> cells/ml). Cultures on agar plates were stored at 4°C up to 1-2 months. For long-term storage, stationary cultures were frozen in 15% (v/v) glycerol solutions at -80°C (Sherman, 1991).

### **Preparation of competent yeast cells**

Cells from a mid-log phase growing culture were harvested by centrifugation (500g, 5 min, room temperature), washed first with 1/5 volume sterile water and then with 1/10 volume SORB solution and resuspended in 360µl SORB solution. After addition of 40µl carrier DNA (salmon sperm DNA, 10mg/ml, Invitrogen), competent cells were stored in 50µl aliquots at -80°C.

### **Transformation of yeast cells**

For transformation, 0,2µg of circular or 2µg linearized plasmid DNA or PCR product was mixed with 10µl or 50µl competent cells, respectively. 6 volumes of PEG solution were added and the cell suspension was incubated at 30°C for 30min. Subsequently, DMSO (final concentration 10%) was added and a heat shock performed at 42°C for 15min. Cells were sedimented by centrifugation (400g for 3min at room temperature) resuspended in 100µl sterile water and plated on the respective SC medium plates. If G418 or Nat were used for selection, transformed cells were first shaken for 3h in liquid YPD medium before plating. Selection of transformants was carried out for 2-3 days at 30°C (or 23°C for temperature sensitive strains). If necessary, transformants were replica-plated on selection plates to remove the background.

### **Genomic integration by homologous recombination**

The Ylplac vector series (Gietz and Sugino, 1988) can be used for the integration of a gene in the yeast genome (integrative transformation). These vectors contain no autonomous replication elements, thus only vectors stably integrated are propagated in yeast. Before transformation, vectors were linearized with the help of a restriction enzyme, which cuts only in the auxotrophy marker gene. Linearized plasmids are inserted in the endogenous locus of the marker gene by homologous recombination.

Chromosomal gene deletions or insertions of epitope tags were performed by a PCR strategy (Janke et al., 2004; Knop et al., 1999; Longtine et al., 1998). The oligonucleotides used contain sequences for amplification of special cassettes, which contain marker genes and target complementary sequences, which allow homologous recombination within the endogenous locus. For gene deletions, the forward primer contains 55bp of the promoter sequence 5' of the start ATG, while the reverse primer has 55bp of the terminator sequence 3' of the stop codon. For the insertion of C-terminal epitope tags, the forward primer contains 55bp 5' of the stop codon instead. After amplification of the cassette, the PCR product was purified by ethanol precipitation and transformed into competent cells.

Recombination leads to replacement of the ORF by a marker gene in the case of gene deletions, while in the case of epitope tag insertion, the STOP codon of the target gene is replaced by the epitope sequence and a marker gene. The correct recombination event was identified by PCR for gene deletions and Western blot for epitope tagging.

### **Mating type analysis of haploid strains**

For mating type identification, the tester strains RC634a and RC75-7 $\alpha$  were used. These strains are hypersensitive to the pheromone secreted by the opposite mating type strain. 50 $\mu$ l of an aqueous cell suspension of each tester strain was mixed with 5ml molten agar (1% w/v), which has been cooled to 45°C, and poured over a YPD plate. Plates containing cultures to be analyzed were replica plated on the a- and  $\alpha$ -tester plates. The tester cells cannot grow in proximity of cells of different mating type. Therefore, after 1-2 days of incubation, a halo of clear agar appears around the colony, if the mating type of the tester strain is different. Diploid cells do not secrete any mating type pheromones, therefore no halo is formed on any mating type tester plate.

### **Mating of haploid *S. cerevisiae* strains**

Haploid strains of opposite mating types (MATa, MAT $\alpha$ ) grown to mid-log growth phase were mixed by spotting 10 $\mu$ l of each on a pre-warmed YPD plate and grown overnight. Cells were streaked on YPD or selection plates and diploids were identified by mating type analyses.

### **Sporulation and tetrad analysis of diploid *S. cerevisiae* strains**

Diploid cells of a 36h stationary culture (500 $\mu$ l) were harvested by centrifugation (500g, 3 min), washed 4 times with sterile water, resuspended in 4ml sporulation medium and incubated on a shaker at 23°C. After 3 days, 10 $\mu$ l of the sporulation culture was mixed with an equal volume of zymolase-100T solution and incubated at 23°C for 7 min. The spores were dissected in tetrads with a micromanipulator (Singer MSM Systems). Germination and growth of the spores were carried out on non-selective YPD plates for 2-3 days. Tetrades were analyzed genotypically by replica plating on selection plates and for known phenotypes, where applicable.

### **Analyses of protein-protein interactions with the Two-Hybrid System**

The two proteins analyzed for interaction were fused to the DNA-binding and, respectively, the activation domain of the Gal4 transcription factor. The expression constructs of the fusion proteins were transformed in PJ69-7A cells (James et al., 1996). An interaction between the two proteins results in the reconstitution of the Gal4 transcription activator. Thus, the expression of reporter genes under the control of Gal4 (i.e. HIS3, ADE2) is turned on, and cells can grow on the respective selection media.

**Synchronization by  $\alpha$ -Factor or Nocodazole**

Yeast cultures were 1:400 inoculums from overnight cultures. All cultures were grown in YP-media containing glucose (2%) as carbon source, with the exception of **Fig. 23-25**, where raffinose and galactose were used instead, as indicated. In order to facilitate adaptation of the DF5 strains to the non-fermentable carbon sources, single colonies were pre-streaked 2-3 times on SC + Raf (2%) + Gal (2%) plates. Synchronization of *MATa BAR1* cells was performed by the addition of 10  $\mu$ M  $\alpha$ -factor mating pheromone into mid-exponential cultures ( $OD_{600} = 0,35$ ) and incubation for 2-3 h at 30°C. For *bar1 $\Delta$*  cells (**Fig. 13**)  $\alpha$ -factor was used at 200nM and release was achieved by addition of pronase (25  $\mu$ g/ml; CALBIOCHEM). G1-arrest was verified microscopically and by FACS analysis. Cells were released into the cell cycle by washing two times in sterile water and two times in fresh YPD at 23°C to remove  $\alpha$ -factor. Cell cycle arrest in G2/M was performed by adding 15  $\mu$ g/ml of the microtubule de-polymerizing agent nocodazole (*SIGMA-ALDRICH*) into mid-exponential cell cultures and incubating at 30°C for 2 hours. Cells arrested in this way were released by washing twice in YPD at 23°C. At the time of the release OD at 600 nm were measured for each parallel culture and corresponding culture volumes were collected for further analysis at every time-point thereafter. Released cultures were grown at the indicated temperatures in pre-warmed or pre-chilled media accordingly.

**Cell Survival Assays**

Qualitative spotting assays were performed from overnight YPD cultures on YPD agar plates, applying  $5 \times 10^4$  cells and consecutive 1:5 serial dilutions. Plates were incubated for 2,5 days at 30°C, 5 days at 17°C, and 9 days at 14°C, unless indicated otherwise, and images were obtained. Treatment of asynchronous cultures with MMS (0,02%) or HU (200 mM) was for 2 h at 30°C, unless mentioned otherwise. For synchronous cultures, MMS was added to G1-arrested cells at 23°C, as indicated and appropriate dilutions were plated on YPD plates to estimate survival rates. Subsequently, the cultures were exposed to sodium thiosulfate (5% final concentration) to inactivate MMS, and were released into the cell cycle. For all other quantitative plating assays, single colony inoculums were grown at 30°C overnight in YPD, subsequently set to  $OD_{600} = 0,625$  in 1 ml sterile water (approximately  $10^7$  cells) and were further diluted appropriately for plating on YPD plates. UV survival curves were estimated after UV irradiation of cells plated on YPD plates in appropriate dilutions. UV-irradiation with the indicated doses was performed within an hour after plating using a UV lamp (254nm) under the constant irradiation rate of  $2,2 \text{ J} \times \text{m}^{-2} \times \text{s}^{-1}$ , plates were incubated in the dark (to avoid photoreactivation) for 2-3 days at 30°C and colonies were counted. Averages were obtained from 2-3 independent experiments.



**Mutagenesis assays**

For estimating rates of spontaneous and UV-induced forward mutagenesis we employed the *CAN1* gene locus. *CAN1* encodes the plasma membrane permease for basic amino-acids (Lysine, Arginine, and Histidine), which in addition can promote the uptake of the toxic Arginine analogue, canavanine. Canavanine incorporation into polypeptides disturbs protein functionality and causes lethality at a concentration > 10-30 mg/ml. Forward mutations take place at the *CAN1* locus (Cassier-Chauvat et al., 1991) and result in loss of function of the Can1 transporter (*can1*) (Grenson et al., 1966). 10 individual YPD cultures were inoculated with a very small number of cells (1:20000 dilution of an overnight culture) that should contain the smallest number of inactivating mutations at the *CAN1* locus possible (usually cultures should contain no such mutation). Cultures were incubated with constant shaking at 30°C for 36 hours, in order to promote the acquisition of additional mutations – some of which at the *CAN1* locus – and appropriate dilutions were washed with sterile water and were plated on YPD plates or SC-Arg+CAN (60 mg/ml). Spontaneous mutation frequencies (number of mutants in culture) were calculated using a fluctuation test (Rosche and Foster, 2000) and the mutation rates were estimated using a maximum-likelihood approach. UV-induced rates were calculated as the ratio of the number of colonies on canavanine plates to the number of total surviving colonies (each plating step was done in triplicates in parallel) (Stelter and Ulrich, 2003). UV-irradiation with the indicated doses was performed within an hour after plating using a UV lamp (254nm) under the constant irradiation rate of  $2,2 \text{ J} \times \text{m}^{-2} \times \text{s}^{-1}$ , plates were incubated in the dark (to avoid photoreactivation) for 2-3 days at 30°C and colonies were counted. Averages were obtained from 2-7 independent experiments.

**Flow cytometry**

For FACS analysis, approximately  $7 \times 10^6$  cells for each time-point were collected, washed in sterile water, and permeabilized in 70% ethanol. Cells were suspended in 10 mM Tris pH 7,5 buffer, and RNA and proteins were removed by RNaseA (0,4 mg/ml final concentration) and proteinase K (1 mg/ml) treatment (*SIGMA-ALDRICH*). Subsequently, cells were stained in SYTOX green (1  $\mu\text{M}$ ) (*Invitrogen*) solution or PI (propidium iodide 50  $\mu\text{g/ml}$ ) (*SIGMA-ALDRICH*) as indicated. SYTOX allows for more accurate cell cycle analysis (Haase and Reed, 2002). Cell cycle profiles were obtained at the FL1 channel (voltage 520; gain 1,00) using a FACSCalibur system operated via the CELLQuest software (Becton Dickinson). Data was analyzed quantitatively with FlowJo (Tree Star).

**Pulse-field gel electrophoresis**

For preparation of PFGE samples,  $4,5 \times 10^7$  cells were treated with sodium azide (0,1% final concentration) and embedded in 1% low-melting agarose (*BIO-RAD*) plugs. Cells were lysed in the gel by incubation with zymolase 100T (1 mg/ml; *SEIKAGAKU*) for 1 h at 37°C and treatment with proteinase K (*SIGMA-*

*ALDRICH*) at 50°C for 36 h. The plugs were then loaded on a 1% agarose gel (*BIO-RAD*) and genomic DNA was resolved using a CHEF-DR III system (*BIO-RAD*) according to the manufacturer's instructions. Gels were stained in 1% ethidium bromide for 1 h and photographed under UV light.

### **Robot-based deletion library screening**

Automated systematic genetic analysis was performed using a library of non-essential deletion mutants (*EUROSCARF*) and the robotic system Biomek FX (*BECKMAN COULTER*). Mating, sporulation, haploid selection, and spore selection were performed on plate by pinning on a 356-format using the robotic system Biomek FX (*BECKMAN COULTER*) essentially as described before (Tong et al., 2001), with the exception that sporulation was prolonged to 14 days. The final spore selection was performed either on plates lacking uracil to select for triple deletion mutants (*mms2Δ pol32Δ xΔ*) or on plates containing 5'-FOA (Boeke Fink Methods Enzymol. 1987) and uracil to allow the growth only of the double deletion mutants (*pol32Δ xΔ*), which retain a WT copy of *MMS2* (**Fig. 22**). Plates were scanned after 3 days of incubation at 23°C and were manually inspected for synthetic interactions.

## **V.3 Molecular biology methods**

### **General buffers and solutions**

TE buffer:	10 mM Tris-HCl, pH 8,0 1 mM EDTA sterilized by autoclaving
TBE buffer 5x:	90 mM Tris 90 mM boric acid 2,5 mM EDTA, pH 8.0 sterilized by autoclaving
DNA loading buffer 6x:	0,5% (w/v) SDS 0,25% (w/v) bromophenol blue or orange G 0,25% (v/v) glycerol 25 mM EDTA, pH 8,0

### **V.3.1 Isolation of DNA**

#### **Isolation of plasmid DNA from *E. coli***

Plasmid DNA was isolated using commercially available kits from either Qiagen (Plasmid Mini Kit) or Macherey-Nagel (Nucleospin Plasmid Quick Pure) according to the manufacturers' instructions. For small DNA preparations

(minipreps) 4ml overnight culture was used, while 500ml cultures were employed for large preparations (maxipreps).

#### **Isolation of plasmid DNA from *S. cerevisiae***

Lysis buffer:                    1% (v/v) SDS  
                                      10 mM Tris-HCl, pH 8,0  
                                      1 mM EDTA, pH 8,0

A fast and easy protocol was used for isolation of plasmid DNA from a transformed yeast strain and its direct propagation in *E. coli*. A single yeast colony was resuspended in 50µl lysis buffer, and, after addition of 50µl phenol/chloroform/isoamyl alcohol (24:24:1 v/v/v; Roth), the liquid volume was filled with acid-washed glass-beads (Ø 425-600µm; Sigma). Cells were lysed by vortexing 1-2min at highest speed. The DNA was recovered by centrifugation at high speed for 3min at room temperature. 0,5µl of the aqueous phase, containing the DNA, were subsequently transformed into *E. coli*.

#### **Isolation of chromosomal DNA from *S. cerevisiae***

Breaking buffer:                2% (v/v) Triton X-100  
                                      1% (v/v) SDS  
                                      100 mM NaCl  
                                      10 mM Tris-HCl, pH 8,0  
                                      1 mM EDTA, pH 8,0

Yeast genomic DNA was prepared to be used as template for amplification of genes via PCR. Cells from a stationary (36h) culture (10ml) were pelleted by centrifugation (1500g, 5 min, 23°C), washed once in 0,5ml water and resuspended in 200µl breaking buffer. Subsequently, 200µl phenol/chloroform/isoamyl alcohol (24:24:1 v/v/v; Roth) and 300mg acidwashed glass beads (Ø 425-600µm; Sigma) were added, and the mixture was vortexed 5 min. The lysate was mixed with 200µl TE buffer, centrifuged for 5 min at 14000rpm at 23°C and the aqueous layer transferred to a microcentrifuge tube. DNA was precipitated by addition of 1ml ethanol (100%) followed by centrifugation at 14000rpm for 3 min at 23°C. The pellet was resuspended in 0.4ml TE buffer and RNA contaminants were destroyed by treatment with 30µl of DNase-free RNase A (1 mg/ml) for 5 min at 37°C. Afterwards, DNA was re-precipitated by mixing with 10µl ammonium acetate (4M) and 1ml ethanol (100%). After a brief centrifugation, the pellet was resuspended in 100µl TE buffer. The yield of isolated DNA was determined photometrically.

#### **Precipitation of DNA**

For ethanol precipitation, 1/10 volume sodium acetate (3M, pH 4,8) and 2,5 volumes ethanol were added to the DNA solution and incubated at -20°C for 30 min. The mixture was then centrifuged at 16000g, at 4°C for 20 min. The DNA

pellet was washed once with 0,5ml 70% ethanol. After centrifugation, the DNA was air-dried and resuspended in an appropriated volume of TE buffer or sterile water.

### **Determination of DNA concentration**

The DNA concentration was determined photometrically, by measuring the absorbance at  $\lambda=260\text{nm}$ . An OD<sub>260</sub> of 1 represents a concentration of 50 $\mu\text{g/ml}$  double-stranded DNA.

### **2D gel analysis of replication intermediates**

Cells were killed in 0,1% sodium azide and immediately chilled on frozen 0,2M Na EDTA. Cells were washed in ice-cold water and pellets were frozen. Cell pellets were resuspended in NIB buffer (17% glycerol, 50mM MOPS, 150mM potassium acetate, 2mM magnesium chloride, 500 $\mu\text{M}$  spermidine and 150 $\mu\text{M}$  spermine (pH 7,2), and cells were broken with glass bead-vortexing. Cell extracts were collected and membranes were disrupted by addition of sarcosyl (1,5%), and proteins were digested with Proteinase K at 37°C. Low-spin supernatants were gently mixed with CsCl and were subsequently loaded on 2ml PA tubes (*BECKMAN*), and were loaded on a VTi65 rotor and sealed, and were processed by ultracentrifugation. Genomic DNA resolved in the CsCl gradients was detected by Hoechst staining and was isolated with a syringe under UV-light. DNA was enriched and concentrated with subsequent isopropanol and 70% ethanol washes; see also (Brewer et al., 1992; Huberman et al., 1987). The DNA concentration was determined, and 12 $\mu\text{g}$  from each condition were subsequently digested with *NheI* and were loaded on a 0,4% agarose gel. First-dimension was run for 22 h and second-dimension (1% agarose) were run for 4,5 hr at 4° in 1xTBE containing 0,3  $\mu\text{g/ml}$  ethidium bromide (Friedman and Brewer, 1995). The probe was a *PvuII-EcoRI* restriction fragment of plasmid pBB-3NTS (Ward et al., 2000). Replication intermediates were quantified and normalized against the 1N spot after subtraction of background signal for each area. Signals were corrected for incomplete release from  $\alpha$ -factor based on quantitative FACS analysis, and unspecific signal from quantification of the G1 samples was subtracted from the mid-late S and late S-G2 samples resulting in the plotted values.

## **V.3.2 Molecular cloning methods**

### **Restriction digest of DNA**

Restriction enzymes were employed for sequence-specific cleavage of DNA according to standard protocols (Sambrock et al., 1989) and the instructions of the manufacturer (New England Biolabs). For the digestion of 1 $\mu\text{g}$  DNA, 5 to 10 units of restriction enzyme were usually used. Reaction samples were incubated at the recommended temperature for 2h. To avoid the recircularization of linearized vectors, the 5' end of vector DNA was dephosphorylated by incubation

with 5-10 units of Calf Intestinal Phosphatase (New England Biolabs) at 37°C for 30 min.

### **Separation of DNA fragments by gel electrophoresis**

For isolation of DNA fragments, 0,8-2% agarose gels, containing 0,5µg/ml ethidium bromide were used. DNA samples were mixed with 6x DNA loading buffer and electrophoretically separated at 120 volts in TBE buffer. Due to the intercalation of ethidium bromide into DNA, DNA fragments could be visualized by using an UV transilluminator (324nm). The size of the fragments was estimated by migration on the same gel of standard size markers (1kb DNA Ladder, Invitrogen).

### **Purification of DNA fragments from agarose gels**

The DNA fragment was excised from the gel, after electrophoresis, using a sterile razor blade. Next DNA purification from the cut agarose block was performed using kits from the companies Qiagen (QIAExII, QIAquick Gel Extraction Kit) or Macherey-Nagel (Nucleospin Extract II) according to the manufacturers' instructions

### **Ligation of DNA fragments**

The amounts of linearized vector and insert required for the ligation reaction were estimated by gel electrophoresis of the purified fragments. A ratio of 1:3–1:10 of vector to insert was used. The 10µl ligation reaction sample contained 100ng of vector DNA and 10 units T4 DNA ligase (New England Biolabs). The ligation was performed at 16°C for 4-12h. Before electroporation of the ligation products into *E. coli*, the sample was dialyzed against deionized water for 15 min using a nitrocellulose filter (pore size 0,05µm, Millipore).

### **DNA sequencing**

DNA sequencing reactions were carried out by the Core Facility of the Max Planck Institute, using an Abi-Prism 377 sequencer. The sample contained 1µg plasmid DNA and 5pmol primer. The sequencing reaction and the subsequent sample preparation were done with the DYEnamic ET terminator cycle sequencing kit (Amersham-Pharmacia), according to the instructions of the manufacturer.

### **V.3.3 Polymerase chain reaction (PCR)**

The PCR technique was used for cloning, for direct yeast transformation and for analysis of chromosomal recombination events. The PCR reactions were performed in a volume of 50µl, containing 50ng plasmid DNA or 0,2µg genomic DNA preparation, 0,6µM of the forward and reverse primers, 1,75µl deoxynucleotide mix (each 10mM, New England Biolabs) and 0,2-5 units DNA polymerase, either Phusion High-Fidelity polymerase (NEB), or a mixture of 4:1

Taq/Vent polymerases (New England Biolabs). The mixture was compiled in the buffer required by the polymerase used (HF buffer was used for Phusion, and Thermo buffer; NEB for Taq/Vent). A PCR Mastercycler (Eppendorf) was used for the reaction. The temperatures for primer annealing and primer extension were been optimized on a case by case basis, taking into consideration the quality of template DNA, the length and the G/C content of the primers. In general, the following program was used:

initial denaturation 95°C 180s  
 9 amplification cycles 95°C 45s  
 45°C 30s  
 68°C 100s  
 18 amplification cycles 94°C 60s  
 54°C 50s  
 +20s / cycle 68°C 100s  
 cooling 4°C

For cloning using Phusion polymerase the following program was used:

initial denaturation 98°C 180s  
 25 amplification cycles 98°C 45s  
 58°C 30s  
 72°C 60-180s  
 final extension 72°C 10 min  
 cooling 4°C

For verification of gene deletions and other chromosomal integrations, the colony PCR method was used. A single yeast colony was resuspended in 20µl NaOH 20mM, the liquid volume was filled with glass beads (Ø 425- 600nm, Sigma), and boiled in a thermomixer at 1400rpm for 5min. After a brief 15s centrifugation, 4µl of the supernatant was removed and used as template for the PCR reaction. The reaction was carried out in a volume of 50µl, containing 0,6µM of each primer, 1,75µl deoxynucleotide mix (each 10mM, New England Biolabs) and 2 units Taq polymerase. The mixture was made in Thermopol buffer (New England Biolabs), and the reaction was performed in a Mastercycler (Eppendorf) using the following program:

initial denaturation 95°C 180s  
 30 amplification cycles 95°C 30s  
 54°C 30s  
 68°C 60s  
 final extension 68°C 10 min  
 cooling 4°C

#### **V.3.4 Site-directed mutagenesis**

The method used for insertion of point mutations, was a PCR-based strategy based on the QuickChange protocol (Stratagene). Two complementary

oligonucleotide primers containing the mutated codon in the middle, flanked by 15 bases of the target sequence on each side were used. The 25µl PCR reaction mixture contained 50ng DNA template (plasmid), 62,5ng of each primer, 0,625µl deoxynucleotide mix (each 10mM, New England Biolabs), and 5 units Phusion HF (NEB) in HF-buffer (NEB). The reaction was performed in a Mastercycler (Eppendorf), with the following program:

initial denaturation	98°C 30s
30 amplification cycles	98°C 30s
	58°C 60s
	72°C 30s / kb plasmid
	cooling 4°C

To eliminate the template DNA, the reaction mixture was incubated at 37°C for 1h with DpnI, a restriction enzyme that cuts specifically methylated DNA. After dialysis, the mixture was transformed in *E. coli* and mutated plasmids were identified by DNA sequencing.

## V.4. Protein biochemistry methods

### V.4.1 Gel electrophoresis and immunoblot techniques

#### General buffers and solutions

HU sample buffer	8 M Urea 5 % SDS 1 mM EDTA 1,5 % DTT 1 % Bromphenolblue
MOPS buffer	50 mM MOPS 50 mM Tris base 3,5 mM SDS 1 mM EDTA
transfer buffer	250 mM Tris base 1,92 M glycine 0,1 % SDS 20 % methanol
TBST	25 mM Tris-HCl, pH 7,5 137 mM NaCl 2,6 mM KCl 0,1 % Tween 20

### **Western blot**

Proteins separated by gel electrophoresis were transferred to a polyvinylidene fluorid (PVDF) membrane (Millipore) in a wet (tank) blot system. The blotting was done in transfer buffer, at a constant voltage of 70V for 90 min at 4°C.

### **Immunological detection of membrane-transferred proteins**

The PVDF membrane with immobilized proteins was blocked with 5% milk in TBST for at least 30 min and incubated over-night with primary antibodies diluted in blocking solution. Afterwards, the membrane was washed 6 times for 5 min with TBST and incubated for 1h with secondary antibodies coupled to horseradish peroxidase (Dianova) diluted 1:5000 in TBST with 5% milk. Subsequently, the membrane was washed again as described. The detection of the protein of interest was carried out using the chemiluminiscence detection kits ECL or ECL Advanced (Amersham), according to the instructions of the manufacturer, followed by exposure to ECL Hyperfilm (Amersham) or to a CCD (charged coupled device) camera (LAS, Fuji). The following primary antibodies were used in this study:

rabbit polyclonal anti-PCNA (1:2000, (Hoege et al., 2002)), rabbit polyclonal anti-Pol32 (Lucian Moldovan PhD Thesis) goat polyclonal anti-Rad53 (1:5000, yC-19, Santa Cruz Biotechnology), goat polyclonal anti-Mcm2 (1:2000, yN-19, Santa Cruz Biotechnology), rabbit polyclonal anti-Clb2 (1:2000, y-180, Santa Cruz Biotechnology; recognizes the N-terminal 180 aa of Clb2), mouse monoclonal anti-HA (1:2000, F-7, Santa Cruz Biotechnology), and mouse monoclonal anti-Pgk1 (1:10000, 22C5; Invitrogen).

## **V.4.2 Preparation of cell extracts**

### **Preparation of denatured yeast extracts**

In order to avoid de-conjugation of posttranslational modifications during lysis, yeast cells were lysed under denaturing conditions. Usually, cells from 1ml of a yeast culture of  $OD_{600}=1$  were harvested by centrifugation, resuspended in 1ml water and lysed by incubation with 150µl 1,85M NaOH/ 7,5% β-mercaptoethanol for 15 min on ice. Proteins were precipitated by addition of 150µl 55% trichloroacetic acid (TCA) followed by incubation on ice for 10min and centrifugation at 20000g for 20min at 4°C. The pellet was resuspended in 50µl HU sample buffer.



## VI LITERATURE

Abdulovic, A.L., and Jinks-Robertson, S. (2006). The in vivo characterization of translesion synthesis across UV-induced lesions in *Saccharomyces cerevisiae*: insights into Pol zeta- and Pol eta-dependent frameshift mutagenesis. *Genetics* 172, 1487-1498.

Acharya, N., Johnson, R.E., Pages, V., Prakash, L., and Prakash, S. (2009). Yeast Rev1 protein promotes complex formation of DNA polymerase zeta with Pol32 subunit of DNA polymerase delta. *Proc Natl Acad Sci U S A* 106, 9631-9636.

Alcasabas, A.A., Osborn, A.J., Bachant, J., Hu, F., Werler, P.J., Bousset, K., Furuya, K., Diffley, J.F., Carr, A.M., and Elledge, S.J. (2001). Mrc1 transduces signals of DNA replication stress to activate Rad53. *Nat Cell Biol* 3, 958-965.

Alvino, G.M., Collingwood, D., Murphy, J.M., Delrow, J., Brewer, B.J., and Raghuraman, M.K. (2007). Replication in hydroxyurea: it's a matter of time. *Mol Cell Biol* 27, 6396-6406.

Amin, N.S., and Holm, C. (1996). In vivo analysis reveals that the interdomain region of the yeast proliferating cell nuclear antigen is important for DNA replication and DNA repair. *Genetics* 144, 479-493.

Amon, A., Irniger, S., and Nasmyth, K. (1994). Closing the cell cycle circle in yeast: G2 cyclin proteolysis initiated at mitosis persists until the activation of G1 cyclins in the next cycle. *Cell* 77, 1037-1050.

Andersen, P.L., Xu, F., and Xiao, W. (2008). Eukaryotic DNA damage tolerance and translesion synthesis through covalent modifications of PCNA. *Cell Res* 18, 162-173.

Arakawa, H., Moldovan, G.L., Saribasak, H., Saribasak, N.N., Jentsch, S., and Buerstedde, J.M. (2006). A role for PCNA ubiquitination in immunoglobulin hypermutation. *PLoS Biol* 4, e366.

Ardley, H.C., and Robinson, P.A. (2004). The role of ubiquitin-protein ligases in neurodegenerative disease. *Neurodegener Dis* 1, 71-87.

Ausubel, F.M., Brent, R., Kingston, R. E., Moore, D. D., Seidmna, J. G., Smith, J. A. und, and Struhl., K. (1994). *Current Protocols in Molecular Biology*, Green and Wiley, New York.

Baba, D., Maita, N., Jee, J.G., Uchimura, Y., Saitoh, H., Sugasawa, K., Hanaoka, F., Tochio, H., Hiroaki, H., and Shirakawa, M. (2005). Crystal structure of thymine DNA glycosylase conjugated to SUMO-1. *Nature* 435, 979-982.

Barbour, L., and Xiao, W. (2003). Regulation of alternative replication bypass pathways at stalled replication forks and its effects on genome stability: a yeast model. *Mutat Res* 532, 137-155.

Bartek, J., Lukas, C., and Lukas, J. (2004). Checking on DNA damage in S phase. *Nat Rev Mol Cell Biol* 5, 792-804.

Baynton, K., and Fuchs, R.P. (2000). Lesions in DNA: hurdles for polymerases. *Trends Biochem Sci* 25, 74-79.

Bell, S.P., and Dutta, A. (2002). DNA replication in eukaryotic cells. *Annu Rev Biochem* 71, 333-374.

Bi, X., Barkley, L.R., Slater, D.M., Tateishi, S., Yamaizumi, M., Ohmori, H., and Vaziri, C. (2006). Rad18 regulates DNA polymerase kappa and is required for recovery from S-phase checkpoint-mediated arrest. *Mol Cell Biol* 26, 3527-3540.

Bienko, M., Green, C.M., Crosetto, N., Rudolf, F., Zapart, G., Coull, B., Kannouche, P., Wider, G., Peter, M., Lehmann, A.R., *et al.* (2005). Ubiquitin-binding domains in Y-family polymerases regulate translesion synthesis. *Science* 310, 1821-1824.

- Blank, A., Kim, B., and Loeb, L.A. (1994). DNA polymerase delta is required for base excision repair of DNA methylation damage in *Saccharomyces cerevisiae*. *Proc Natl Acad Sci U S A* **91**, 9047-9051.
- Blank, A., and Loeb, L.A. (1991). Isolation of temperature-sensitive DNA polymerase III from *Saccharomyces cerevisiae* cdc2-2. *Biochemistry* **30**, 8092-8096.
- Blasius, M., Sommer, S., and Hubscher, U. (2008). *Deinococcus radiodurans*: what belongs to the survival kit? *Crit Rev Biochem Mol Biol* **43**, 221-238.
- Blastyak, A., Pinter, L., Unk, I., Prakash, L., Prakash, S., and Haracska, L. (2007). Yeast Rad5 protein required for postreplication repair has a DNA helicase activity specific for replication fork regression. *Mol Cell* **28**, 167-175.
- Bomar, M.G., D'Souza, S., Bienko, M., Dikic, I., Walker, G.C., and Zhou, P. (2010). Unconventional ubiquitin recognition by the ubiquitin-binding motif within the Y family DNA polymerases iota and Rev1. *Mol Cell* **37**, 408-417.
- Branzei, D., and Foiani, M. (2009). The checkpoint response to replication stress. *DNA Repair (Amst)* **8**, 1038-1046.
- Branzei, D., and Foiani, M. (2010). Maintaining genome stability at the replication fork. *Nat Rev Mol Cell Biol* **11**, 208-219.
- Branzei, D., Seki, M., and Enomoto, T. (2004). Rad18/Rad5/Mms2-mediated polyubiquitination of PCNA is implicated in replication completion during replication stress. *Genes Cells* **9**, 1031-1042.
- Branzei, D., Seki, M., Onoda, F., and Enomoto, T. (2002). The product of *Saccharomyces cerevisiae* WHIP/MGS1, a gene related to replication factor C genes, interacts functionally with DNA polymerase delta. *Mol Genet Genomics* **268**, 371-386.
- Branzei, D., Vanoli, F., and Foiani, M. (2008). SUMOylation regulates Rad18-mediated template switch. *Nature* **456**, 915-920.
- Bresson, A., and Fuchs, R.P. (2002). Lesion bypass in yeast cells: Pol eta participates in a multi-DNA polymerase process. *Embo J* **21**, 3881-3887.
- Brewer, B.J., Lockshon, D., and Fangman, W.L. (1992). The arrest of replication forks in the rDNA of yeast occurs independently of transcription. *Cell* **71**, 267-276.
- Brewer, B.J., Zakian, V.A., and Fangman, W.L. (1980). Replication and meiotic transmission of yeast ribosomal RNA genes. *Proc Natl Acad Sci U S A* **77**, 6739-6743.
- Bridges, B.A., Law, J., and Munson, R.J. (1968). Mutagenesis in *Escherichia coli*. II. Evidence for a common pathway for mutagenesis by ultraviolet light, ionizing radiation and thymine deprivation. *Mol Gen Genet* **103**, 266-273.
- Briggs, S.D., Xiao, T., Sun, Z.W., Caldwell, J.A., Shabanowitz, J., Hunt, D.F., Allis, C.D., and Strahl, B.D. (2002). Gene silencing: trans-histone regulatory pathway in chromatin. *Nature* **418**, 498.
- Broomfield, S., Chow, B.L., and Xiao, W. (1998a). MMS2, encoding a ubiquitin-conjugating-enzyme-like protein, is a member of the yeast error-free postreplication repair pathway. *Proc Natl Acad Sci U S A* **95**, 5678-5683.
- Broomfield, S., Chow, B.L., and Xiao, W. (1998b). MMS2, encoding a ubiquitin-conjugating-enzyme-like protein, is a member of the yeast error-free postreplication repair pathway. *Proc Natl Acad Sci U S A* **95**, 5678-5683.

- Broomfield, S., Hryciw, T., and Xiao, W. (2001). DNA postreplication repair and mutagenesis in *Saccharomyces cerevisiae*. *Mutat Res* 486, 167-184.
- Brown, S., Niimi, A., and Lehmann, A.R. (2009). Ubiquitination and deubiquitination of PCNA in response to stalling of the replication fork. *Cell Cycle* 8, 689-692.
- Budzowska, M., and Kanaar, R. (2009). Mechanisms of dealing with DNA damage-induced replication problems. *Cell Biochem Biophys* 53, 17-31.
- Burgers, P.M., and Gerik, K.J. (1998). Structure and processivity of two forms of *Saccharomyces cerevisiae* DNA polymerase delta. *J Biol Chem* 273, 19756-19762.
- Byun, T.S., Pacek, M., Yee, M.C., Walter, J.C., and Cimprich, K.A. (2005). Functional uncoupling of MCM helicase and DNA polymerase activities activates the ATR-dependent checkpoint. *Genes Dev* 19, 1040-1052.
- Cao, K., Nakajima, R., Meyer, H.H., and Zheng, Y. (2003). The AAA-ATPase Cdc48/p97 regulates spindle disassembly at the end of mitosis. *Cell* 115, 355-367.
- Carroll, C.W., and Morgan, D.O. (2002). The Doc1 subunit is a processivity factor for the anaphase-promoting complex. *Nat Cell Biol* 4, 880-887.
- Cassier-Chauvat, C., and Fabre, F. (1991). A similar defect in UV-induced mutagenesis conferred by the *rad6* and *rad18* mutations of *Saccharomyces cerevisiae*. *Mutat Res* 254, 247-253.
- Chang, D.J., and Cimprich, K.A. (2009). DNA damage tolerance: when it's OK to make mistakes. *Nat Chem Biol* 5, 82-90.
- Chen, S.H., Albuquerque, C.P., Liang, J., Suhandynata, R.T., and Zhou, H. (2010). A proteome-wide analysis of kinase-substrate network in the DNA damage response. *J Biol Chem* 285, 12803-12812.
- Ciechanover, A., Finley, D., and Varshavsky, A. (1984). Ubiquitin dependence of selective protein degradation demonstrated in the mammalian cell cycle mutant ts85. *Cell* 37, 57-66.
- Cobb, J.A., Bjergbaek, L., Shimada, K., Frei, C., and Gasser, S.M. (2003). DNA polymerase stabilization at stalled replication forks requires Mec1 and the RecQ helicase Sgs1. *Embo J* 22, 4325-4336.
- Cobb, J.A., Schleker, T., Rojas, V., Bjergbaek, L., Tercero, J.A., and Gasser, S.M. (2005). Replisome instability, fork collapse, and gross chromosomal rearrangements arise synergistically from Mec1 kinase and RecQ helicase mutations. *Genes Dev* 19, 3055-3069.
- Courcelle, J., and Hanawalt, P.C. (2001). Participation of recombination proteins in rescue of arrested replication forks in UV-irradiated *Escherichia coli* need not involve recombination. *Proc Natl Acad Sci U S A* 98, 8196-8202.
- Courcelle, J., and Hanawalt, P.C. (2003). RecA-dependent recovery of arrested DNA replication forks. *Annu Rev Genet* 37, 611-646.
- Cox, M.M., Goodman, M.F., Kreuzer, K.N., Sherratt, D.J., Sandler, S.J., and Marians, K.J. (2000). The importance of repairing stalled replication forks. *Nature* 404, 37-41.
- Das, R., Mariano, J., Tsai, Y.C., Kalathur, R.C., Kostova, Z., Li, J., Tarasov, S.G., McFeeters, R.L., Altieri, A.S., Ji, X., *et al.* (2009). Allosteric activation of E2-RING finger-mediated ubiquitylation by a structurally defined specific E2-binding region of gp78. *Mol Cell* 34, 674-685.
- David, Y., Ziv, T., Admon, A., and Navon, A. (2010). The E2 ubiquitin-conjugating enzymes direct polyubiquitination to preferred lysines. *J Biol Chem* 285, 8595-8604.

- Davies, A.A., Huttner, D., Daigaku, Y., Chen, S., and Ulrich, H.D. (2008). Activation of ubiquitin-dependent DNA damage bypass is mediated by replication protein a. *Mol Cell* 29, 625-636.
- de Padula, M., Slezak, G., Auffret van Der Kemp, P., and Boiteux, S. (2004). The post-replication repair RAD18 and RAD6 genes are involved in the prevention of spontaneous mutations caused by 7,8-dihydro-8-oxoguanine in *Saccharomyces cerevisiae*. *Nucleic Acids Res* 32, 5003-5010.
- Deng, L., Wang, C., Spencer, E., Yang, L., Braun, A., You, J., Slaughter, C., Pickart, C., and Chen, Z.J. (2000). Activation of the I $\kappa$ B kinase complex by TRAF6 requires a dimeric ubiquitin-conjugating enzyme complex and a unique polyubiquitin chain. *Cell* 103, 351-361.
- Dupre, S., Urban-Grimal, D., and Haguenauer-Tsapis, R. (2004). Ubiquitin and endocytic internalization in yeast and animal cells. *Biochim Biophys Acta* 1695, 89-111.
- Duval, D., Duval, G., Kedinger, C., Poch, O., and Boeuf, H. (2003). The 'PINIT' motif, of a newly identified conserved domain of the PIAS protein family, is essential for nuclear retention of PIAS3L. *FEBS Lett* 554, 111-118.
- Eddins, M.J., Carlile, C.M., Gomez, K.M., Pickart, C.M., and Wolberger, C. (2006). Mms2-Ubc13 covalently bound to ubiquitin reveals the structural basis of linkage-specific polyubiquitin chain formation. *Nat Struct Mol Biol* 13, 915-920.
- Edmunds, C.E., Simpson, L.J., and Sale, J.E. (2008). PCNA ubiquitination and REV1 define temporally distinct mechanisms for controlling translesion synthesis in the avian cell line DT40. *Mol Cell* 30, 519-529.
- Eluere, R., Offner, N., Varlet, I., Motteux, O., Signon, L., Picard, A., Bailly, E., and Simon, M.N. (2007). Compartmentalization of the functions and regulation of the mitotic cyclin Clb2 in *S. cerevisiae*. *J Cell Sci* 120, 702-711.
- Feng, W., Collingwood, D., Boeck, M.E., Fox, L.A., Alvino, G.M., Fangman, W.L., Raghuraman, M.K., and Brewer, B.J. (2006). Genomic mapping of single-stranded DNA in hydroxyurea-challenged yeasts identifies origins of replication. *Nat Cell Biol* 8, 148-155.
- Finley, D., Ciechanover, A., and Varshavsky, A. (1984). Thermolability of ubiquitin-activating enzyme from the mammalian cell cycle mutant ts85. *Cell* 37, 43-55.
- Frei, C., and Gasser, S.M. (2000). The yeast Sgs1p helicase acts upstream of Rad53p in the DNA replication checkpoint and colocalizes with Rad53p in S-phase-specific foci. *Genes Dev* 14, 81-96.
- Friedberg, E.C. (2005). Suffering in silence: the tolerance of DNA damage. *Nat Rev Mol Cell Biol* 6, 943-953.
- Friedberg, E.C., Fischhaber, P.L., and Kisker, C. (2001). Error-prone DNA polymerases: novel structures and the benefits of infidelity. *Cell* 107, 9-12.
- Friedberg, E.C., and Gerlach, V.L. (1999). Novel DNA polymerases offer clues to the molecular basis of mutagenesis. *Cell* 98, 413-416.
- Friedberg, E.C., Wagner, R., and Radman, M. (2002). Specialized DNA polymerases, cellular survival, and the genesis of mutations. *Science* 296, 1627-1630.
- Friedman, K.L., and Brewer, B.J. (1995). Analysis of replication intermediates by two-dimensional agarose gel electrophoresis. *Methods Enzymol* 262, 613-627.
- Fronza, G., Campomenosi, P., Iannone, R., and Abbondandolo, A. (1992). The 4-nitroquinoline 1-oxide mutational spectrum in single stranded DNA is characterized by guanine to pyrimidine transversions. *Nucleic Acids Res* 20, 1283-1287.

- Fu, H., Lin, Y.L., and Fatimababy, A.S. Proteasomal recognition of ubiquitylated substrates. *Trends Plant Sci.*
- Fukui, T., Yamauchi, K., Muroya, T., Akiyama, M., Maki, H., Sugino, A., and Waga, S. (2004). Distinct roles of DNA polymerases delta and epsilon at the replication fork in *Xenopus* egg extracts. *Genes Cells* 9, 179-191.
- Ganesan, A.K. (1974). Persistence of pyrimidine dimers during post-replication repair in ultraviolet light-irradiated *Escherichia coli* K12. *J Mol Biol* 87, 103-119.
- Gangavarapu, V., Haracska, L., Unk, I., Johnson, R.E., Prakash, S., and Prakash, L. (2006). Mms2-Ubc13-dependent and -independent roles of Rad5 ubiquitin ligase in postreplication repair and translesion DNA synthesis in *Saccharomyces cerevisiae*. *Mol Cell Biol* 26, 7783-7790.
- Garcia-Higuera, I., Taniguchi, T., Ganesan, S., Meyn, M.S., Timmers, C., Hejna, J., Grompe, M., and D'Andrea, A.D. (2001). Interaction of the Fanconi anemia proteins and BRCA1 in a common pathway. *Mol Cell* 7, 249-262.
- Gerik, K.J., Li, X., Pautz, A., and Burgers, P.M. (1998). Characterization of the two small subunits of *Saccharomyces cerevisiae* DNA polymerase delta. *J Biol Chem* 273, 19747-19755.
- Gietz, R.D., and Sugino, A. (1988). New yeast-*Escherichia coli* shuttle vectors constructed with in vitro mutagenized yeast genes lacking six-base pair restriction sites. *Gene* 74, 527-534.
- Giot, L., Chanut, R., Simon, M., Facca, C., and Faye, G. (1997). Involvement of the yeast DNA polymerase delta in DNA repair in vivo. *Genetics* 146, 1239-1251.
- Girdwood, D., Bumpass, D., Vaughan, O.A., Thain, A., Anderson, L.A., Snowden, A.W., Garcia-Wilson, E., Perkins, N.D., and Hay, R.T. (2003). P300 transcriptional repression is mediated by SUMO modification. *Mol Cell* 11, 1043-1054.
- Glutzer, M., Murray, A.W., and Kirschner, M.W. (1991). Cyclin is degraded by the ubiquitin pathway. *Nature* 349, 132-138.
- Gohler, T., Munoz, I.M., Rouse, J., and Blow, J.J. (2008). PTIP/Swift is required for efficient PCNA ubiquitination in response to DNA damage. *DNA Repair (Amst)* 7, 775-787.
- Grabbe, C., and Dikic, I. (2009). Functional roles of ubiquitin-like domain (ULD) and ubiquitin-binding domain (UBD) containing proteins. *Chem Rev* 109, 1481-1494.
- Grenson, M., Mousset, M., Wiame, J.M., and Bechet, J. (1966). Multiplicity of the amino acid permeases in *Saccharomyces cerevisiae*. I. Evidence for a specific arginine-transporting system. *Biochim Biophys Acta* 127, 325-338.
- Haglund, K., Di Fiore, P.P., and Dikic, I. (2003). Distinct monoubiquitin signals in receptor endocytosis. *Trends Biochem Sci* 28, 598-603.
- Hanna, M., Ball, L.G., Tong, A.H., Boone, C., and Xiao, W. (2007). Pol32 is required for Pol zeta-dependent translesion synthesis and prevents double-strand breaks at the replication fork. *Mutat Res* 625, 164-176.
- Hannich, J.T., Lewis, A., Kroetz, M.B., Li, S.J., Heide, H., Emili, A., and Hochstrasser, M. (2005). Defining the SUMO-modified proteome by multiple approaches in *Saccharomyces cerevisiae*. *J Biol Chem* 280, 4102-4110.
- Hardeland, U., Steinacher, R., Jiricny, J., and Schar, P. (2002). Modification of the human thymine-DNA glycosylase by ubiquitin-like proteins facilitates enzymatic turnover. *Embo J* 21, 1456-1464.

- Hartwell, L.H., and Smith, D. (1985). Altered fidelity of mitotic chromosome transmission in cell cycle mutants of *S. cerevisiae*. *Genetics* **110**, 381-395.
- Hastings, P.J., Quah, S.K., and von Borstel, R.C. (1976). Spontaneous mutation by mutagenic repair of spontaneous lesions in DNA. *Nature* **264**, 719-722.
- Heller, R.C., and Marians, K.J. (2006). Replisome assembly and the direct restart of stalled replication forks. *Nat Rev Mol Cell Biol* **7**, 932-943.
- Hendrickson, C., Meyn, M.A., 3rd, Morabito, L., and Holloway, S.L. (2001). The KEN box regulates Clb2 proteolysis in G1 and at the metaphase-to-anaphase transition. *Curr Biol* **11**, 1781-1787.
- Hershko, A., and Ciechanover, A. (1998). The ubiquitin system. *Annu Rev Biochem* **67**, 425-479.
- Herzberg, K., Bashkurov, V.I., Rolfsmeier, M., Haghnazari, E., McDonald, W.H., Anderson, S., Bashkurova, E.V., Yates, J.R., 3rd, and Heyer, W.D. (2006). Phosphorylation of Rad55 on serines 2, 8, and 14 is required for efficient homologous recombination in the recovery of stalled replication forks. *Mol Cell Biol* **26**, 8396-8409.
- Heyer, W.D., Li, X., Rolfsmeier, M., and Zhang, X.P. (2006). Rad54: the Swiss Army knife of homologous recombination? *Nucleic Acids Res* **34**, 4115-4125.
- Hicke, L., and Dunn, R. (2003). Regulation of membrane protein transport by ubiquitin and ubiquitin-binding proteins. *Annu Rev Cell Dev Biol* **19**, 141-172.
- Higgins, N.P., Kato, K., and Strauss, B. (1976). A model for replication repair in mammalian cells. *J Mol Biol* **101**, 417-425.
- Hishida, T., Kubota, Y., Carr, A.M., and Iwasaki, H. (2009). RAD6-RAD18-RAD5-pathway-dependent tolerance to chronic low-dose ultraviolet light. *Nature* **457**, 612-615.
- Hochstrasser, M. (1996). Ubiquitin-dependent protein degradation. *Annu Rev Genet* **30**, 405-439.
- Hochstrasser, M. (2006). Lingering mysteries of ubiquitin-chain assembly. *Cell* **124**, 27-34.
- Hoegel, C., Pfander, B., Moldovan, G.L., Pyrowolakis, G., and Jentsch, S. (2002). RAD6-dependent DNA repair is linked to modification of PCNA by ubiquitin and SUMO. *Nature* **419**, 135-141.
- Hoeijmakers, J.H. (2001). Genome maintenance mechanisms for preventing cancer. *Nature* **411**, 366-374.
- Hofmann, R.M., and Pickart, C.M. (1999). Noncanonical MMS2-encoded ubiquitin-conjugating enzyme functions in assembly of novel polyubiquitin chains for DNA repair. *Cell* **96**, 645-653.
- Hood, J.K., Hwang, W.W., and Silver, P.A. (2001). The *Saccharomyces cerevisiae* cyclin Clb2p is targeted to multiple subcellular locations by cis- and trans-acting determinants. *J Cell Sci* **114**, 589-597.
- Howard-Flanders, P. (1968). DNA repair. *Annu Rev Biochem* **37**, 175-200.
- Huang, M.E., Cadieu, E., Souciet, J.L., and Galibert, F. (1997). Disruption of six novel yeast genes reveals three genes essential for vegetative growth and one required for growth at low temperature. *Yeast* **13**, 1181-1194.
- Huang, M.E., de Calignon, A., Nicolas, A., and Galibert, F. (2000). POL32, a subunit of the *Saccharomyces cerevisiae* DNA polymerase delta, defines a link between DNA replication and the mutagenic bypass repair pathway. *Curr Genet* **38**, 178-187.

- Huang, M.E., Rio, A.G., Galibert, M.D., and Galibert, F. (2002). Pol32, a subunit of *Saccharomyces cerevisiae* DNA polymerase delta, suppresses genomic deletions and is involved in the mutagenic bypass pathway. *Genetics* **160**, 1409-1422.
- Huberman, J.A., Spotila, L.D., Nawotka, K.A., el-Assouli, S.M., and Davis, L.R. (1987). The in vivo replication origin of the yeast 2 microns plasmid. *Cell* **51**, 473-481.
- Hubscher, U. (2009). DNA replication fork proteins. *Methods Mol Biol* **521**, 19-33.
- Huen, M.S., Sy, S.M., and Chen, J. (2010). BRCA1 and its toolbox for the maintenance of genome integrity. *Nat Rev Mol Cell Biol* **11**, 138-148.
- Ikeda, F., and Dikic, I. (2008). Atypical ubiquitin chains: new molecular signals. 'Protein Modifications: Beyond the Usual Suspects' review series. *EMBO Rep* **9**, 536-542.
- Jackson, S.P., and Bartek, J. (2009). The DNA-damage response in human biology and disease. *Nature* **461**, 1071-1078.
- Janion, C. (2008). Inducible SOS response system of DNA repair and mutagenesis in *Escherichia coli*. *Int J Biol Sci* **4**, 338-344.
- Janke, C., Magiera, M.M., Rathfelder, N., Taxis, C., Reber, S., Maekawa, H., Moreno-Borchart, A., Doenges, G., Schwob, E., Schiebel, E., *et al.* (2004). A versatile toolbox for PCR-based tagging of yeast genes: new fluorescent proteins, more markers and promoter substitution cassettes. *Yeast* **21**, 947-962.
- Jansen, J.G., Tsaalbi-Shtylik, A., Hendriks, G., Gali, H., Hendel, A., Johansson, F., Erixon, K., Livneh, Z., Mullenders, L.H., Haracska, L., *et al.* (2009a). Separate domains of Rev1 mediate two modes of DNA damage bypass in mammalian cells. *Mol Cell Biol* **29**, 3113-3123.
- Jansen, J.G., Tsaalbi-Shtylik, A., Hendriks, G., Verspuy, J., Gali, H., Haracska, L., and de Wind, N. (2009b). Mammalian polymerase zeta is essential for post-replication repair of UV-induced DNA lesions. *DNA Repair (Amst)* **8**, 1444-1451.
- Jeltsch, A., and Rathert, P. (2008). Putting the pieces together: histone H2B ubiquitylation directly stimulates histone H3K79 methylation. *Chembiochem* **9**, 2193-2195.
- Jentsch, S. (1992). The ubiquitin-conjugation system. *Annu Rev Genet* **26**, 179-207.
- Jentsch, S., McGrath, J.P., and Varshavsky, A. (1987). The yeast DNA repair gene *RAD6* encodes a ubiquitin-conjugating enzyme. *Nature* **329**, 131-134.
- Jentsch, S., and Pyrowolakis, G. (2000). Ubiquitin and its kin: how close are the family ties? *Trends Cell Biol* **10**, 335-342.
- Jentsch, S., and Rumpf, S. (2007). Cdc48 (p97): a "molecular gearbox" in the ubiquitin pathway? *Trends Biochem Sci* **32**, 6-11.
- Johansson, E., Garg, P., and Burgers, P.M. (2004). The Pol32 subunit of DNA polymerase delta contains separable domains for processive replication and proliferating cell nuclear antigen (PCNA) binding. *J Biol Chem* **279**, 1907-1915.
- Kannouche, P.L., Wing, J., and Lehmann, A.R. (2004). Interaction of human DNA polymerase eta with monoubiquitinated PCNA: a possible mechanism for the polymerase switch in response to DNA damage. *Mol Cell* **14**, 491-500.
- Katou, Y., Kanoh, Y., Bando, M., Noguchi, H., Tanaka, H., Ashikari, T., Sugimoto, K., and Shirahige, K. (2003). S-phase checkpoint proteins Tof1 and Mrc1 form a stable replication-pausing complex. *Nature* **424**, 1078-1083.

- Katzmann, D.J., Babst, M., and Emr, S.D. (2001). Ubiquitin-dependent sorting into the multivesicular body pathway requires the function of a conserved endosomal protein sorting complex, ESCRT-I. *Cell* **106**, 145-155.
- Keeney, S., Giroux, C.N., and Kleckner, N. (1997). Meiosis-specific DNA double-strand breaks are catalyzed by Spo11, a member of a widely conserved protein family. *Cell* **88**, 375-384.
- Khan, M.M., Nomura, T., Kim, H., Kaul, S.C., Wadhwa, R., Shinagawa, T., Ichikawa-Iwata, E., Zhong, S., Pandolfi, P.P., and Ishii, S. (2001). Role of PML and PML-RARalpha in Mad-mediated transcriptional repression. *Mol Cell* **7**, 1233-1243.
- Knipscheer, P., Raschle, M., Smogorzewska, A., Enou, M., Ho, T.V., Scharer, O.D., Elledge, S.J., and Walter, J.C. (2009). The Fanconi anemia pathway promotes replication-dependent DNA interstrand cross-link repair. *Science* **326**, 1698-1701.
- Knop, M., Siegers, K., Pereira, G., Zachariae, W., Winsor, B., Nasmyth, K., and Schiebel, E. (1999). Epitope tagging of yeast genes using a PCR-based strategy: more tags and improved practical routines. *Yeast* **15**, 963-972.
- Koegl, M., Hoppe, T., Schlenker, S., Ulrich, H.D., Mayer, T.U., and Jentsch, S. (1999). A novel ubiquitination factor, E4, is involved in multiubiquitin chain assembly. *Cell* **96**, 635-644.
- Komata, M., Bando, M., Araki, H., and Shirahige, K. (2009). The direct binding of Mrc1, a checkpoint mediator, to Mcm6, a replication helicase, is essential for the replication checkpoint against methyl methanesulfonate-induced stress. *Mol Cell Biol* **29**, 5008-5019.
- Kostova, Z., Tsai, Y.C., and Weissman, A.M. (2007). Ubiquitin ligases, critical mediators of endoplasmic reticulum-associated degradation. *Semin Cell Dev Biol* **18**, 770-779.
- Krejci, L., Macris, M., Li, Y., Van Komen, S., Villemain, J., Ellenberger, T., Klein, H., and Sung, P. (2004). Role of ATP hydrolysis in the antirecombinase function of *Saccharomyces cerevisiae* Srs2 protein. *J Biol Chem* **279**, 23193-23199.
- Kunkel, T.A., and Burgers, P.M. (2008). Dividing the workload at a eukaryotic replication fork. *Trends Cell Biol* **18**, 521-527.
- Kunkel, T.A., Pavlov, Y.I., and Bebenek, K. (2003). Functions of human DNA polymerases eta, kappa and iota suggested by their properties, including fidelity with undamaged DNA templates. *DNA Repair (Amst)* **2**, 135-149.
- Kunz, B.A., Straffon, A.F., and Vonnar, E.J. (2000). DNA damage-induced mutation: tolerance via translesion synthesis. *Mutat Res* **451**, 169-185.
- Lawrence, C.W., and Christensen, R. (1976). UV mutagenesis in radiation-sensitive strains of yeast. *Genetics* **82**, 207-232.
- Lawrence, C.W., Stewart, J.W., Sherman, F., and Christensen, R. (1974). Specificity and frequency of ultraviolet-induced reversion of an iso-1-cytochrome c ochre mutant in radiation-sensitive strains of yeast. *J Mol Biol* **85**, 137-162.
- Leach, C.A., and Michael, W.M. (2005). Ubiquitin/SUMO modification of PCNA promotes replication fork progression in *Xenopus laevis* egg extracts. *J Cell Biol* **171**, 947-954.
- Lee, K.Y., and Myung, K. (2008). PCNA modifications for regulation of post-replication repair pathways. *Mol Cells* **26**, 5-11.
- Lee, S.J., Duong, J.K., and Stern, D.F. (2004). A Ddc2-Rad53 fusion protein can bypass the requirements for RAD9 and MRC1 in Rad53 activation. *Mol Biol Cell* **15**, 5443-5455.



- Lehmann, A.R., and Fuchs, R.P. (2006). Gaps and forks in DNA replication: Rediscovering old models. *DNA Repair (Amst)* 5, 1495-1498.
- Lehmann, A.R., Niimi, A., Ogi, T., Brown, S., Sabbioneda, S., Wing, J.F., Kannouche, P.L., and Green, C.M. (2007). Translesion synthesis: Y-family polymerases and the polymerase switch. *DNA Repair (Amst)* 6, 891-899.
- Lemontt, J.F. (1971). Mutants of Yeast Defective in Mutation Induced by Ultraviolet Light. *Genetics* 68, 21-33.
- Lengronne, A., Pasero, P., Bensimon, A., and Schwob, E. (2001). Monitoring S phase progression globally and locally using BrdU incorporation in TK(+) yeast strains. *Nucleic Acids Res* 29, 1433-1442.
- Liberi, G., Maffioletti, G., Lucca, C., Chiolo, I., Baryshnikova, A., Cotta-Ramusino, C., Lopes, M., Pelliccioli, A., Haber, J.E., and Foiani, M. (2005). Rad51-dependent DNA structures accumulate at damaged replication forks in *sgs1* mutants defective in the yeast ortholog of BLM RecQ helicase. *Genes Dev* 19, 339-350.
- Liefshitz, B., Steinlauf, R., Friedl, A., Eckardt-Schupp, F., and Kupiec, M. (1998). Genetic interactions between mutants of the 'error-prone' repair group of *Saccharomyces cerevisiae* and their effect on recombination and mutagenesis. *Mutat Res* 407, 135-145.
- Little, J.W., and Mount, D.W. (1982). The SOS regulatory system of *Escherichia coli*. *Cell* 29, 11-22.
- Liu, F., and Walters, K.J. (2010). Multitasking with ubiquitin through multivalent interactions. *Trends Biochem Sci*.
- Longtine, M.S., McKenzie, A., 3rd, Demarini, D.J., Shah, N.G., Wach, A., Brachat, A., Philippsen, P., and Pringle, J.R. (1998). Additional modules for versatile and economical PCR-based gene deletion and modification in *Saccharomyces cerevisiae*. *Yeast* 14, 953-961.
- Lopes, M., Cotta-Ramusino, C., Liberi, G., and Foiani, M. (2003). Branch migrating sister chromatid junctions form at replication origins through Rad51/Rad52-independent mechanisms. *Mol Cell* 12, 1499-1510.
- Lopes, M., Foiani, M., and Sogo, J.M. (2006). Multiple mechanisms control chromosome integrity after replication fork uncoupling and restart at irreparable UV lesions. *Mol Cell* 21, 15-27.
- Lorenz, M.C., Muir, R.S., Lim, E., McElver, J., Weber, S.C., and Heitman, J. (1995). Gene disruption with PCR products in *Saccharomyces cerevisiae*. *Gene* 158, 113-117.
- Lou, H., Komata, M., Katou, Y., Guan, Z., Reis, C.C., Budd, M., Shirahige, K., and Campbell, J.L. (2008). Mrc1 and DNA polymerase epsilon function together in linking DNA replication and the S phase checkpoint. *Mol Cell* 32, 106-117.
- Lundin, C., North, M., Erixon, K., Walters, K., Jenssen, D., Goldman, A.S., and Helleday, T. (2005). Methyl methanesulfonate (MMS) produces heat-labile DNA damage but no detectable in vivo DNA double-strand breaks. *Nucleic Acids Res* 33, 3799-3811.
- Ma, W., Resnick, M.A., and Gordenin, D.A. (2008). Apn1 and Apn2 endonucleases prevent accumulation of repair-associated DNA breaks in budding yeast as revealed by direct chromosomal analysis. *Nucleic Acids Res* 36, 1836-1846.
- Maher, M., Cong, F., Kindelberger, D., Nasmyth, K., and Dalton, S. (1995). Cell cycle-regulated transcription of the *CLB2* gene is dependent on Mcm1 and a ternary complex factor. *Mol Cell Biol* 15, 3129-3137.
- Martini, E.M., Keeney, S., and Osley, M.A. (2002). A role for histone H2B during repair of UV-induced DNA damage in *Saccharomyces cerevisiae*. *Genetics* 160, 1375-1387.

- Masuda, Y., Suzuki, M., Piao, J., Gu, Y., Tsurimoto, T., and Kamiya, K. (2007). Dynamics of human replication factors in the elongation phase of DNA replication. *Nucleic Acids Res* 35, 6904-6916.
- Matta-Camacho, E., Kozlov, G., Trempe, J.F., and Gehring, K. (2009). Atypical binding of the Swa2p UBA domain to ubiquitin. *J Mol Biol* 386, 569-577.
- Merrill, B.J., and Holm, C. (1998). The RAD52 recombinational repair pathway is essential in pol30 (PCNA) mutants that accumulate small single-stranded DNA fragments during DNA synthesis. *Genetics* 148, 611-624.
- Minty, A., Dumont, X., Kaghad, M., and Caput, D. (2000). Covalent modification of p73alpha by SUMO-1. Two-hybrid screening with p73 identifies novel SUMO-1-interacting proteins and a SUMO-1 interaction motif. *J Biol Chem* 275, 36316-36323.
- Mirzayans, R., Paterson, M.C., and Waters, R. (1985). Defective repair of a class of 4NQO-induced alkali-labile DNA lesions in xeroderma pigmentosum complementation group A fibroblasts. *Carcinogenesis* 6, 555-559.
- Mizuno, K., Lambert, S., Baldacci, G., Murray, J.M., and Carr, A.M. (2009). Nearby inverted repeats fuse to generate acentric and dicentric palindromic chromosomes by a replication template exchange mechanism. *Genes Dev* 23, 2876-2886.
- Moldovan, G.L. (2006). Regulation of replication-linked functions by PCNA and SUMO. PhD Thesis.
- Moldovan, G.L., Pfander, B., and Jentsch, S. (2007). PCNA, the maestro of the replication fork. *Cell* 129, 665-679.
- Moriel-Carretero, M., and Aguilera, A. (2010). A postincision-deficient TFIIF causes replication fork breakage and uncovers alternative Rad51- or Pol32-mediated restart mechanisms. *Mol Cell* 37, 690-701.
- Morrison, A., Christensen, R.B., Alley, J., Beck, A.K., Bernstine, E.G., Lemontt, J.F., and Lawrence, C.W. (1989). REV3, a *Saccharomyces cerevisiae* gene whose function is required for induced mutagenesis, is predicted to encode a nonessential DNA polymerase. *J Bacteriol* 171, 5659-5667.
- Myung, K., and Smith, S. (2008). The RAD5-dependent postreplication repair pathway is important to suppress gross chromosomal rearrangements. *J Natl Cancer Inst Monogr*, 12-15.
- Nick McElhinny, S.A., Gordenin, D.A., Stith, C.M., Burgers, P.M., and Kunkel, T.A. (2008). Division of labor at the eukaryotic replication fork. *Mol Cell* 30, 137-144.
- Niimi, A., Brown, S., Sabbioneda, S., Kannouche, P.L., Scott, A., Yasui, A., Green, C.M., and Lehmann, A.R. (2008). Regulation of proliferating cell nuclear antigen ubiquitination in mammalian cells. *Proc Natl Acad Sci U S A* 105, 16125-16130.
- Northam, M.R., Garg, P., Baitin, D.M., Burgers, P.M., and Shcherbakova, P.V. (2006). A novel function of DNA polymerase zeta regulated by PCNA. *Embo J* 25, 4316-4325.
- Ogi, T., and Lehmann, A.R. (2006). The Y-family DNA polymerase kappa (pol kappa) functions in mammalian nucleotide-excision repair. *Nat Cell Biol* 8, 640-642.
- Olsen, S.K., Capili, A.D., Lu, X., Tan, D.S., and Lima, C.D. (2010). Active site remodelling accompanies thioester bond formation in the SUMO E1. *Nature* 463, 906-912.
- Osborn, A.J., and Elledge, S.J. (2003). Mrc1 is a replication fork component whose phosphorylation in response to DNA replication stress activates Rad53. *Genes Dev* 17, 1755-1767.
- Osborn, A.J., Elledge, S.J., and Zou, L. (2002). Checking on the fork: the DNA-replication stress-response pathway. *Trends Cell Biol* 12, 509-516.

- Osley, M.A. (2004). H2B ubiquitylation: the end is in sight. *Biochim Biophys Acta* 1677, 74-78.
- Paek, A.L., Kaochar, S., Jones, H., Elezaby, A., Shanks, L., and Weinert, T. (2009). Fusion of nearby inverted repeats by a replication-based mechanism leads to formation of dicentric and acentric chromosomes that cause genome instability in budding yeast. *Genes Dev* 23, 2861-2875.
- Pages, V., and Fuchs, R.P. (2002). How DNA lesions are turned into mutations within cells? *Oncogene* 21, 8957-8966.
- Pages, V., Santa Maria, S.R., Prakash, L., and Prakash, S. (2009). Role of DNA damage-induced replication checkpoint in promoting lesion bypass by translesion synthesis in yeast. *Genes Dev* 23, 1438-1449.
- Papouli, E., Chen, S., Davies, A.A., Huttner, D., Krejci, L., Sung, P., and Ulrich, H.D. (2005). Crosstalk between SUMO and ubiquitin on PCNA is mediated by recruitment of the helicase Srs2p. *Mol Cell* 19, 123-133.
- Parrilla-Castellar, E.R., Arlander, S.J., and Karnitz, L. (2004). Dial 9-1-1 for DNA damage: the Rad9-Hus1-Rad1 (9-1-1) clamp complex. *DNA Repair (Amst)* 3, 1009-1014.
- Paulovich, A.G., Armour, C.D., and Hartwell, L.H. (1998). The *Saccharomyces cerevisiae* RAD9, RAD17, RAD24 and MEC3 genes are required for tolerating irreparable, ultraviolet-induced DNA damage. *Genetics* 150, 75-93.
- Paulovich, A.G., and Hartwell, L.H. (1995). A checkpoint regulates the rate of progression through S phase in *S. cerevisiae* in response to DNA damage. *Cell* 82, 841-847.
- Paulovich, A.G., Margulies, R.U., Garvik, B.M., and Hartwell, L.H. (1997). RAD9, RAD17, and RAD24 are required for S phase regulation in *Saccharomyces cerevisiae* in response to DNA damage. *Genetics* 145, 45-62.
- Pavlov, Y.I., Shcherbakova, P.V., and Kunkel, T.A. (2001). In vivo consequences of putative active site mutations in yeast DNA polymerases alpha, epsilon, delta, and zeta. *Genetics* 159, 47-64.
- Perry, J.J., Tainer, J.A., and Boddy, M.N. (2008). A SIM-ultaneous role for SUMO and ubiquitin. *Trends Biochem Sci* 33, 201-208.
- Petroski, M.D., and Deshaies, R.J. (2005). Mechanism of lysine 48-linked ubiquitin-chain synthesis by the cullin-RING ubiquitin-ligase complex SCF-Cdc34. *Cell* 123, 1107-1120.
- Pfander, B. (2005). *Regulation der Genomstabilität durch SUMO- und Ubiquitin-Modifikation von PCNA*. PhD Thesis.
- Pfander, B., Moldovan, G.L., Sacher, M., Hoege, C., and Jentsch, S. (2005). SUMO-modified PCNA recruits Srs2 to prevent recombination during S phase. *Nature* 436, 428-433.
- Pfleger, C.M., and Kirschner, M.W. (2000). The KEN box: an APC recognition signal distinct from the D box targeted by Cdh1. *Genes Dev* 14, 655-665.
- Pichler, A., Knipscheer, P., Saitoh, H., Sixma, T.K., and Melchior, F. (2004). The RanBP2 SUMO E3 ligase is neither HECT- nor RING-type. *Nat Struct Mol Biol* 11, 984-991.
- Pickart, C.M. (2001). Ubiquitin enters the new millennium. *Mol Cell* 8, 499-504.
- Pickart, C.M. (2004). Back to the future with ubiquitin. *Cell* 116, 181-190.
- Prakash, S., Johnson, R.E., and Prakash, L. (2005). Eukaryotic translesion synthesis DNA polymerases: specificity of structure and function. *Annu Rev Biochem* 74, 317-353.

- Raghuraman, M.K., Winzeler, E.A., Collingwood, D., Hunt, S., Wodicka, L., Conway, A., Lockhart, D.J., Davis, R.W., Brewer, B.J., and Fangman, W.L. (2001). Replication dynamics of the yeast genome. *Science* **294**, 115-121.
- Rape, M., Reddy, S.K., and Kirschner, M.W. (2006). The processivity of multiubiquitination by the APC determines the order of substrate degradation. *Cell* **124**, 89-103.
- Raschle, M., Knipscheer, P., Enoiu, M., Angelov, T., Sun, J., Griffith, J.D., Ellenberger, T.E., Scharer, O.D., and Walter, J.C. (2008). Mechanism of replication-coupled DNA interstrand crosslink repair. *Cell* **134**, 969-980.
- Reindle, A., Belichenko, I., Bylebyl, G.R., Chen, X.L., Gandhi, N., and Johnson, E.S. (2006). Multiple domains in Siz SUMO ligases contribute to substrate selectivity. *J Cell Sci* **119**, 4749-4757.
- Reverter, D., and Lima, C.D. (2005). Insights into E3 ligase activity revealed by a SUMO-RanGAP1-Ubc9-Nup358 complex. *Nature* **435**, 687-692.
- Richly, H., Rape, M., Braun, S., Rumpf, S., Hoege, C., and Jentsch, S. (2005). A series of ubiquitin binding factors connects CDC48/p97 to substrate multiubiquitylation and proteasomal targeting. *Cell* **120**, 73-84.
- Rodrigo-Brenni, M.C., and Morgan, D.O. (2007). Sequential E2s drive polyubiquitin chain assembly on APC targets. *Cell* **130**, 127-139.
- Romisch, K. (2005). Endoplasmic reticulum-associated degradation. *Annu Rev Cell Dev Biol* **21**, 435-456.
- Rossi, M.L., Ghosh, A.K., and Bohr, V.A. (2010). Roles of Werner syndrome protein in protection of genome integrity. *DNA Repair (Amst)* **9**, 331-344.
- Rotin, D., and Kumar, S. (2009). Physiological functions of the HECT family of ubiquitin ligases. *Nat Rev Mol Cell Biol* **10**, 398-409.
- Rupp, W.D., and Howard-Flanders, P. (1968). Discontinuities in the DNA synthesized in an excision-defective strain of *Escherichia coli* following ultraviolet irradiation. *J Mol Biol* **31**, 291-304.
- Sabbioneda, S., Bortolomai, I., Giannattasio, M., Plevani, P., and Muzi-Falconi, M. (2007). Yeast Rev1 is cell cycle regulated, phosphorylated in response to DNA damage and its binding to chromosomes is dependent upon MEC1. *DNA Repair (Amst)* **6**, 121-127.
- Sabbioneda, S., Minesinger, B.K., Giannattasio, M., Plevani, P., Muzi-Falconi, M., and Jinks-Robertson, S. (2005). The 9-1-1 checkpoint clamp physically interacts with polzeta and is partially required for spontaneous polzeta-dependent mutagenesis in *Saccharomyces cerevisiae*. *J Biol Chem* **280**, 38657-38665.
- Sambrook, J., Fritsch, E. F. und Maniatis, T (1989). *Molecular Cloning*, CSH Laboratory Press.
- Sancar, A., Lindsey-Boltz, L.A., Unsal-Kacmaz, K., and Linn, S. (2004). Molecular mechanisms of mammalian DNA repair and the DNA damage checkpoints. *Annu Rev Biochem* **73**, 39-85.
- Schiestl, R.H., and Wintersberger, U. (1992). DNA damage induced mating type switching in *Saccharomyces cerevisiae*. *Mutat Res* **284**, 111-123.
- Schwab, M., Lutum, A.S., and Seufert, W. (1997). Yeast Hct1 is a regulator of Clb2 cyclin proteolysis. *Cell* **90**, 683-693.
- Sekiyama, N., Arita, K., Ikeda, Y., Hashiguchi, K., Ariyoshi, M., Tochio, H., Saitoh, H., and Shirakawa, M. (2010). Structural basis for regulation of poly-SUMO chain by a SUMO-like domain of Nip45. *Proteins* **78**, 1491-1502.

- Sherman, F. (1991). Getting started with yeast. *Methods Enzymol* 194, 3-21.
- Smirnova, M., and Klein, H.L. (2003). Role of the error-free damage bypass postreplication repair pathway in the maintenance of genomic stability. *Mutat Res* 532, 117-135.
- Sobhian, B., Shao, G., Lilli, D.R., Culhane, A.C., Moreau, L.A., Xia, B., Livingston, D.M., and Greenberg, R.A. (2007). RAP80 targets BRCA1 to specific ubiquitin structures at DNA damage sites. *Science* 316, 1198-1202.
- Sogo, J.M., Lopes, M., and Foiani, M. (2002). Fork reversal and ssDNA accumulation at stalled replication forks owing to checkpoint defects. *Science* 297, 599-602.
- Song, J., Durrin, L.K., Wilkinson, T.A., Krontiris, T.G., and Chen, Y. (2004). Identification of a SUMO-binding motif that recognizes SUMO-modified proteins. *Proc Natl Acad Sci U S A* 101, 14373-14378.
- Soria, G., Podhajcer, O., Prives, C., and Gottifredi, V. (2006). P21Cip1/WAF1 downregulation is required for efficient PCNA ubiquitination after UV irradiation. *Oncogene* 25, 2829-2838.
- Stelter, P., and Ulrich, H.D. (2003). Control of spontaneous and damage-induced mutagenesis by SUMO and ubiquitin conjugation. *Nature* 425, 188-191.
- Stillman, B. (2008). DNA polymerases at the replication fork in eukaryotes. *Mol Cell* 30, 259-260.
- Sun, L., and Chen, Z.J. (2004). The novel functions of ubiquitination in signaling. *Curr Opin Cell Biol* 16, 119-126.
- Sun, Z.W., and Allis, C.D. (2002). Ubiquitination of histone H2B regulates H3 methylation and gene silencing in yeast. *Nature* 418, 104-108.
- Thrower, J.S., Hoffman, L., Rechsteiner, M., and Pickart, C.M. (2000). Recognition of the polyubiquitin proteolytic signal. *Embo J* 19, 94-102.
- Tong, A.H., Evangelista, M., Parsons, A.B., Xu, H., Bader, G.D., Page, N., Robinson, M., Raghibizadeh, S., Hogue, C.W., Bussey, H., *et al.* (2001). Systematic genetic analysis with ordered arrays of yeast deletion mutants. *Science* 294, 2364-2368.
- Tornaletti, S., and Hanawalt, P.C. (1999). Effect of DNA lesions on transcription elongation. *Biochimie* 81, 139-146.
- Torres-Ramos, C.A., Prakash, S., and Prakash, L. (2002). Requirement of RAD5 and MMS2 for postreplication repair of UV-damaged DNA in *Saccharomyces cerevisiae*. *Mol Cell Biol* 22, 2419-2426.
- Tourriere, H., and Pasero, P. (2007). Maintenance of fork integrity at damaged DNA and natural pause sites. *DNA Repair (Amst)* 6, 900-913.
- Tourriere, H., Versini, G., Cordon-Preciado, V., Alabert, C., and Pasero, P. (2005). Mrc1 and Tof1 promote replication fork progression and recovery independently of Rad53. *Mol Cell* 19, 699-706.
- Tsurimoto, T. (1999). PCNA binding proteins. *Front Biosci* 4, D849-858.
- Ulrich, H.D. (2009). Regulating post-translational modifications of the eukaryotic replication clamp PCNA. *DNA Repair (Amst)* 8, 461-469.
- Ulrich, H.D., and Jentsch, S. (2000). Two RING finger proteins mediate cooperation between ubiquitin-conjugating enzymes in DNA repair. *Embo J* 19, 3388-3397.

- Usui, T., Foster, S.S., and Petrini, J.H. (2009). Maintenance of the DNA-damage checkpoint requires DNA-damage-induced mediator protein oligomerization. *Mol Cell* 33, 147-159.
- VanDemark, A.P., Hofmann, R.M., Tsui, C., Pickart, C.M., and Wolberger, C. (2001). Molecular insights into polyubiquitin chain assembly: crystal structure of the Mms2/Ubc13 heterodimer. *Cell* 105, 711-720.
- Varshavsky, A. (1996). The N-end rule: functions, mysteries, uses. *Proc Natl Acad Sci U S A* 93, 12142-12149.
- Veaute, X., Jeusset, J., Soustelle, C., Kowalczykowski, S.C., Le Cam, E., and Fabre, F. (2003). The Srs2 helicase prevents recombination by disrupting Rad51 nucleoprotein filaments. *Nature* 423, 309-312.
- Vertegaal, A.C. (2010). SUMO chains: polymeric signals. *Biochem Soc Trans* 38, 46-49.
- Vialard, J.E., Gilbert, C.S., Green, C.M., and Lowndes, N.F. (1998). The budding yeast Rad9 checkpoint protein is subjected to Mec1/Tel1-dependent hyperphosphorylation and interacts with Rad53 after DNA damage. *Embo J* 17, 5679-5688.
- Vijeh Motlagh, N.D., Seki, M., Branzei, D., and Enomoto, T. (2006). Mgs1 and Rad18/Rad5/Mms2 are required for survival of *Saccharomyces cerevisiae* mutants with novel temperature/cold sensitive alleles of the DNA polymerase delta subunit, Pol31. *DNA Repair (Amst)* 5, 1459-1474.
- Visintin, R., Prinz, S., and Amon, A. (1997). CDC20 and CDH1: a family of substrate-specific activators of APC-dependent proteolysis. *Science* 278, 460-463.
- Waga, S., and Stillman, B. (1998). The DNA replication fork in eukaryotic cells. *Annu Rev Biochem* 67, 721-751.
- Wang, J., Lee, B., Cai, S., Fukui, L., Hu, W., and Chen, Y. (2009). Conformational transition associated with E1-E2 interaction in small ubiquitin-like modifications. *J Biol Chem* 284, 20340-20348.
- Warbrick, E. (2000). The puzzle of PCNA's many partners. *Bioessays* 22, 997-1006.
- Ward, T.R., Hoang, M.L., Prusty, R., Lau, C.K., Keil, R.L., Fangman, W.L., and Brewer, B.J. (2000). Ribosomal DNA replication fork barrier and HOT1 recombination hot spot: shared sequences but independent activities. *Mol Cell Biol* 20, 4948-4957.
- Wasch, R., and Cross, F.R. (2002). APC-dependent proteolysis of the mitotic cyclin Clb2 is essential for mitotic exit. *Nature* 418, 556-562.
- Watanabe, K., Tateishi, S., Kawasuji, M., Tsurimoto, T., Inoue, H., and Yamaizumi, M. (2004). Rad18 guides poleta to replication stalling sites through physical interaction and PCNA monoubiquitination. *Embo J* 23, 3886-3896.
- Waters, L.S., Minesinger, B.K., Wiltrot, M.E., D'Souza, S., Woodruff, R.V., and Walker, G.C. (2009). Eukaryotic translesion polymerases and their roles and regulation in DNA damage tolerance. *Microbiol Mol Biol Rev* 73, 134-154.
- Waters, L.S., and Walker, G.C. (2006). The critical mutagenic translesion DNA polymerase Rev1 is highly expressed during G(2)/M phase rather than S phase. *Proc Natl Acad Sci U S A* 103, 8971-8976.
- Weinert, T. (2007). Cell biology. What a cell should know (but may not). *Science* 315, 1374-1375.
- Wu, C.J., Conze, D.B., Li, T., Srinivasula, S.M., and Ashwell, J.D. (2006). Sensing of Lys 63-linked polyubiquitination by NEMO is a key event in NF-kappaB activation [corrected]. *Nat Cell Biol* 8, 398-406.

- Xiao, W., Chow, B.L., Fontanie, T., Ma, L., Bacchetti, S., Hryciw, T., and Broomfield, S. (1999). Genetic interactions between error-prone and error-free postreplication repair pathways in *Saccharomyces cerevisiae*. *Mutat Res* **435**, 1-11.
- Yang, W., and Woodgate, R. (2007). What a difference a decade makes: insights into translesion DNA synthesis. *Proc Natl Acad Sci U S A* **104**, 15591-15598.
- Yang, X.H., Shiotani, B., Classon, M., and Zou, L. (2008). Chk1 and Claspin potentiate PCNA ubiquitination. *Genes Dev* **22**, 1147-1152.
- Yang, X.H., and Zou, L. (2009). Dual functions of DNA replication forks in checkpoint signaling and PCNA ubiquitination. *Cell Cycle* **8**, 191-194.
- Yunus, A.A., and Lima, C.D. (2009). Structure of the Siz/PIAS SUMO E3 ligase Siz1 and determinants required for SUMO modification of PCNA. *Mol Cell* **35**, 669-682.
- Zhang, H., and Lawrence, C.W. (2005). The error-free component of the RAD6/RAD18 DNA damage tolerance pathway of budding yeast employs sister-strand recombination. *Proc Natl Acad Sci U S A* **102**, 15954-15959.
- Zhang, T., Nirantar, S., Lim, H.H., Sinha, I., and Surana, U. (2009). DNA damage checkpoint maintains CDH1 in an active state to inhibit anaphase progression. *Dev Cell* **17**, 541-551.
- Zhou, B.B., and Elledge, S.J. (2000). The DNA damage response: putting checkpoints in perspective. *Nature* **408**, 433-439.

## Abbreviations

Ψ	aliphatic aminoacid
μ	micro
2D	two-dimensional
4NQO	4-nitro quinoline-1-oxide
5'-FOA	5'-fluoroorotic acid
AD	Gal4 Activation Domain
Amp	ampicillin
APC/C	Anaphase Promoting Complex / Cyclosome
ATP	adenosine 5'-triphosphate
BD	Gal4 DNA Binding Domain
BER	base excision repair
bp	base pairs
BRCA	BReast CAncer
BSA	Bovine Serum Albumin
CDC	Cell Division Cycle
CDH	CDC20 Homolog
CDK	Cyclin-Dependent Kinase
CLB	Cyclin B
C-terminal, C-ter	carboxy-terminal
D-box	Destruction box
D-loop	displacement loop
DDK	Dbf4-Dependent Kinase
DDT	DNA Damage Tolerance
DMSO	dimethylsulfoxide
DNA	deoxyribonucleic acid
DNAase	deoxyribonuclease
dNTP	deoxy nucleoside triphosphate
DSB	double-strand break
DTT	dithiothreitol
DUB	de-ubiquitylating enzyme
E1	ubiquitin activation enzyme
E2	ubiquitin conjugation enzyme
E3	ubiquitin ligase
E4	ubiquitin chain elongation enzyme
EDTA	ethylenediaminetetraacidic acid
EtBr	ethidium bromide
FACS	Fluorescence Activated Cell Sorting
g	gram, gravitational constant
GCR	gross chromosomal rearrangement
GINS	go-ichi-ni-san, 5, 1, 2, 3 for Sld5, Psf1, Psf2, Psf3
h	hours
H2B	histone 2B



HA	hemagglutinin
HDR	homology-dependent repair
HECT	homologous to E6-AP C-terminus
HR	homologous recombination
HRP	Horse Radish Peroxidase
HU	hydroxyurea
Ig	immunoglobulin
k	kilo
kb	kilo base pairs
kDa	kilo Daltons
LB	Luria-Bertani
m	milli
M	molar
MAT	mating type
MCM	Mini-Chromosome Maintenance
min	minutes
MMR	mismatch repair
MMS	methyl methane sulfonate (sensitivity)
MOPS	3-N-Morpholinopropane sulfonic acid
MRC	Mediator of the Replication Checkpoint
mRNA	messenger RNA
MW	molecular weight
n	nano
NER	nucleotide-excision repair
NF- $\kappa$ B	Nuclear Factor "kappa-light-chain-enhancer" of activated B-cells
N-terminal, N-ter	aminoterminal
OD	optical density
ORC	Origin Recognition Complex
ORF	Open Reading Frame
PAGE	Polyacrylamide Gel Electrophoresis
PBS	phosphate-buffered saline
PCNA	Proliferating Cell Nuclear Antigen
PCR	polymerase chain reaction
PDS	Precocious Dissociation of Sisters
PEG	polyethylene glycol
PFGE	pulse-field gel electrophoresis
PIAS	protein inhibitor of activated STAT
PIP	PCNA-Interacting Protein
PMSF	phenylmethylsulfonyl fluoride
POL	polymerase
RAD	RADiation sensitive
REV	REVersionless
RFC	Replication Factor C

RING	Really Interesting New Gene
RNase	ribonuclease
RPA	Replication Protein A
rpm	rounds per minute
RT	room temperature
s	seconds
S	sedimentation coefficient (Svedberg)
SAP	Saf-A/B, Acinus and PIAS
SBD	SUMO Binding Domain
SCF	Skp1-Cullin-F-Box complex
SCJ	sister-chromatid junction
SDS	sodium dodecylsulfate
SGS	Slow Growth Suppressor
SRS	Suppressor of Rad Six
STAT	signal transducer and activator of transcription
SUMO	Small Ubiquitin-related Modifier
TBS	tris-buffered saline
TCA	trichloro acidic acid
TEMED	N,N,N',N'-tetramethylethylene diamine
TLS	translesion synthesis
Tris	Tris (hydroxymethyl) aminomethane
U	unit
Ub	ubiquitin
UBA	ubiquitin-associated domain
Ubc	ubiquitin conjugating enzyme
Ubl	ubiquitin-like
UV	ultraviolet light
V	Volt
v/v	volume per volume
w/v	weight per volume
WT	wild-type
YPD	yeast bactopectone dextrose

## **Acknowledgements**

I would like to thank my research advisor, Stefan Jentsch, for his trust in my work and his continuous support. I have been very privileged to have a generous, open-minded, and enthusiastic mentor, who gave me the freedom to explore my ideas, and prompted with his generosity to my scientific education and growth, and to the success of this work.

I would also like to thank Prof. Dr. Peter Becker for kindly accepting to co-referee this work.

I am obliged to Bonny Brewer, MK Raghuraman Wenyi Feng and Vernon, D. Collingwood, and all members of the Brewer/Raghuraman lab at the University of Washington in Seattle, for hosting me in September 2009, for the demonstration of purification and detection of DNA replication intermediates, as well as for the great time we had.

In addition, I would like to express my gratitude to all members of the lab and especially to Lucian, Sandrine, Christian P, Christian E, Wojtek, Nicole, Greg, and Ivan for the pleasure it has been to work with them. Alex provided excellent technical assistance, for which I am very grateful.

I owe everything to the love of my parents, Effie and Yannis, and my sister, Nadia, to whom this work is dedicated.

# Lebenslauf

**Name** Georgios Ioannis Karras  
**Adresse** Implersstrasse 22  
81371, München  
**Geburtsdatum** 19 November 1982  
**Geburtsort** Cholargos/Athen, Griechenland

## Schulbildung

1988-1995 Grundschole, Kareas/Athen, Griechenland  
1994-1997 Gymnasium No. 7, Ilioupolis/Athen, Griechenland  
1997-2000 Lyceum No. 2, Ilioupolis/Athen, Griechenland  
Abschluss mit Abitur im Juni 2000

## Studium

2000-2004 Democritus University of Thrace  
Department of Molecular Biology and Genetics  
Studiengang: Molekulare Biologie- Genetik (Diplom)  
  
Diplomarbeit über "Structure and Function of a Novel  
Domain Involved in Chromatin Regulation" am EMBL,  
Heidelberg (Arbeitsgruppe Dr. Andreas G. Ladurner)  
  
Abschluss mit Diplom im Oktober 2004

## Doktorarbeit

Seit Oktober 2004 Max-Planck-Institut für Biochemie  
Abteilung Molekulare Zellbiologie (Prof. Dr. Stefan Jentsch)